

2008

Finite element analysis of a steel girder bridge subjected to blast load

Mayik Kornelio Koriom
University of Dayton

Follow this and additional works at: https://ecommons.udayton.edu/graduate_theses

Recommended Citation

Koriom, Mayik Kornelio, "Finite element analysis of a steel girder bridge subjected to blast load" (2008).
Graduate Theses and Dissertations. 4009.
https://ecommons.udayton.edu/graduate_theses/4009

This Thesis is brought to you for free and open access by the Theses and Dissertations at eCommons. It has been accepted for inclusion in Graduate Theses and Dissertations by an authorized administrator of eCommons. For more information, please contact mschlangen1@udayton.edu, ecommons@udayton.edu.

**FINITE ELEMENT ANALYSIS OF A STEEL GIRDER BRIDGE
SUBJECTED TO BLAST LOAD**

Thesis

Submitted to

The School of Engineering of the

University of Dayton

in Partial Fulfillment of the Requirements for

The Degree

Master of Science in Civil Engineering

by

Mayik Kornelio Koriom

University of Dayton

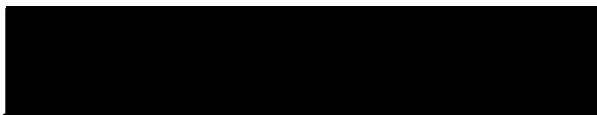
Dayton, Ohio

December, 2008

APPROVED BY:



Robert A. Brockman, committee member



Steven L. Donaldson, committee member



Patrick J. Fortney, committee member



Faris A. Malhas, Advisor, Chairman of the committee

ABSTRACT

FINITE ELEMENT ANALYSIS OF A STEEL GIRDER BRIDGE SUBJECTED TO BLAST LOAD

Name: Koriom, Mayik Kornelio
University of Dayton

Advisor: Dr. Faris .A Malhas

The content of this thesis presents a study of a typical highway steel bridge subjected to blast load resulting from a vehicular explosion 5 feet above the deck. The research identifies and studies critical parameters that define the structural response of the bridge superstructure to blast loads i.e. charge size, location, ductility and strength of both the concrete deck and steel girders. Finite element software ABAQUS is used to evaluate the structural response and behavior of the superstructure during the blast. The software is capable of accurately simulating the initiation and propagation of damage and failure in concrete deck and steel girders during a blast event. The results are presented in 3-D diagrams that depict the actual damages. Structural integrity of the bridge is assessed after the explosion by application of a live load to the bridge to determine the residual strength of critical components. Subjective recommendation on designing a blast-resistant steel bridge is presented based on the assumption that all members should have enough ductility and strength to resist failure.

**THIS THESIS IS DEDICATED TO
MY FATHER KORNELIO KORION**

AND

MY MOTHER REGINA NYBOL

AND

MY WIFE MARY SUKEJI WANI

YOUR SUPPORT MADE THIS WORK POSSIBLE

ACKNOWLEDGEMENT

I am extremely grateful to my supervisor Dr. Faris A. Malhas, who dedicated valuable time in guiding me towards completion of this work. The thesis would not have been accomplished without his knowledgeable supervision. I am also very much appreciative to Dr. Robert Brockman, finite element expert, who assisted me a lot with constructive suggestion. I am extremely thankful to Dr. Patrick Fortney and Dr. Stephen Donaldson for sharing thoughts and suggestions on the thesis work. Finally I am very much appreciative to my wife and parents. Your moral support was a valuable asset that always inspired me to achieve the best.

TABLE OF CONTENTS

ABSTRACT.....	iii
DEDICATION.....	iv
ACKNOWLEDGEMENT.....	v
LIST OF ILLUSTRATIONS	viii
LIST OF TABLES.....	xi
I. INTRODUCTION.....	1
Objective of the study.....	2
Scope and parametric study.....	3
II. LITERATURE REVIEW.....	4
Vulnerability assessment.....	4
Numerical analysis review.....	8
III. FINITE ELEMENT ANALYSIS.....	12
Bridge geometry.....	12
Limitation of the study.....	12
Element type.....	15
Modeling of reinforced concrete slab.....	16
Modeling of steel girders.....	20
Bridge model verification.....	21
IV. BLAST LOAD AND MESH REFINEMENT.....	22
Introduction to blast load.....	22
Mesh refinement and result convergence.....	30
V. FINITE ELEMENT ANALYSIS OF THE BRIDGE SUBJECTED TO BLAST LOAD.....	33
Response of concrete deck of various strength to blast load.....	33
Analysis and results.....	36

Effect of charge sizes on bridge damage.....	35
Blast analysis.....	42
Discussion of results.....	63
Post-blast analysis.....	68
 VI. CONCLUSION AND FUTURE RESEARCH.....	 75
Conclusion.....	75
Future research.....	77
 APPENDICES.....	 78
A. VERIFICATION EXAMPLES.....	78
B. ALTERNATIVE REFINEMENT MESH STUDY.....	92
C. DISTRIBUTION OF BLAST LOAD.....	97
D. CONSTITUTIVE CONCRETE MODEL.....	101
 BIBLIOGRAPHY.....	 103

LIST OF ILLUSTRATIONS

	ILLUSTRATION NAME	PAGE
Figure 1	Destroyed Sarafiya Bridge, Baghdad, Iraq	1
Figure 2	Displacement of composite plate girder deck (Astaneh)	10
Figure 3	Damage to composite plate girder (Astaneh)	10
Figure 4	Structural response of bridge to blast loading (islam)	11
Figure 5	Composite steel bridge	13
Figure 6	Bridge geometry	14
Figure 7	S4R shell element	16
Figure 8	Uniaxial stress-strain curve for concrete	16
Figure 9	Tension stiffening model for concrete	19
Figure 10	Response of concrete to uniaxial loading in (a) tension (b) compression	19
Figure 11	Stress-strain curve of steel	20
Figure 12	Finite element model and mesh	21
Figure 13	Simplified pressure-time profile of blast load	23
Figure 14	Reflected pressure coefficient vs. angle of incidence	24
Figure 15	Maximum and minimum over-pressure with spherical blasts	25
Figure 16	Application of blast load on concrete deck	28
Figure 17	Distribution of pressure load of 0.5N-lb TNT	28
Figure 18	Pressure-distant distribution of 0.5N-lb blast load	29
Figure 19	Explosion locations	32
Figure 20	Concrete stress-strain curves in compression	34
Figure 21	Compressive strain values on concrete deck	38
Figure 22	Deflection of deck due to 0.5N-lb blast load	43
Figure 23	Damage due to 0.5N-lb blast load	43
Figure 24	Longitudinal stress and strain of deck and rebar due to 0.5N-lb blast	44
Figure 25	Deflection, longitudinal stress and strains at girder due to 0.5N-lb blast	45

Figure 26	Displacement at concrete deck due to 1N-lb blast load	47
Figure 27	Damage due to 1N-lb blast load	47
Figure 28	Longitudinal stress and strain of deck and rebar due to 1N-lb blast	48
Figure 29	Deflection, longitudinal stress and strain at girders due to 1N-lb blast	49
Figure 30	Displacement at deck due to 2N-lb blast load	51
Figure 31	Damage due to 2N-lb blast load	51
Figure 32	Longitudinal stress and strain of deck and rebar due to 2N-lb blast	52
Figure 33	Deflection, longitudinal stress and strain at girders due to 2N-lb blast	53
Figure 34	Deflection at deck due to 3N-lb blast load	55
Figure 35	Damage due to 3N-lb blast load	55
Figure 36	Longitudinal stress and strain of deck and rebar due to 3N-lb blast	56
Figure 37	Deflection, longitudinal stress and strain at girders due to 3N-lb blast	57
Figure 38	Deflection of deck due to 4N-lb blast load	59
Figure 39	Damage due 4N-lb blast load	59
Figure 40	Longitudinal stress and strain of deck and rebar due to 4N-lb blast	60
Figure 41	Deflection, longitudinal stress and strain at girders due to 4N-lb blast	61
Figure 42	Comparison of blast loads	64
Figure 43	Comparison of displacement	65
Figure 44	Comparison of strain of girders	66
Figure 45	Comparison of stresses at girders	66
Figure 46	Damage at girder1	67
Figure 47	Damage at girder2	67
Figure 48	Design Load	69
Figure 49	Structural response of the bridge due to 0.5N-lb blast and live load	70
Figure 50	Structural response of the bridge due to 1N-lb blast and live load	71
Figure 51	Structural response of the bridge due to 2N-lb blast and live load	72
Figure 52	Structural response of the bridge due to 3N-lb blast and live load	73
Figure 53	Structural response of the bridge due to 4N-lb blast and live load	74

Figure 54	ABAQUS results	79
Figure 55	Deflection across half of the beam	79
Figure 56	Compressive stress at the top of the beam	80
Figure 57	Response of reinforced concrete beam	81
Figure 58	Moment-curvature for reinforced concrete beam	81
Figure 59	Load-deflection diagram, Tension stiffening = 0.0015	83
Figure 60	Load-deflection diagram, Tension stiffening = 0.003	83
Figure 61	Concrete slab response to failure load	84
Figure 62	Structural response of the steel reinforcement	85
Figure 63	Cross-section of the composite beam	87
Figure 64	Response of composite beam	88
Figure 65	Plastic stress and strain distribution at ultimate moment	90
Figure 66	Moment curvature and moment strain diagram	90
Figure 67	Plastic analysis of concrete beam	91
Figure 68	Mesh of bridge “simplified model”	93
Figure 69	Distribution of pressure due to overpressure and reflected pressure	93
Figure 70	Stress and strain response for mesh refinement	95
Figure 71	Deflection at mid-span due to mesh refinement	95
Figure 72	Blast load profile	97

LIST OF TABLES

	Name	Page
Table 1	Concrete Material properties	18
Table 2	Steel material properties	20
Table 3	Charge sizes	39
Table 4	Damage limits of steel girder	41
Table 5	Table (5) Allowable compressive strains of concrete deck	42
Table 6	Summary of structural response of girders	46
Table 7	Structural response of steel girders to 1N-lb blast load	50
Table 8	Structural response of steel girders to 2N-lb blast load	54
Table 9	Structural response of steel girders to 3N-lb blast load	58
Table 10	Structural response of steel girders to 4N-lb blast load	62
Table 11	Response of girders to 0.5N-lb blast load	70
Table 12	Response of girders to 1N-lb blast load	71
Table 13	Response of girders to 2N-lb blast load	72
Table 14	Response of girders to 3N-lb blast load	73
Table 15	Response of girders to 4N-lb blast load	74
Table 16	Stress and strain of the girder	89
Table 17	Analytical values of stress and strain of the composite beam	91
Table 18	Response due to mesh refinement	96
Table 19	Distribution of 5N blast load	100

Table 20	Concrete properties	101
Table 21	Properties of low strength concrete	101
Table 22	Properties of high strength concrete	101
Table 23	Strain for non-ductile concrete	102
Table 24	Strain for ductile concrete	102
Table 25	Longitudinal strain for high strength concrete	102

CHAPTER I

INTRODUCTION

Bridges are imperative transportation infrastructures that provide means of communication over natural and artificial barriers. Due to their socio-economic importance, bridges have been lucrative targets to terrorist. A memo disclosed by the Federal Transportation Association in 1998, showed that 58% of terrorist attacks worldwide targeted transportation facilities (FTA 2001). Since September 11th 2001, there has been an increase in terrorist threats against economic infrastructure with an aim to inflict massive human casualties, and severe crippling of economy. This intention was apparent in a testimony from several captured terrorists and manuals. One such manual, released by the US Department of Justice, instructs terrorist to “destroy bridges in order to instill terror in the hearts of enemies” (USDJ 2002). The destruction of the Sarafiya Bridge over the Tigris River (Figure (1)) in Iraq in April 2007 is another evidence of terrorists’ determination to target transportation facilities.

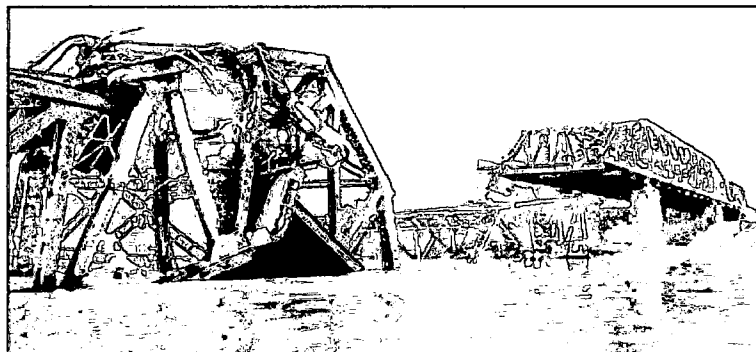


Figure (1) Destroyed Sarafiya Bridge, Baghdad, Iraq.

There are over 600,000 bridges in the USA that are important to the country's economic prosperity. Protecting these bridges from a multitude of unpredictable terrorist threats is a daunting task that was assigned to the Department of Homeland Security by Presidential Directive HSPD 7⁽¹⁾. Protection can theoretically be achieved through the provision of three factors: (1) Gathering good intelligence information, which is a preemptive measure to thwart any attack; (2) Through structural hardening of existing bridge which is done by increasing redundancy and capacity of various structural members such as decks, columns and connections to carry extreme loads, and; (3) Designing blast-resistant bridges. A Blue Ribbon Panel on Bridge and Tunnel Security has issued a list of measures to enhance security of critical bridges across the country (Recommendation on Bridge and Tunnel Security (RBTS), September 2003)⁽²⁾. The RBTS has identified a variety of threats and vulnerabilities of bridges and tunnels. Although hosts of impending threats are listed in the Blue Ribbon study, the nature of a terrorist attack is unpredictable, hence complicating the design process, which depends in large part on exact comprehension of applied loads, seen and unforeseen. To date, limited research has focused on the structural response of bridges subjected to blast load relative to studies of buildings subjected to blast loads. The research presented in this paper advances the knowledge and understanding of the behavior of composite bridges subjected to blast loads.

1.1 Objective of the study

The use of vehicles rigged with explosives as weapons of destruction has been a frequent terrorist strategy for inflicting structural damage to bridges and other vital structures. The damage resulting from such attacks is dependent on factors such as the weight and positioning of explosives on the bridge. Damage generally ranges from local structural damage that can be easily retrofitted, to major structural damage that requires extensive repair. Since bridges are important transportation infrastructures,

putting a bridge out of service for an extended period of time can have a severe economic impact. The worst scenario is the total destruction of the bridge. In this study failure is the state when the bridge cannot safely carry design loads.

To develop reliable procedures to protect steel bridges against explosive attacks, engineers must develop a better understanding of the level of damage that can be inflicted on bridges by explosives. Conducting assessment studies is a viable method for advancing knowledge in this area. One tool of assessment is nonlinear finite element analysis of three dimensional bridge models. The study presented considers the response to explosive loading of steel bridges typically found in the US.

The current thesis tackles a case of a typical highway steel bridge subjected to over deck blast load resulting from explosion. The main objective is to evaluate the structural behavior of the bridge's superstructure during a blast event. Damage analysis following the blast event is conducted to assess the structural integrity of the bridge. Recommendations on retrofitting measures and design of blast-resistant steel bridges are presented based on the fact that all members should have enough ductility and strength to resist failure.

1.2 Scope and Parametric Study

The primary focus of this thesis is to explore parameters that affect the structural response of concrete deck and steel girders, and they are: (1) Explosive charge size; (2) Location of explosive charge; (3) Material characteristics of both concrete deck and steel girder; and (4) Ductility and strength of concrete deck and girders.

A detailed 3-D finite element model of the bridge is developed using general purpose finite element software ABAQUS. The model is capable of capturing both geometric and material nonlinearities of a bridge when subjected to blast loads. The structural response parameters investigated in the analysis are stresses and strains due to flexure.

CHAPTER II

LITERATURE REVIEW

Security Design of bridges has been evaluated by various panels, agencies, and engineers. The American Society of Civil Engineering (ASCE) discussion on Transportation Security Dialogue on May 2002, outlined three areas of interest to be thoroughly investigated which are: (1) Identification of threats and study of vulnerabilities; (2) Emergency response, and; (3) Mitigation measures. This chapter is a review of the available material on vulnerability assessment, numerical analysis of blast load, and mitigation measures.

2.1 Vulnerability Assessment

The September 11th 2001 attack exposed terrorists' intentions to target transportation facilities in the US and around the world. To protect these vital facilities, several transportation agencies in the US decided to formulate subjective methodologies to reveal threats, comprehend vulnerabilities, and mitigate risks of those impending threats. Since terrorists are known to be adaptive to any kind of security measures, it is unreasonable to presume that a specific risk assessment or security measure methodology will absolutely result in a secure facility. So the decision to support and implement one assessment methodology over others relies exclusively on factors such as importance of the facility, vulnerability level, and cost benefit analysis. In this section the most recent literature review of risk assessment methodologies as proposed by various agencies and researchers are presented.

One of the first studies on risk assessment of transportation facilities was outlined by Stephen Polzin⁽³⁾ who suggested that several factors are to be considered while conducting security risk assessment. According to Polzin, the mathematical relationship between those factors and security risk is:

$$\text{Security Risk} = \text{Probability of Incident Attempt} \times \text{Vulnerability} \times \text{Damage}$$

Polzin concluded that in the post September 11th era, security risk on transportation facilities rose sharply due to an increase in probability of incident attempt, i.e., terrorist threats. Polzin also identified means of mitigating risks through reduction of probabilities of threats and minimizing vulnerabilities to decrease damages. Though many subsequent studies based risk and vulnerability assessment methodologies on Polzin's study, the method is neither explicit in defining all the three components of security risk, nor how to quantify each one. Some researchers suggested that the method works the best at the planning or the global level, and is very hard to be implemented on the operational or the local level.

Whereas Polzin considers risk and vulnerability assessment a "simple mathematical function", Karthik Srinivasan considers risk assessment a complex nonlinear problem that should be incorporated in all levels of planning and design ⁽⁴⁾. Srinivasan proposed a quantitative metrics system able to identify vulnerabilities and assess security risks. The proposed methodology has the ability to assess vulnerabilities at the individual component level as well as at the global system level. The methodology identifies specific issues to be explored while conducting risk assessment, i.e., examining vulnerabilities of structures, deterring terrorist attacks, mitigating impact of attacks in the event they happen, formation of a knowledgeable committee to oversee risk assessment studies, and finally, sharing information among various agencies that are responsible for planning, design and operational efforts.

The highly regarded study on risk and vulnerability assessment was published by the Transportation Policy and Analysis Center of Science Applications International Cooperation (SAIC). The study⁽⁵⁾ which was prepared for the American Association of State Highway and Transportation Officials (AASHTO) is the reference that most State Department of Transportation agencies and engineers use when analyzing risk and vulnerability assessment of transportation facilities. The Guide suggests that risk assessment is a complex problem of six main components that have to be addressed individually. The components are: (1) Identification of important infrastructures; (2) Assessing vulnerabilities "both structural and non-structural"; (3) Assessing consequences; (4) Choosing mitigation measures; (5) Conducting benefit-cost analysis, and finally; (6) Reviewing operational security. The methodology recommends formation of a team to administer each of the six components indicated above. Any team is composed of experts in related fields of planning, security, analysis, design, and risk management. All teams should have complete access to a wide range database of information relevant to their field of investigation. The final risk assessment report is a concerted decision of all six teams combined.

SAIC gives vulnerability factor (y) by the expression:

$$\text{Vulnerability Factor (y)} = (A * B) + (C * D) + (E * F)$$

The vulnerability factor, Y, ranges from 1 to 75. (A*B) is attractiveness of site, (C*D) is accessibility to site, and (D*E) is hazard consequence. The SAIC report meticulously elaborated on issues to be investigated at the level of all six teams, and hence represents the most comprehensive guide in regard to the security of bridge infrastructures. The Blue Ribbon Panel report on Bridge and Tunnel Security⁽⁶⁾, released in 2003, and used the SAIC report to assess risk and vulnerability on bridges and tunnels. The report outlined the most practical and scientific step-by-step risk assessment analysis for bridges and tunnels. Firstly it starts with conducting inventory

surveys to identify the country's critical bridges and ranking them based on importance. Secondly, risk assessment study of threats and vulnerabilities are performed to predict resulting damages. Finally effective measures, both engineering and operational, are employed to mitigate damages. The panel also recommended improving codes of practice and specifications to incorporate extreme blast loads as a design parameter. The panel developed an expression to determine Risk "R" based on the equation:

$$R = O \times V \times I$$

The risk, R, is a function of a possibility of occurrence of threat, O, vulnerability, V, and importance of the structure, I. Vulnerability of a structure is an indication of structural damage sustained, and Importance is realized from adverse impact that a destroyed or damaged infrastructure may have on the area or the region.

The Blue Ribbon report has been investigated thoroughly and elaborated on by engineers and transportation agencies based on specific circumstances of various states. While no specific new methodologies have been suggested since 2003, attention has been focused on proper implementation of the panel recommendations regarding vulnerability assessment. Several states' departments of transportation decided to introduce modifications to the panel's recommendations and tailoring them to meet their local state capacity. The State of Alabama was among the first states to publish its vulnerability assessment methodology (December 2004⁽⁷⁾).

Another study that was based also on the Blue Ribbon Panel report was presented by Eric B. William and Davis G. Winget in 2005. The method, which was titled "Risk Assessment and design of critical bridges for terrorist attacks,"⁽⁸⁾ has the advantage of assigning scores to threat scenarios based on severity. This score is then multiplied by criterion weight, 'a function of target importance', to give a final score, which is a likelihood of occurrence of an attack.

2.2 Numerical Analysis Review

Investigations of different types of bridges subjected to blast loads were conducted over the past few years. Astaneh examined a variety of bridges subjected to blast loads. All his models were 3-D and accounted for material and geometric nonlinearity of structures. Figure (2) shows displacement of normal and high strength concrete deck due to 10A and 20A blast loads (the actual value of blast load was obscured for security purposes). The displacement of the concrete deck is a function of blast size. Figure (3) shows resulting damage due to 10A and 20A blast load. Astaneh concluded that ductility of the bridge deck, rather than strength, is instrumental in determining the response of bridges to blast load⁽⁹⁾. Also, in another study Astaneh concluded that introducing axial load effect to the concrete deck will help delay progressive collapse of deck⁽¹⁰⁾.

A.K.M Anawrul Islam analyzed the response of type III AASHTO Girder Bridge to blast loads⁽¹¹⁾, but the scope of study conducted in his research was simplified in terms of geometry and load application. Islam modeled girders as line models and ignored modeling concrete deck. Islam also assumed a very conservative approach in distributing blast loads on girder, and didn't use reflected pressure as a design load, instead he used incident pressure. Using this model, Islam obtained bending moment and shear force for a two span bridge subjected to a blast load of 500 lb of TNT explosives as shown in Figure (4). Islam recommended that blast resistant bridge design and retrofit techniques should be developed to protect important bridges against explosion.

Winget, Marchant and Williamson studied the effect of blast loads on type V prestressed concrete bridges. They came to various conclusions that bridge geometry directly and crucially affect the response of bridge due to blast load occurring beneath the deck. Winget, Marchant and Williamson pointed out that explosion occurring in

confined regions below bridges will be amplified and hence cause more damage. The study recommended the use of fiber-reinforced polymers (FRPs) for designing and retrofitting bridges. The study also recommended higher steel reinforcement ratios at top and bottom faces of concrete decks in case of explosion below the concrete deck.

Winget and Astaneh recommended that all important bridges should have the ability to redistribute loads, through restraining the deck and girders at the support regions with steel cables to prevent collapse in case that any pier of support is lost.

Currently several agencies such as Center for Infrastructure Engineering studies and Federal Highway Agency and others are researching and exploring the feasibility of developing a blast-resistant design codes similar to the American Society of Civil Engineering set of provisions "Blast Protection of Building Standards" which is due to be released.

This thesis will focus on a rigorous modeling of the whole bridge using shell elements for all members. The blast load will be distributed over the entire bridge using a model presented in chapter (IV).

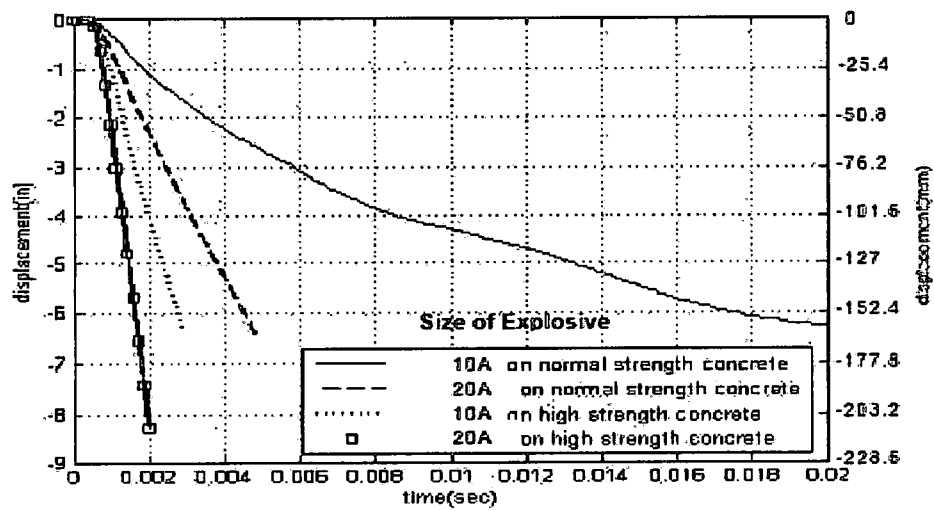


Figure (2) Displacement of composite plate girder deck (Astaneh⁹).

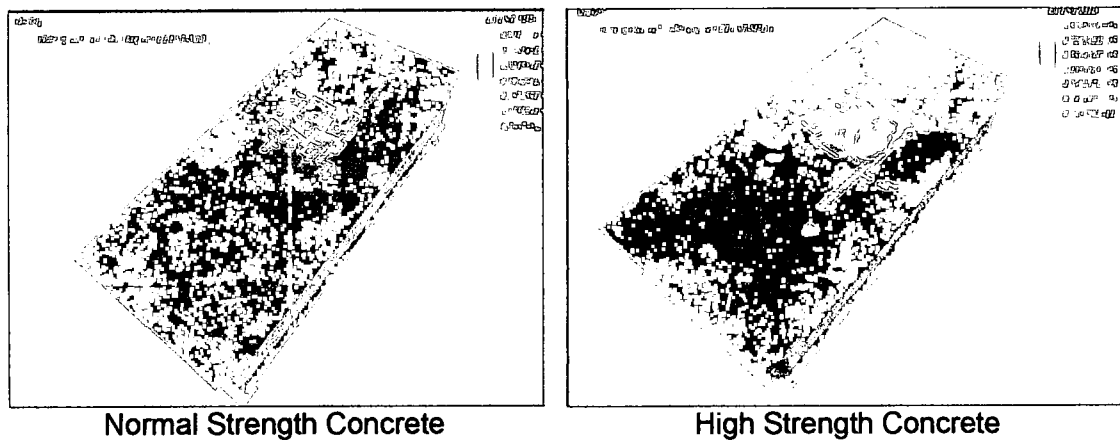
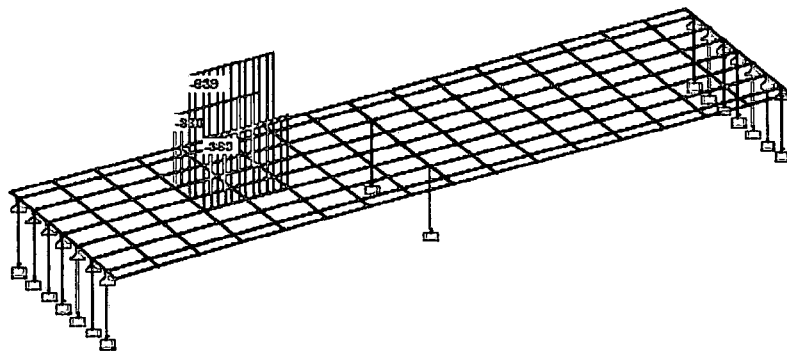
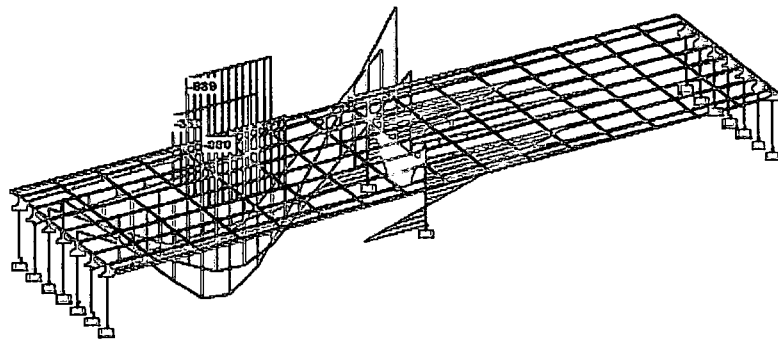


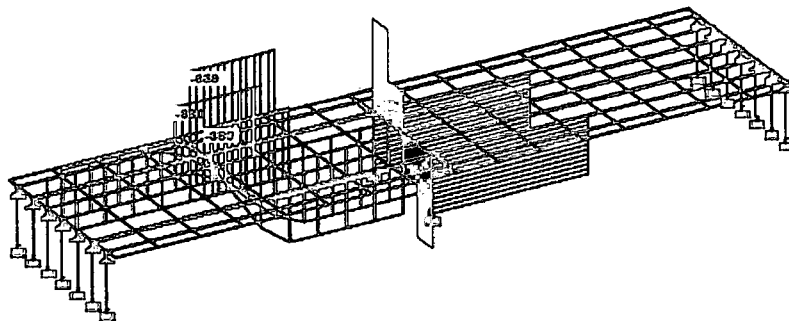
Figure (3) Damage to composite plate girder deck (Ataneh⁹)



(a) Position of blast loading



(b) Moment diagram



(c) Shear Force diagram

Figure (4) Structural response of deck and columns due to blast loading (Islam ¹¹)

CHAPTER III

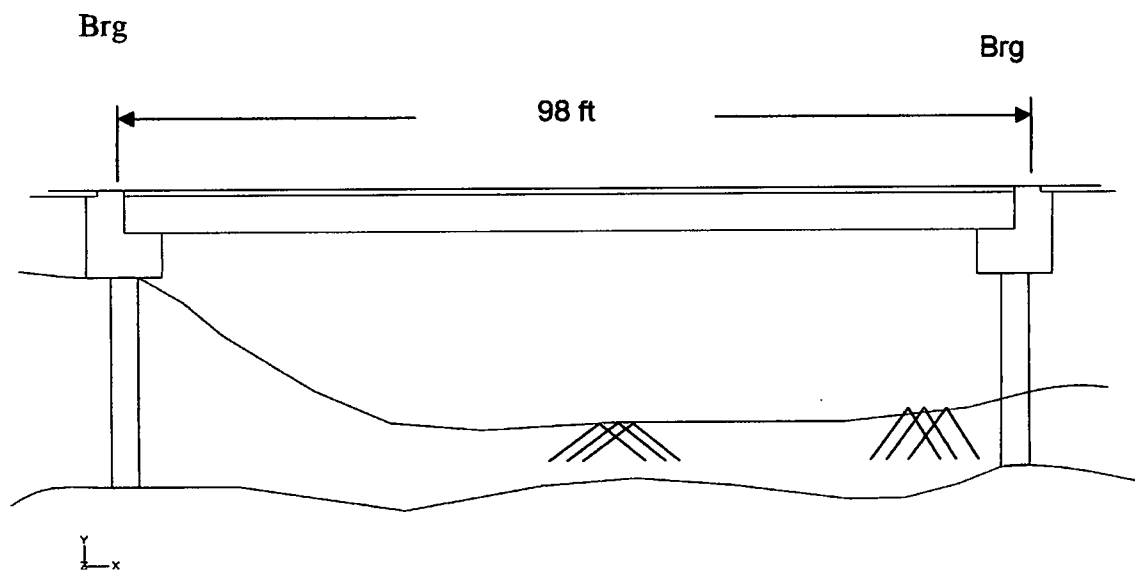
FINITE ELEMENT ANALYSIS

3.1 Bridge Geometry

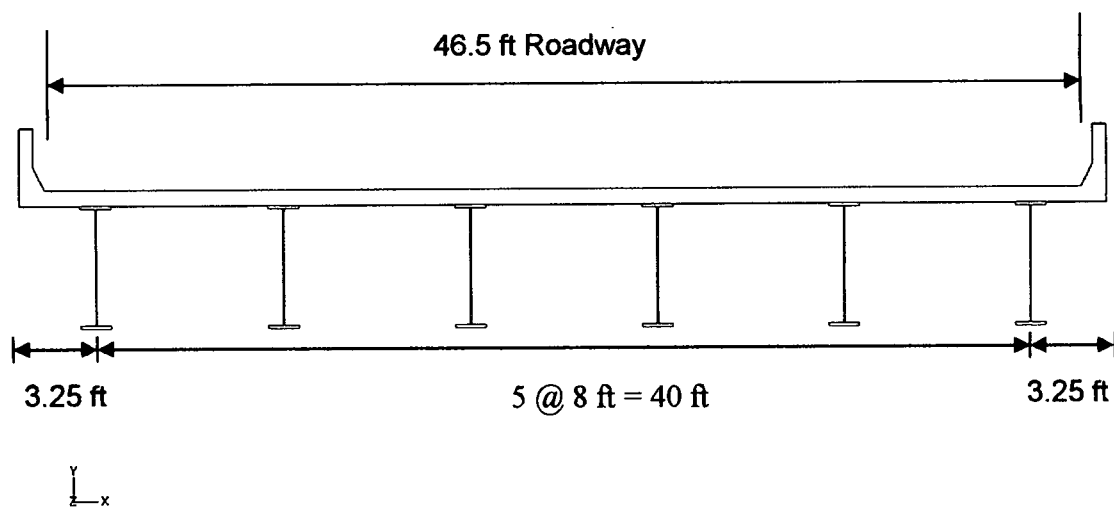
The type of bridge considered in this study is a simply supported typical highway composite steel bridge shown in Figure (5). The bridge has a span of 98 ft and width of 46.5 ft. It consists of a concrete deck that has a thickness of 8.0 in and six steel girders spaced at 8 ft apart. The dimensions and cross sections of girders and reinforcement details are shown in Figure (6-a). The arrangements of stiffeners and cross frames are shown in Figure (6-b) and Figure (6-c), respectively. All structural members of the bridge are modeled using shell element S4R available in the ABAQUS element library.

3.2 Limitation of the study conducted

The scenario of an explosion that occurs at mid-span of the deck of a typical highway composite steel bridge of the type shown in Figure (5) is considered in this study. The bridge has a concrete deck and six steel girders. Arrangement of stiffeners, cross-frames, and steel reinforcement are shown in Figure (6). Hence, results of this evaluation apply only for these types of highway bridges, and other bridges that may have fewer or more girders on the superstructure.



(a)



(b)

Figure (5) Composite Steel bridge (a) General elevation (b) cross section

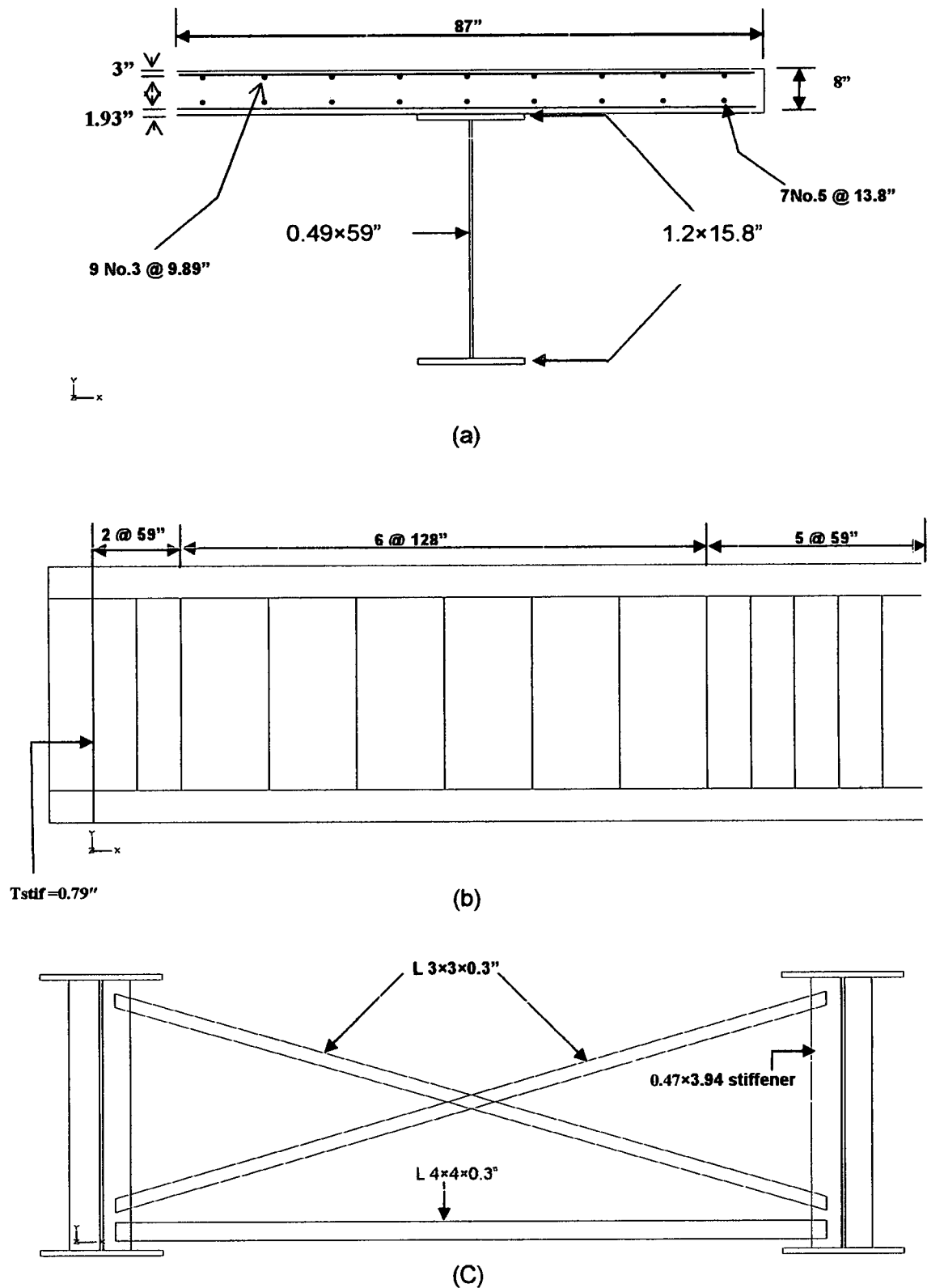


Figure (6) Bridge geometry. (a) Cross section. (b) Stiffener detail. (c) Cross frame details (the drawing is not to scale)

3.3 Element Type

Several studies were conducted by Jiang et al. (2002)⁽¹²⁾ and Liew (2004)⁽¹³⁾ to identify elements that are capable of accurately representing the state of high inelastic response of structures to blast loads. Their studies concluded that shell elements can capture extensive geometric nonlinearity and inelastic behavior of materials, as well as accurately representing lateral-torsional buckling resulting from extreme blast pressure. Hence shell element S4R available in ABAQUS library ⁽¹⁴⁾ is used to model all structural components of the bridge in this study.

Shell elements are basically used to model structures where the thickness ratio to other dimensions is less than 1/10. S4R shell element is a multi-purpose quadrilateral element with reduced integration that has 4 nodes as shown in Figure (7). Each node has three translational (u_x, u_y, u_z) and three rotational (Φ_x, Φ_y, Φ_z) degrees of freedom. S4R has, by default, five integration points across the thickness. These points are used by ABAQUS to compute responses such as stresses and strains. Depending on the nature of problems, the number of integration points can be increased (in case of extreme non-linear problems) or decreased (in case of linear static problems). By default the top surface of the shell element has a positive normal (SPOS) and the bottom has a negative normal (SNEG), both are defined using OFFSET command in section property. S4R shell element exhibits excellent bending and membrane strain behavior, and generates precise solutions for various types of loadings. They are used to model both thin and thick shell elements.

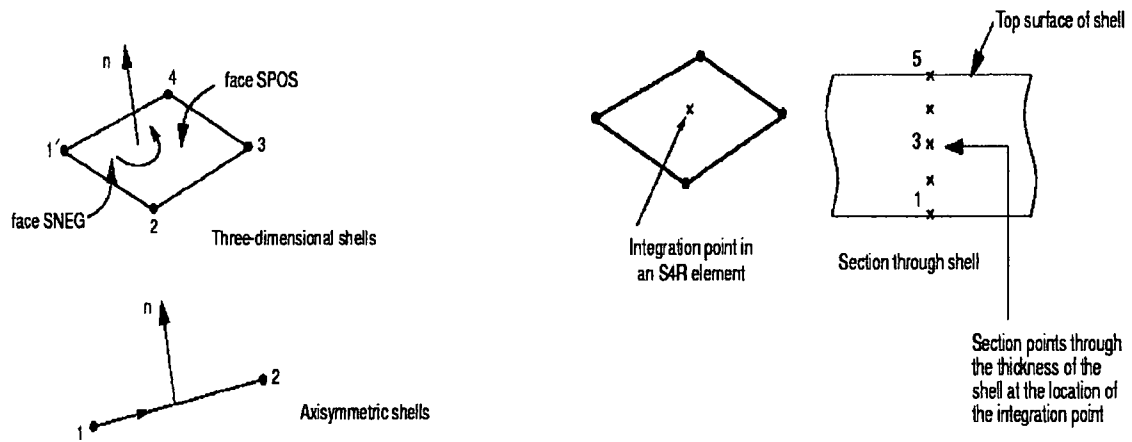


Figure (7) S4R shell element.

3.4 Modeling of reinforced concrete deck slab

Concrete is a material that possesses different behavior in tension and compression as shown in figure (8). Concrete has two failure modes; tensile cracking or compressive crushing.

ABAQUS models concrete by using Concrete Smeared Cracking in ABAQUS/Standard, and Brittle Cracking in ABAQUS/Explicit.

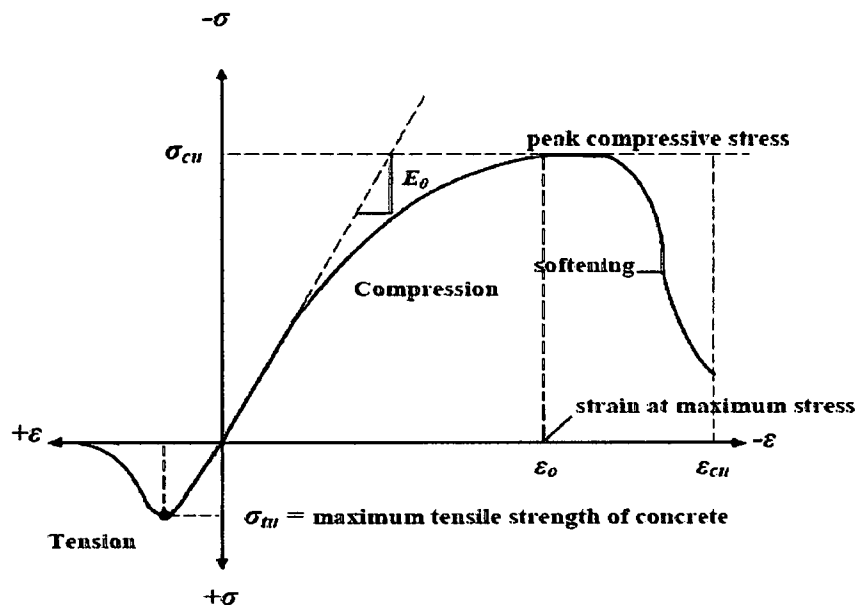


Figure (8) Uniaxial stress-strain curve for concrete.

3.4.1 Smeared Concrete Cracking

Smeared concrete cracking is used to model plain concrete in ABAQUS when the load produces excessive compressive stresses. The values of responses at integration points are performed and calculated after assuming that crack affects only material stiffness at that particular integration point. Tension stiffening concept is used to model the interaction between reinforcement bars and plain concrete. Tension stiffening concept replicates concrete steel carry loads due to loss of stiffness in concrete by formation of cracks.

3.4.2 Tension Stiffening

The interaction between concrete and reinforcing steel is introduced into the plain concrete by addition of tension stiffening. Usually the cracked concrete section is capable of resisting compressive stress while its tensile stress value decreases. In its simplest definition tension stiffness is a linear reduction in tensile strength after the cracking strain of concrete has been reached. The complex relationship between stress and strain of tension stiffening is shown in Figure (9). Basically it is assumed that the tensile strength of concrete is lost when the strain reaches the value of 5×10^{-4} past the failure value in ABAQUS/Standard. This value may be slightly higher in ABAQUS/Explicit.

3.4.3 Concrete Damaged Plasticity

Concrete damaged plasticity in ABAQUS can be used to assess damage in a concrete model subjected to blast load. It has the capability to model damage initiation and evolution in reinforced concrete. The concrete damage model for both uniaxial tension loading and uniaxial compression loading are shown in Figure (10). The model indicates that the stiffness of concrete material degrades when unloaded from the strain-softening branch. The slope of degradation of stiffness is directly related to a

tensile damage variable d_t and compressive damage variable d_c . These damage variables assume values of '0', a no damage state, and '1' which is a full damage of the model. Hence damage or failure of a reinforced concrete model in ABAQUS is basically a function of two hardening variables i.e. tensile equivalent plastic strain, and compressive equivalent plastic strain. The stress-strain relationship of concrete for uniaxial tension and uniaxial compression is given by expression 3.1

$$\begin{aligned}\sigma_t &= (1 - d_t)E_0(\varepsilon_t - \tilde{\varepsilon}_t^{pl}), \\ \sigma_c &= (1 - d_c)E_0(\varepsilon_c - \tilde{\varepsilon}_c^{pl}).\end{aligned}\quad (3.1)$$

With E_0 being the undamaged modulus of elasticity.

Hence, the scope or magnitude of damage will be determined using effective tensile stress and effective compressive stresses given by expression 3.2

$$\begin{aligned}\bar{\sigma}_t &= \frac{\sigma_t}{(1 - d_t)} = E_0(\varepsilon_t - \tilde{\varepsilon}_t^{pl}), \\ \bar{\sigma}_c &= \frac{\sigma_c}{(1 - d_c)} = E_0(\varepsilon_c - \tilde{\varepsilon}_c^{pl}).\end{aligned}\quad (3.2)$$

3.4.4 Material Properties of Concrete

The material properties of the deck are shown in Table (1)

Elastic modulus	$E_c = 4070 \text{ ksi}$
Uniaxial compressive Strength	$f_c = 5000 \text{ psi}$
Uniaxial tensile Strength	$f_t = 530 \text{ psi}$
Strain at ultimate compressive strength	$\varepsilon_{cu} = 0.05$
Poisson's ratio	$\nu = 0.2$
Density	$\rho = 0.084 \text{ lb/in}^3$

Table (1) Concrete material properties

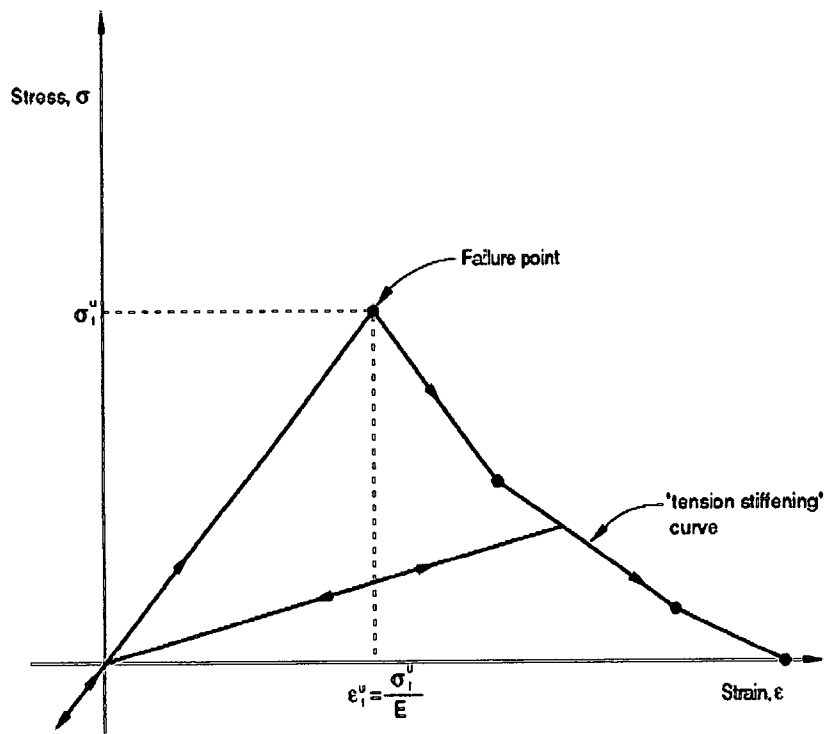


Figure (9) Tension stiffening Model for Concrete

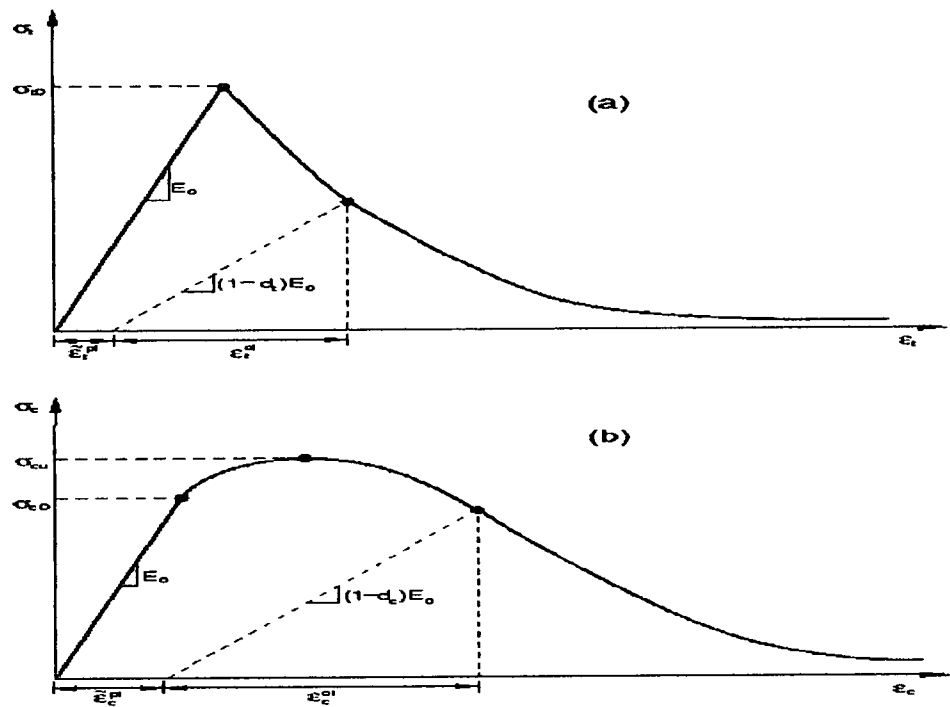


Figure (10) Response of concrete to uniaxial loading in (a) tension and (b) compression

3.5 Modeling of steel girders

The reinforcing steel is Grade 60 and Grade 50 steel is used for the girders. Steel material is modeled assuming an elastic-perfectly plastic material that has both stress values in tension and in compression as shown in figure (11). Girder elements are modeled using shell elements S4R which has a characteristic explained in section 3.3.

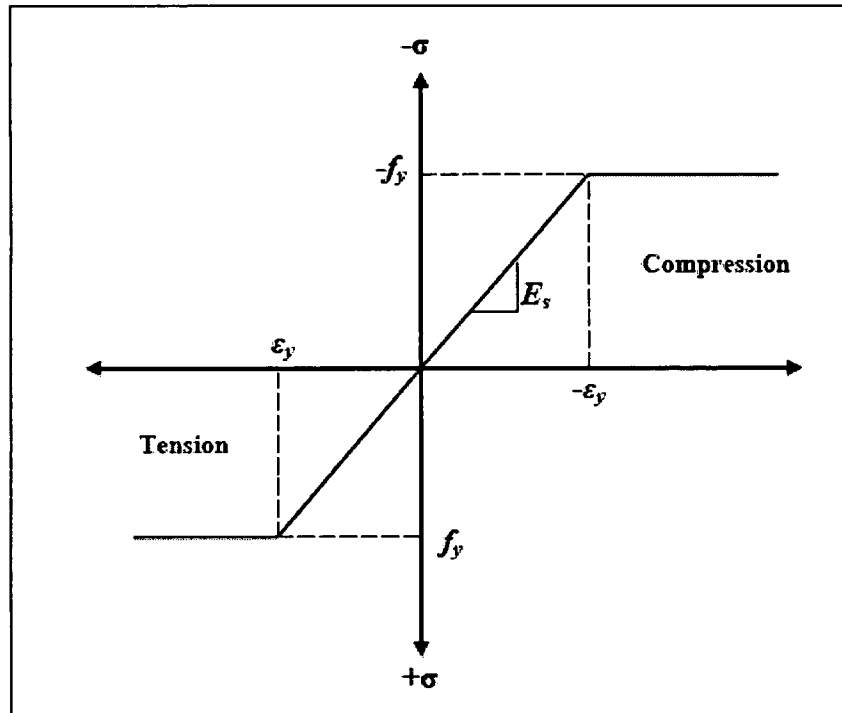


Figure (11) Stress-strain curve of steel material

The properties of steel material used in analysis are shown in Table (2):

Density	$\rho = 0.284 \text{ lb/in}^3$
Elastic modulus	$E_s = 29000 \text{ ksi}$
Yield stress	$f_y = 50,000 \text{ psi} = -f_y$
Yield strain	$\epsilon_y = 0.001724$
Plastic strain	P.S = .15
Poisson's ratio	$\gamma = 0.3$

Table (2) Steel material properties

3.6 Bridge Model and verification

For the purpose of verifying the ability of ABAQUS to accurately model the bridge structural components, a series of quasi static and nonlinear analyses were performed on steel sections representing girders and concrete sections representing deck slabs, as well as on a composite beam. Results of these analyses (Appendix A) were compared to published values to determine accuracy and legitimize the use of these elements in analysis of a bridge subjected to blast load. Based on discussion in section 3.3 and Appendix (A), all constituent elements of the bridge such as deck, girders, cross frames and stiffeners are modeled using shell elements. The number of elements chosen to discretize the concrete deck and individual steel girders, based on convergence results discussed in section 4.2, are found to be 10335 and 2850 respectively. Each cross frame is modeled using 34 elements, and each stiffener is modeled using 24 elements. The end condition is assumed fixed. The finite element model of the superstructure studied in this study is shown in Figure (12)

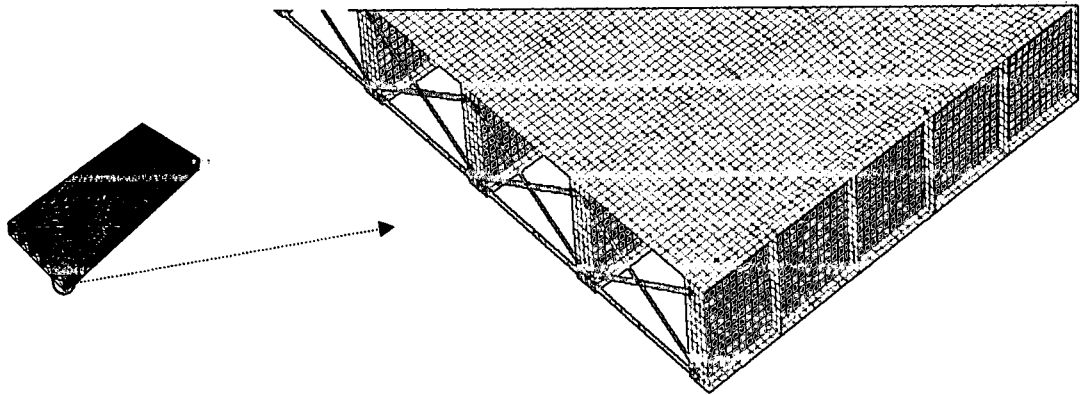


Figure (12) Finite Element model and mesh.

CHAPTER IV

BLAST LOAD AND MESH REFINEMENT

4.1 Introduction to Blast Load

4.1.1 Blast load

Detonation of an explosive device releases a very high energy that travels from the source at a supersonic speed. Physical explosion results in two principal events, i.e. thermal energy leading to a rapid increase in temperature, and air-blast that raises air pressure at proximity of the source of explosion. Though the temperature released can be very high, the air-blast component of the explosion usually causes the bulk of structural damage that is inflicted on structures. When an explosion occurs, the blast wave released expands almost instantaneously to a positive peak value called overpressure (defined as P_{so}^+) which is much higher than the ambient atmospheric pressure (defined as P_o). The shock wave then propagates outwards from the source of explosion while the pressure intensity decays rapidly and exponentially with time and distance. Most of structural damages occur during this positive phase of explosion. The pressure then ultimately drops to a negative value (P_{so}^-) below the ambient pressure, creating a suction pressure that causes debris to be thrown around and far away from the structure inducing more structural damage. The negative phase of pressure usually has longer duration compared to positive phase, but is of much less intensity. The air-pressure profile of an air-blast is shown in Figure (13-a). While conducting nonlinear dynamic analysis of an explosive event, most analysts ignore the effect of the negative phase of pressure, and the positive overpressure is further assumed to decay linearly with time instead of exponentially as shown in Figure (13b).

When a blast wave incident normally interacts with a surface (structure) obstructing its path of propagation, it will be reflected. The reflected overpressure P_r is augmented by a reflection factors, and is usually larger than the peak overpressure. Though reflected pressure varies with the angle of incidence, Smith⁽¹⁵⁾ found that reflection factors values are not greatly changed by incident angles less than 40 degrees.

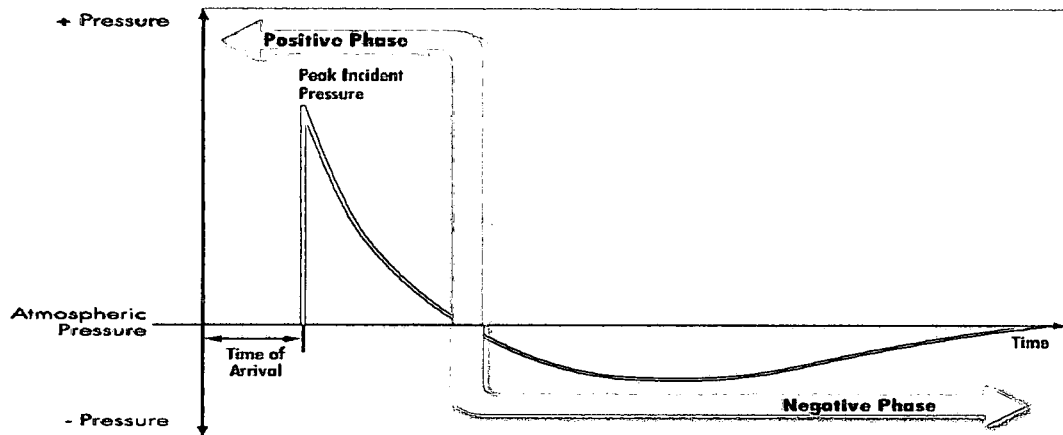


Figure (13) (a) Air pressure profile of an air blast (FEMA 2003)

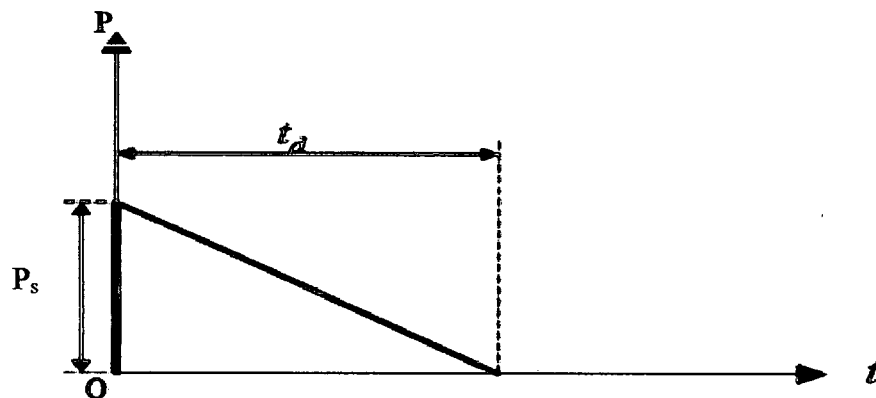


Figure (13) (b) Simplified pressure-time profile of blast wave

It is conservatively assumed that reflected pressure values are the same for incident angles less than 40 degrees. The reflected overpressure is given by expression (4.1)

$$P_r = 2 P_{smax} \left[\frac{7 P_o + 4 P_{smax}}{7 P_o + P_{smax}} \right] \quad (4.1)$$

The values of reflection factors for various incident pressures and angle of incidence are discussed thoroughly in reference (16) and shown in Figure (14). For example a peak incident pressure of 500 psi has a reflection factor of 5, making the reflected pressure P_r equal to 2500 psi. Another parameter that is instrumental in determining the structural response is impulse (I) which is a measure of energy released by an explosion. Impulse can be represented by the following expression

$$I = \frac{1}{2} (P_r \cdot t_d) \quad (4.2)$$

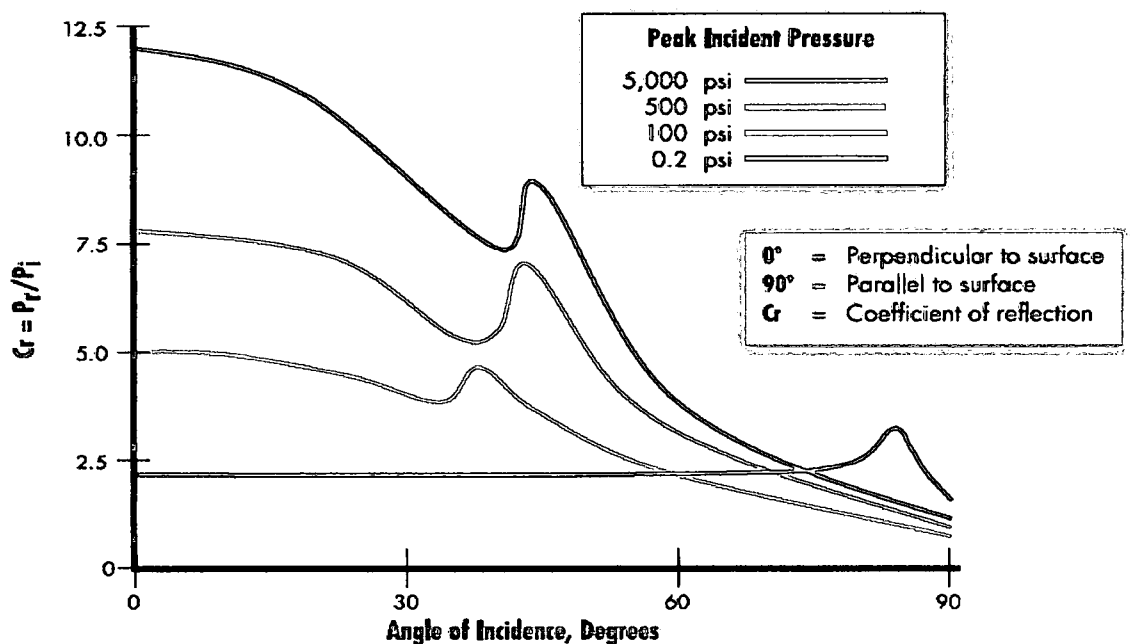


Figure (14) Reflected Pressure coefficient vs. angle of incident [FEMA 2003]

4.1.2 Distribution of Blast Load:

The intensity of blast load, and its capability to inflict damage, is characterized by three main factors: (1) Weight of explosives W (measured in pounds of TNT); (2) The distance of explosion source from the target, usually called the standoff distance R (measured in feet) and; (3) The angle of incidence at which the air-blast encounters any obstruction. Smith⁽¹⁵⁾ concluded that the angle of incidence of a blast load of 40

degrees or less can be neglected in analysis with minimal difference in results. The scaled distance Z , which is essential in estimating blast pressure, is given by the expression

$$Z = \frac{R}{W^{1/3}} \quad (4.3)$$

Using the scaled distance, the value of overpressure P_{Smax} can be obtained from various published curves and charts. Brode⁽¹⁷⁾ developed a curve shown in Figure (15) to compute P_{Smax} for spherical blast. Similar curves and tables have been generated by General Service Administration GSA⁽¹⁸⁾.

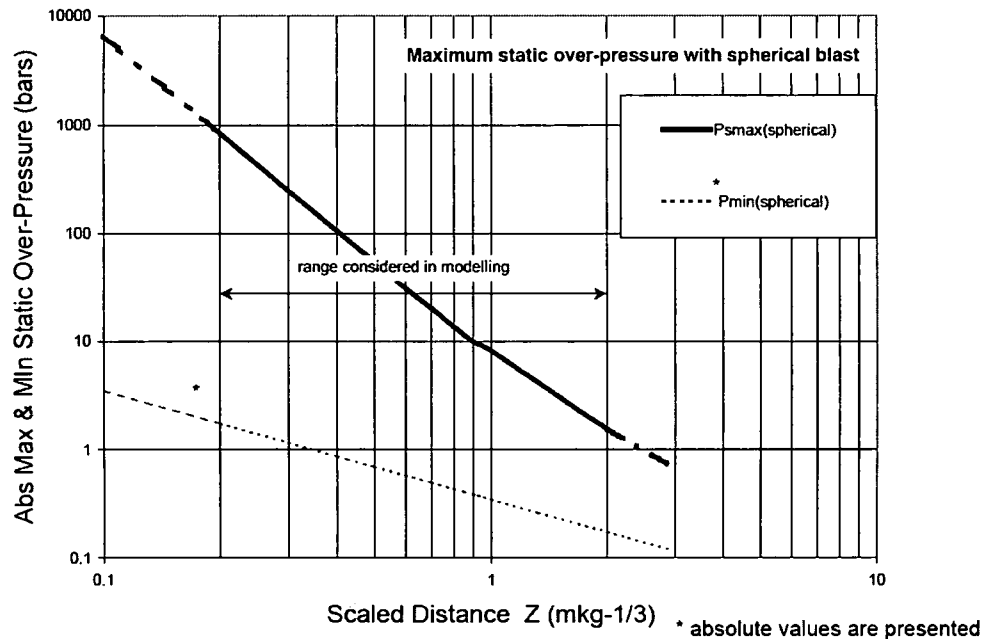


Figure (15) Maximum and minimum over-pressure from spherical blast

The value of pressure at any time t is given by expression (4.4)

$$P(t) = P_o \{ 1 - t/t_d \} \exp^{-(\alpha t/t_d)} \quad (4.4)$$

P_o = maximum overpressure at time $t=0$. P_a = Atmospheric pressure.

α = decay factor.

The maximum overpressure is

$$P_o = \frac{808 \times P_a [1 + (Z/4.5)^2]}{\sqrt{1 + (Z/0.048)^2} \times \sqrt{1 + (Z/0.32)^2} \times \sqrt{1 + (Z/91.35)^2}} \quad (4.5)$$

The duration of blast load t_d is

$$t_d = \frac{980 \times W^{1/3} [1 + (Z/0.54)^{10}]}{[1 + (Z/0.02)^3] \times [1 + (Z/0.74)^6] \times \sqrt{1 + (Z/6.9)^2}} \quad (4.6)$$

The decay factor α is

$$\alpha = 0.3306Z^4 - 3.188Z^3 + 11.755Z^2 - 20.308Z + 15.12 \quad (4.7)$$

Computer software such as ATBlast⁽¹⁹⁾ is capable of computing the value of overpressure, and converting the dynamic air-blast pressure into an equivalent static pressure. ATBlast, developed by Applied Research Association (ARA) for GSA in June 2004, generates values for pressure, impulse, velocity, and duration of blast wave as it decays with distance and time. The graph in Figure (17) depicts a reflected air pressure value resulting from a detonation of 4000 lb of TNT explosives at standoff distance of 10 ft, "similar to explosives used to attack the Murrah Federal building in Oklahoma". The average peak pressure is around 19,000 psi and the duration of loading is 34 milliseconds.

In an explosion event, structures normally respond to reflected pressure P_r (or average reflected pressure over a tributary area) and impulse rather than incident pressure, then maximum reflected pressure is considered as a design blast load in this study. Since the maximum reflected pressure is multiple times greater than incident pressure, safety requirements imply using the worst possible load scenario in analysis and design.

4.1.3 Approximate Distribution of Blast Load on Bridge's Deck

After predicting the peak design pressure, the propagation of shock wave and its encounter with structures has to be examined carefully. Available literature assumes that blast wave travels spherically in air, mainly in a circular manner as it decays with time. The value of peak pressure and reflected pressure can easily be predicted from charts and computer software, but the distribution of blast pressure on structure surfaces is a complex process to represent, and often depends on the structure's profile. Hence, in this study, assumptions have been made to accurately model blast load in a simple fashion.

The maximum distance beyond which pressure value is insignificant is determined from ATBlast software. Since blast wave propagates in a spherical manner, the circle is divided into a group of spheres or rings; each ring represents a contour of equal pressure "or average pressure" profile, and has a standoff distance, and a pressure-time behavior that is different from other rings as suggested in reference (12).

The distribution of blast pressure on the deck surface is done assuming that the first ring has a radius of 12 in, and each subsequent ring has radius of 12 in more than the previous ring. The arrangement of rings and application of blast pressure on the bridge deck is shown in Figure (16). The accuracy of the applied load using this method increases with the decrease of the radius of each ring. This method of applying blast pressure was first discussed by Coggin in 2004 ⁽²⁰⁾.

For example, in this study 23 rings have been used to model blast load. The first seven blast load rings are shown in Figure (17).

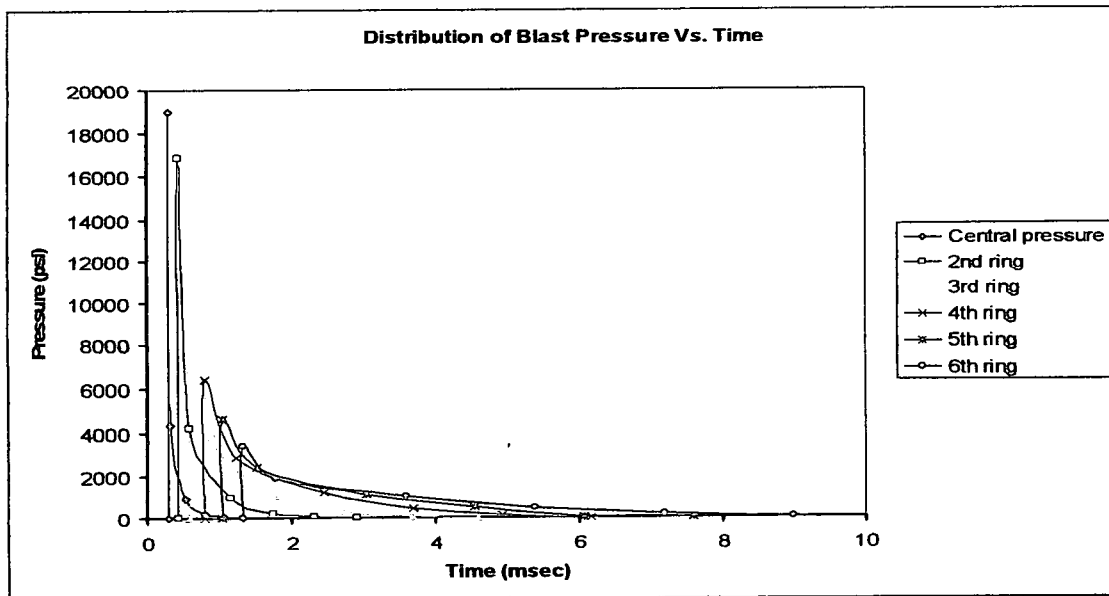


Figure (16) distribution of pressure load of 500 lb TNT.

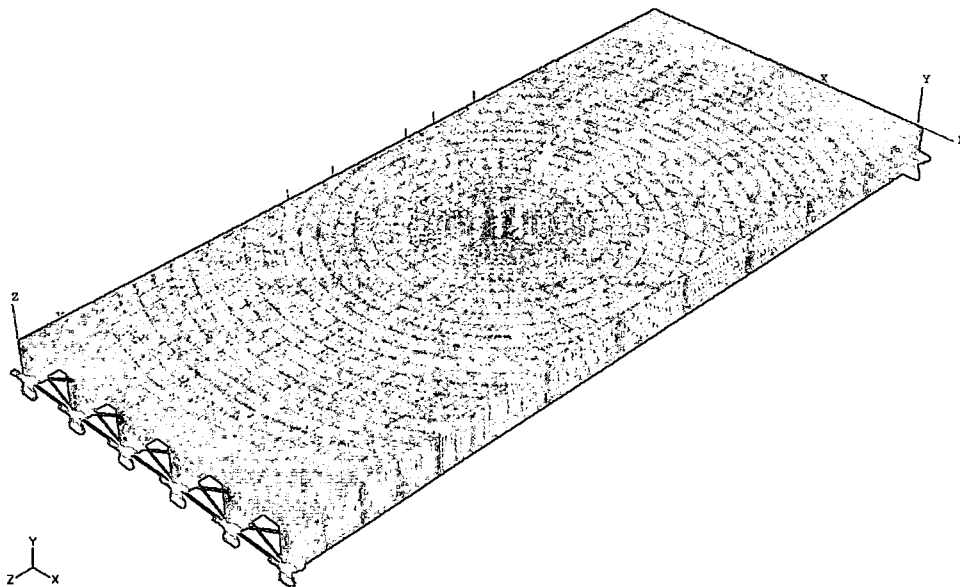


Figure (17) Application of blast load on the concrete deck

The peak pressure at each ring is determined using ATBlast software⁽¹⁹⁾. Since each ring has a unique pressure-time history, the duration of each pressure is determined using equation (4.6), and the value of corresponding value of pressure $P(t_i)$ can be calculated using equation (4.4). This practice is repeated for all rings used to apply

blast pressure on the bridge. In the study, five charge sizes are considered. The blast pressure for each charge size and its distribution on the deck is discussed thoroughly in appendix (c), and omitted from this discussion for security purposes.

4.1.4 Blast Loads

The structural response of a bridge is evaluated based on five charge sizes threats i.e. 0.5N-lb, 1N-lb, 2N-lb, 3N-lb and 4N-lb, 'N' is a multiplier omitted for security purposes. The Blue Ribbon Panel on Bridge and Tunnel Security suggested that a car bomb of charge 500 lb TNT is the likely scenario of a terrorist attack, with 5N-lb vehicle bomb being the highest possible charge used in vehicular explosions. To understand the structural behavior of bridges to blast loads, charge sizes less than and greater than the minimum specified charge are studied thoroughly. The pressure-distance profile of a 5N lb blast load is shown in Figure (18).

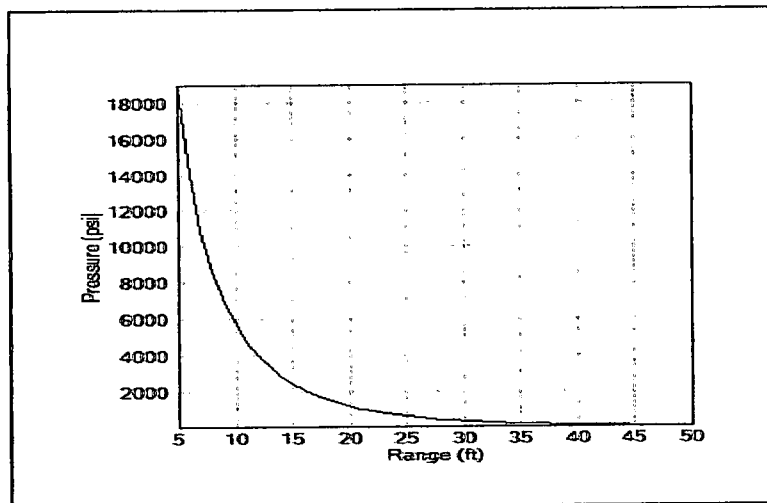


Figure (18) Pressure-distance distribution of 0.5N-lb blast load

4.1.5 Structural response to blast waves

The response of structures to blast loads depends on factors such as the weight (W) of explosives, stand-off distance (R) and angle of incident of blast load. It is also a

function of structural strength, redundancy and geometry. Explosion produces dynamic loads that are characterized by a very high pressure and strong dragging load. Depending on the position and intensity of the blast from the structure, the structure may sustain different levels of deformation and damages. If the source of blast is very close to the structure, it may sustain severe localized damages because the incident blast will travel a short distance while retaining much of its initial intensity. If the source of blast is far from the structure, the incident blast pressure will have a relatively long distance to travel, thus its intensity decays but its duration increases as it interacts with structures. The further the source of the blast from a structure, the larger the area of the structure affected by blast wave causing global damage.

4.2 MESH REFINEMENT AND RESULTS CONVERGENCE

Proper meshing of the bridge model is an important analytical step to obtain an accurate solution in ABAQUS. Accuracy of numerical solutions increase as the number of elements used in a mesh is increased. On the other hand, having more elements in a model means increasing the computing time of the analysis process. Hence a balance between accuracy and reduction of the cost of solutions is investigated in this chapter. Blast load is a dynamic impact load that results in sudden and rapid increase of pressure at and around the source of explosion followed by instant reduction in pressure. The dynamic response of structures to severe blast load is characterized by high strain rate deformation and plasticity. Hence the mesh used to discretize models subjected to blasts loads should be fine enough to capture high-rate structural damages locally as well as globally.

4.2.1 Mesh study based on wave speed of stress propagation

A blast event generates a wave that travels at high speed producing fast rate of stress application. To accurately account for stress wave propagation, the F.E. model

must be refined based on the proposition that the blast duration t_d multiplied by wave speed equals the length of ten elements. The longitudinal wave speed propagation C_d in the structural materials is given by the expression⁽²⁰⁾

$$C_d = (E/\rho)^{1/2} \quad (4.7)$$

E is modulus of elasticity and ρ is material density

The length of ten elements L_{10ele}

$$L_{10ele} = t_d \times C_d \quad (4.8)$$

For 1000 lb TNT explosive positioned at 10 ft above the concrete deck, the duration of highest peak reflected pressure is 0.73 msec, hence the length of 10 elements to capture stress propagation is computed as:

$$L_{10ele} = .01223 \times (3.2E+6 / .087)^{1/2} = 74.17 \text{ in}$$

Hence the length of one element is 7.42 in, making the total number of elements along the length approximately 159 elements and 65 elements across the width, for a total of 10,335 elements for the deck. A mesh of the bridge model is shown in Figure (12). Following the same calculations, the number of elements across the height of girder is 5 elements and 95 along the girder length, for a total of 475 elements per girder. In general, we will have over 13,185 elements for the superstructure. An alternative study for mesh refinement independent of stress wave propagation is presented in Appendix (B). Either method can be used for mesh refinement.

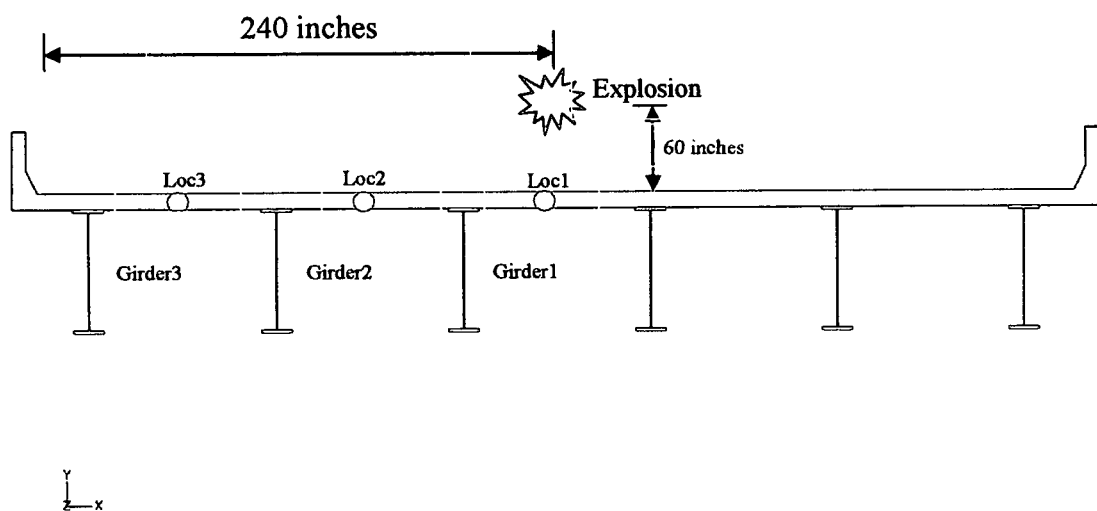
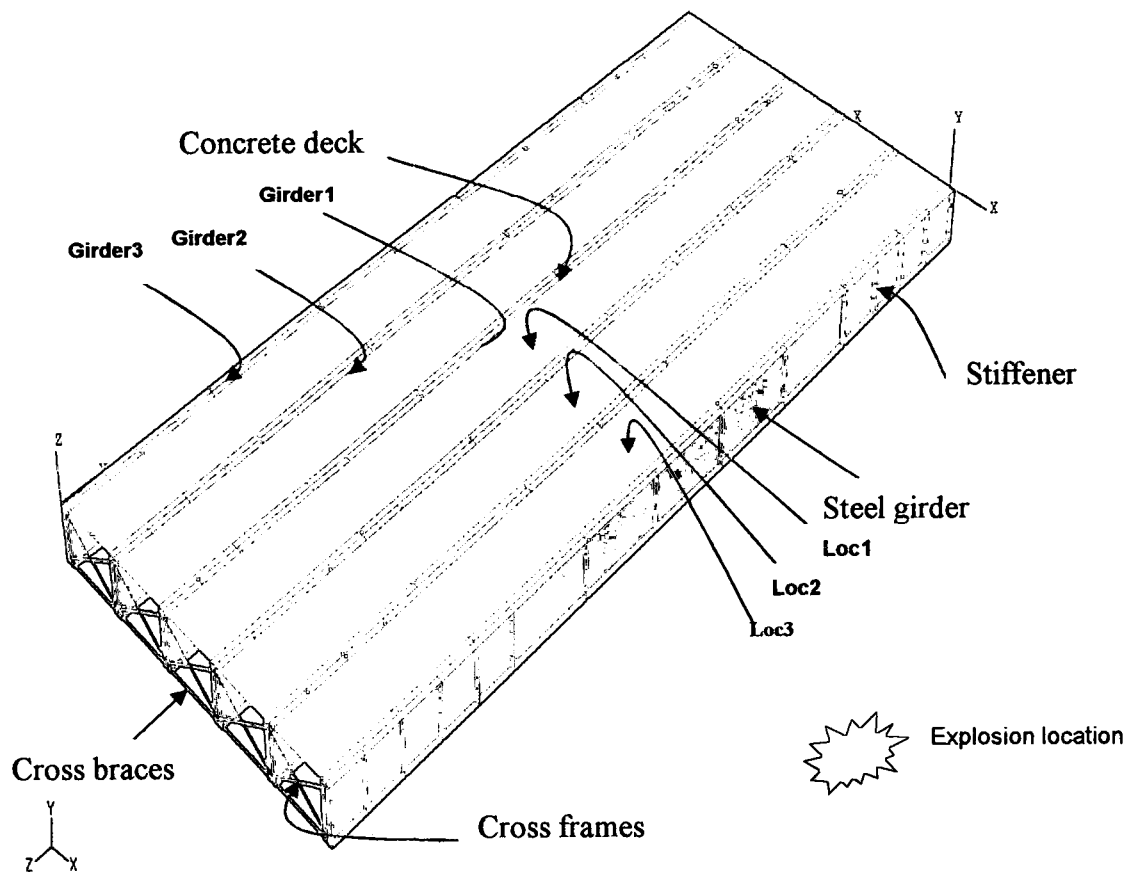


Figure (19) Explosion location

CHAPTER V

FINITE ELEMENT ANALYSIS OF THE BRIDGE FOR BLAST LOAD

5.1 Response of Concrete Deck of Various Strengths to Blast Loads

Structural ductility is a critical feature that has significant impact on the behavior of a concrete deck when subjected to blast load. The stress-strain curve of concrete material, Figure 20(a), has a linear ascending portion with a slope representing modulus of elasticity E_c . Ductility is represented by the descending portion of the stress-strain curve. The material is ductile if the slope is less steep. Usually lower-strength concrete exhibits more ductile behavior than high-strength concrete, as seen in Figure 20 (a,b). The aim of the current practice is to study which factor contributes the most in improving the response of concrete deck to blast. The study compares ductility and strength factors.

5.1.1 Concrete Constitutive Model

ACI '318' (2008) relates the modulus of elasticity E_c , unit weight of concrete ω_c and concrete compressive stress f'_c with the following expression:

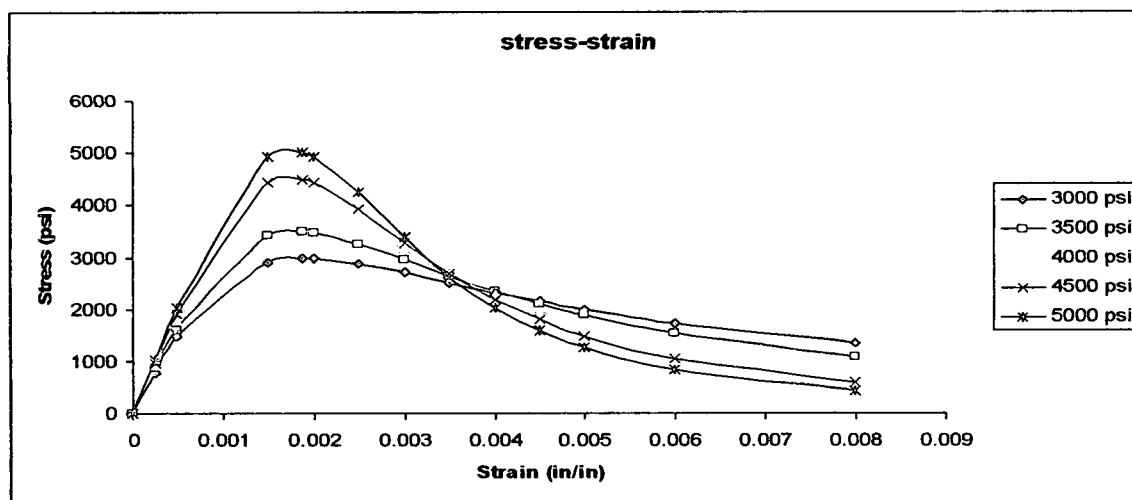
$$E_c = 33 \omega_c^{1.5} \sqrt{f'_c} \quad (5.1)$$

The tensile strength for low and high strength concrete from ACI (2008) is given by

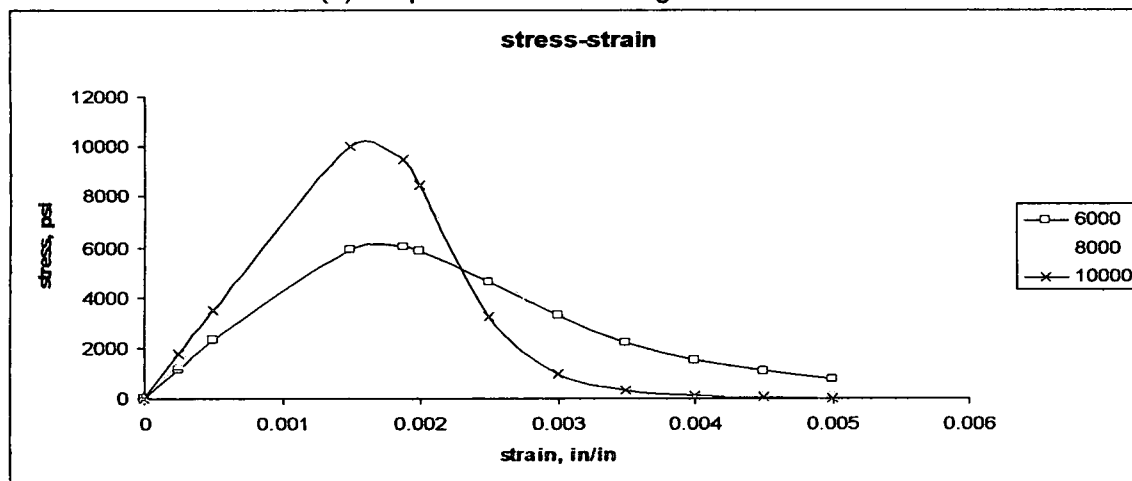
$$f'_t = 6.4 (f'_c)^{1/2} \quad (5.2)$$

$$f'_t = 6.7 (f'_c)^{1/2} \quad (5.3)$$

The stress-strain curve for various models of concrete studied based on expressions 5.1, 5.2, and 5.3 are presented in figure 20 (a,b) and also Table (21) and Table (22) of Appendix (D). The concrete model for low strength concrete is a modified Hognestad* stress-strain curve, and the high strength concrete is Thorenfeldt, Tomaszewicz and Jensen** model. To account for the high rate application of load, the ultimate compressive strain was increased by 15 percent.



(a) Properties of low strength concrete



(b) Properties of high-strength concrete

Figure (20) Concrete stress-strain curves in compression

* ** Reinforced Concrete Mechanics and Design, Fourth Edition, James Macgregor and James Wright

5.1.2 Analysis Methodology

The structural response of a bridge deck to dynamic blast loads is dictated by the following properties:

1. Size of blast load and proximity to deck,
2. Concrete strength and ductility,
3. Yield stress of reinforcing steel.

The effects of concrete strength and ductility on the deck response have been investigated in this section. Concrete decks built of materials that have compressive strength of 3000, 3500, 4000, 4500, 5000, 6000, 8000 and 10,000 psi respectively are considered in this study. The yield stress of the steel girder is kept constant at a value of 50,000 psi. Material properties for the bridge's structural components are similar to those considered in Section (3.3.5) and Section (3.4).

5.1.3 Low Strength Concrete

For low strength concrete, i.e. 3000 through 5000 psi, the analysis is run twice; the first analysis assuming the concrete material has an ultimate crushing strain of 0.003. The second analysis is run for a ductile concrete material that has an ultimate crushing strain of 0.008. The constitutive material properties of low strength concrete are shown in Table (20) and Table (21) of Appendix (D), and the stress-strain curves are shown in Figure (20-a).

5.1.4 High Strength Concrete

High strength concrete is typically used in prestressed concrete structures, but recently there has been an increasing trend to use high strength concrete in deck slabs of composite steel girder bridges. Though there are discussions about the practicality and cost of using high strength concrete deck in non-prestressed

structures, as clarified in FHWA-HRT-05-058⁽²²⁾ study, it is worthy to examine the effect a high strength concrete material may have in improving the structural response of decks to blast loads. Three high strength concretes of 6000, 8000 and 10,000 psi strength have been selected for analysis. The constitutive material property of high strength concrete is illustrated in Table (22) of Appendix (D). The stress-strain curves are shown in Figure 20, b. It is assumed that the maximum stress is reached at a strain value between 0.002 and 0.0025. Ductility is not considered in the analysis, since high strength concrete rarely exhibits ductile behavior compared to low strength concrete, hence the ultimate crushing strain is taken as 0.005 for all high strength concrete.

5.2 Analysis and Results

The bridge was evaluated for a blast load of 500 lb TNT explosive charge detonated at a height of 60 in above the bridge deck at mid-span. The distribution of blast pressure and pressure history profile are shown in Figure (16), Figure (17) and Figure (18), respectively. Structural responses such as deflection, longitudinal stress and strain are obtained at locations loc1, loc2 and loc3 of concrete deck, which are points between girders, as well as on girder1, girder2, and girder3 as seen in Figure (19). The analysis step time is 0.05 sec which is enough to capture structural response due to this blast event. The value of strain, displacement and strain energy are determined for all material models. The results are compared and conclusions are made on how material strength and ductility influence bridge deck resistance to blast load.

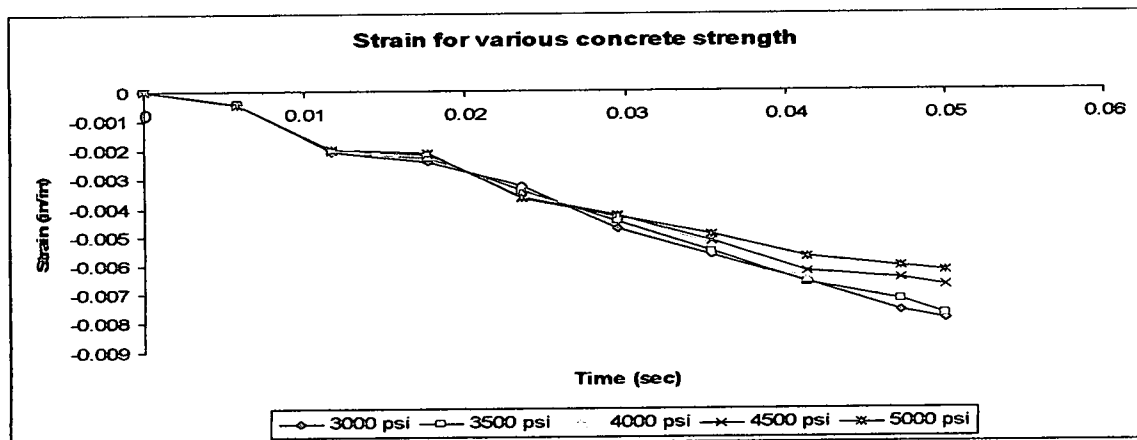
5.2.1 Induced Strain for Low Strength Concrete

Strain values obtained at top surface of the deck are illustrated in Figure (21, a-b) and tabulated in Table (23) and Table (24) in Appendix (D). After 0.05 sec of analysis,

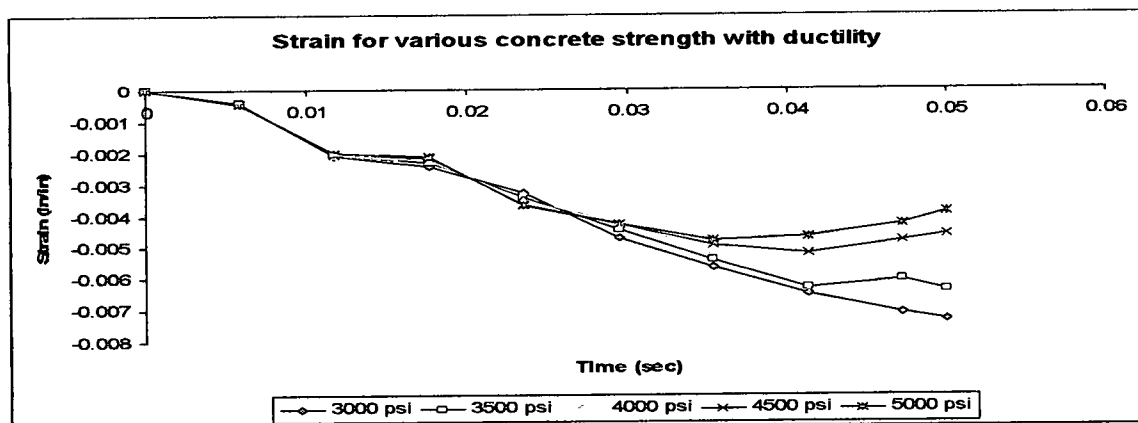
strain values have exceeded the ultimate strain for all five 'low strength' concrete material types. It can deduced that by using 5000 psi concrete the value of strain is reduced by 21 percent compared to using 3000 psi. The value of strain for the four concrete strengths decreased by 2, 6, 15 and 21 percent, respectively, compared to 3000 psi concrete. When the same analyses are repeated, this time assuming a maximum crushing strain of 0.008, all strain values obtained again exceeded 0.002 strain, but did not exceed crushing strain. The decrease in strain in the deck due to added ductility are 7, 17, 19, 22.7, 32 percent, respectively, for all five material strengths compared to one with no ductility. The ductile 5000 psi concrete has a maximum strain of 0.00479 which is 35 percent higher than strain of ductile 3000 psi concrete. Hence it can be concluded that ductility increases the ability of the concrete deck to withstand blast load. It also proves that high strength concrete with ductility yields better results than lower strength concrete with ductility. On other hand, results also show that a ductile 3500 psi concrete performs better than that of 4000 psi and 5000 psi. Also a ductile 4000 psi concrete gives performs better than the 4500 psi and 5000 psi. Hence, low strength concrete gives better structural resistance to blast loads than normal strength concrete.

5.2.2 Induced Strain for High Strength Concrete

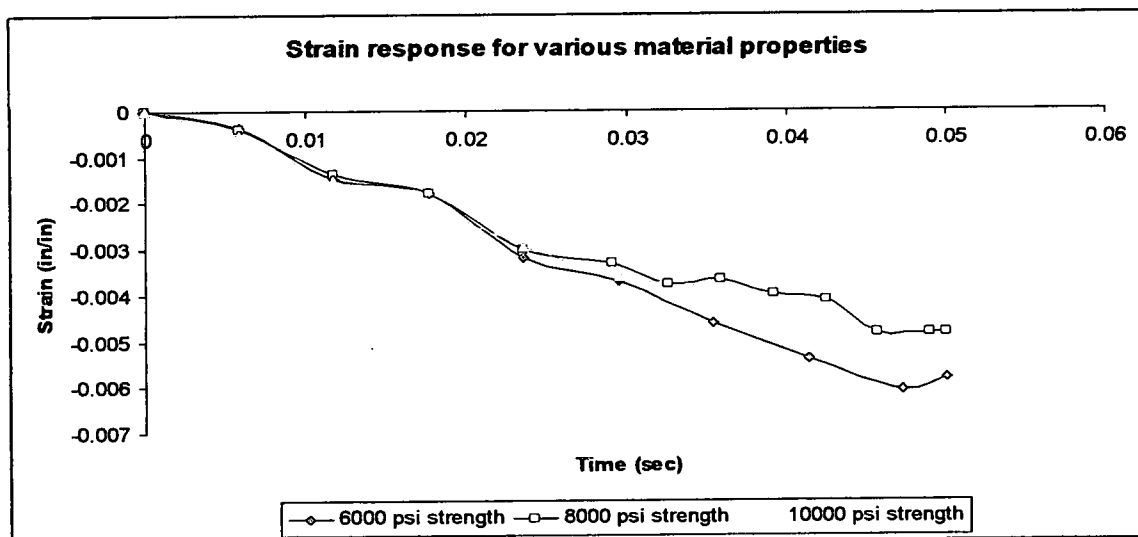
As indicated in Figure 21,c and Table (24) of Appendix (D), the maximum strain for a 6000 psi concrete is 0.00582, which exceeds the maximum allowable strain value of 0.003. The maximum strain for 8000 psi concrete is 0.00487, and for 10000 psi strength concrete is 0.00493. Hence, a deck constructed from the above three materials suffers extensive damage to blast loads unless they have crushing strain capacity of 0.005.



(a) Strain at ultimate crushing strain of 0.003 in/in



(b) Strain at ultimate crushing strain of 0.008



(c) Strain on the concrete deck for high strength concrete

Figure (21) Compressive strain of concrete deck

5.3 EFFECT OF CHARGE SIZES ON BRIDGE DAMAGE

The structural response of the superstructure of the bridge subjected to different blast charges is presented in this section. There are no codes of practice that list possible failure criteria for bridges due to blast loads, hence general failure criteria are proposed for concrete deck and steel girder based on the assumption that failure is the state where the bridge can no longer safely carry design loads.

The bridge model illustrated in Figure (5) and Figure (6) is subjected to various sizes of explosives positioned at a distance of 60 in above the concrete deck. Blast load is distributed on the deck based on the procedure outlined in Section (4.1.2) and (4.1.3). Structural responses of deck and girders (i.e. deflections, longitudinal stresses and strains) are obtained at locations shown in Figure (19). Blast charges for various loading scenarios are listed in Table (3)

Load Scenario	Charge Size
Scenario 1	0.5N-lb
Scenario 2	1N-lb
Scenario 3	2N-lb
Scenario 4	3N-lb
Scenario 5	4N-lb

Table (3) Charge Sizes

5.3.1 Failure Criteria

The structural response of a bridge's superstructure subjected to blast load determines whether the bridge will safely resist blast effect or fail. Though the main concept of safety is that the bridge should continue to function satisfactorily after explosion occurs, a degree of damage will be inflicted on the bridge due to any explosion event.

There is no unified established definition of damage in structural engineering. All structures vary in importance and strength, hence, the level of 'acceptable' damage varies too. In this thesis damage is defined as change(s) that occur(s) to the structural

system and permanently impairs its ability to perform its designed function currently or in the future. Damage is better perceived by comparing two different states, i.e. one before changes occurs and one after changes. The Center for Infrastructure Engineering Studies explains that damage is "the change to material and/or geometric properties of the system including changes to boundary conditions. Abolhassan et-al⁽⁹⁾, in a study of bridges subjected to blast loads, explained that damage to gravity load-carrying members should be minor, and not jeopardize the ability of structures to carry design loads after explosion, and added that progressive collapse of the bridge should not be allowed. The study concluded that ductility of materials contributes more than strength in resisting blast loads.

Winget⁽⁸⁾ is very specific in defining damage concept of bridges due to blast. He concluded that damage should be confined to local deck failure, and allowable 5 percent deflection to span length ratio for girders in case of small bomb sizes, and 12 percent maximum deflection to length ratio for large loads sizes.

The basic concept of failure due to an extreme event is to prevent the bridge from losing its structural integrity and its ability to perform its designed duty. The Federal Department of Transportation (FDOT) has no definite provision for failure due to blast loads, hence failure criteria for girders and decks can be assumed as explained in the following sections.

5.3.1.2 Steel Girder

The structural integrity of bridges can be assessed based on the flexural behavior of girders. The higher the flexural capacity of girders, the more strain energy created to absorb the kinetic energy of blast loads. Hence deflection can be a good indicator of failure. Based on the static analysis conducted on girders, Appendix (A-4), a steel girder section starts to yield when it deflects 3.27 in ($L/360$), and reaches a full plastic strength when it deflects downwards by 13.105 in. These values are used as baseline

values to determine damage levels at girders. The highly dynamic and impulsive nature of blast load may also have a direct and localized impact on parts of girders. In ABAQUS, Von Mises stress gives an instantaneous response of local elements and potential of metals to yield. Effective plastic strain gives the cumulative effect of structural behavior due to applied loading. Hence, failure of steel girders is avoided if deflections, longitudinal stresses and strains at specific locations are within acceptable damage limits specified in Table (4).

Parameter	Damage limit
Deflection	13.105 in
Yield stress	50,000 psi
Plastic hardening stress	60,000 psi
Yield Strain	0.00172
Plastic hardening strain	0.15

Table (4) Damage limit of steel girders

5.3.1.3 Concrete Deck

Concrete can be damaged through spalling or crushing. Allowable response limits of concrete deck are shown in Table (5). A static analysis conducted on concrete deck with steel reinforcement, Appendix (A-4), revealed that the deck spalls when it deflects by 3.079 in and crushes when it deflects by 10.47 in. Also, the same analysis indicated that rebar yields when the deck deflects by 2.56 in and ruptures when it deflects by 12.28 in. Hence, deflection criterion is used as a damage index in this study. All structural members that have response higher than the allowable values are removed in visualization results of ABAQUS.

5.3.1.4 Repairable and Irreparable Damage

The Applied Technology Council⁽²²⁾ listed three levels of damage for deck:

1. Minimal damage: flexural cracking of concrete members while there is no plastic deformation.

2. Repairable Damage: Inelastic response in concrete members coupled with yielding of reinforcement and spalling of cover concrete. Rehabilitation of damage should be done without replacing of concrete members or reinforcements.
3. Significant Damage: Comprises cracking, major spalling, crushing of concrete, and yielding of reinforcement. Repair requires partial or complete replacement of members.

Based on the above definition, minimal and repairable damage represents a tolerable extent of damage, while significant damage is considered a structural failure. In this study, a significant damage to two-third area of the concrete deck is sufficient to put the bridge out of service for an extended period of time.

Parameter	Damage limit
Ultimate stress	5,000 psi
Ultimate Strain (%)	0.003
Spall strain (%)	0.007
Crushing strain (%)	0.012

Table (5) Allowable compressive strains of concrete deck

5.4 Blast Analysis

The bridge deck is subjected to blast loads listed in Table (3). Structural response such as deflection, stresses and strains at locations shown in Figure (19) are computed and compared to damage criteria shown in Table (4) and Table (5) for girders and decks respectively. Evaluations of results determine the level of damage as outlined in section (5.3.1.2) and (5.3.1.4).

5.4.1 Scenario (1) 0.5N-lb Blast Load

The bridge deck is subjected to 0.5N-lb blast load at a distance of 5 ft above the bridge's deck. The distribution of blast load is described in Section (4.1.3) and Appendix (C).

5.4.1.1 Structural response of deck and girder

Figure (22) through Figure (25) shows deflections, plastic strains and stresses in concrete deck, rebar and steel girders.

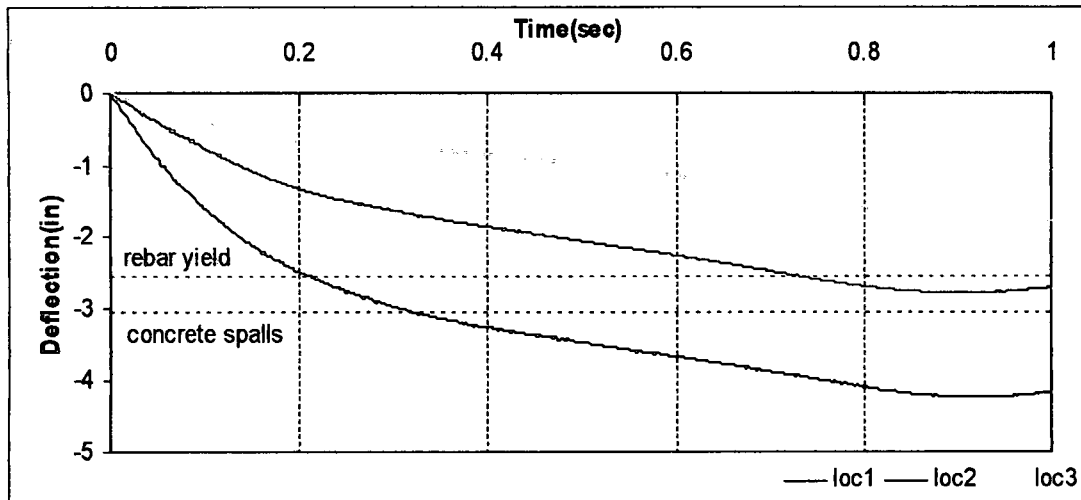
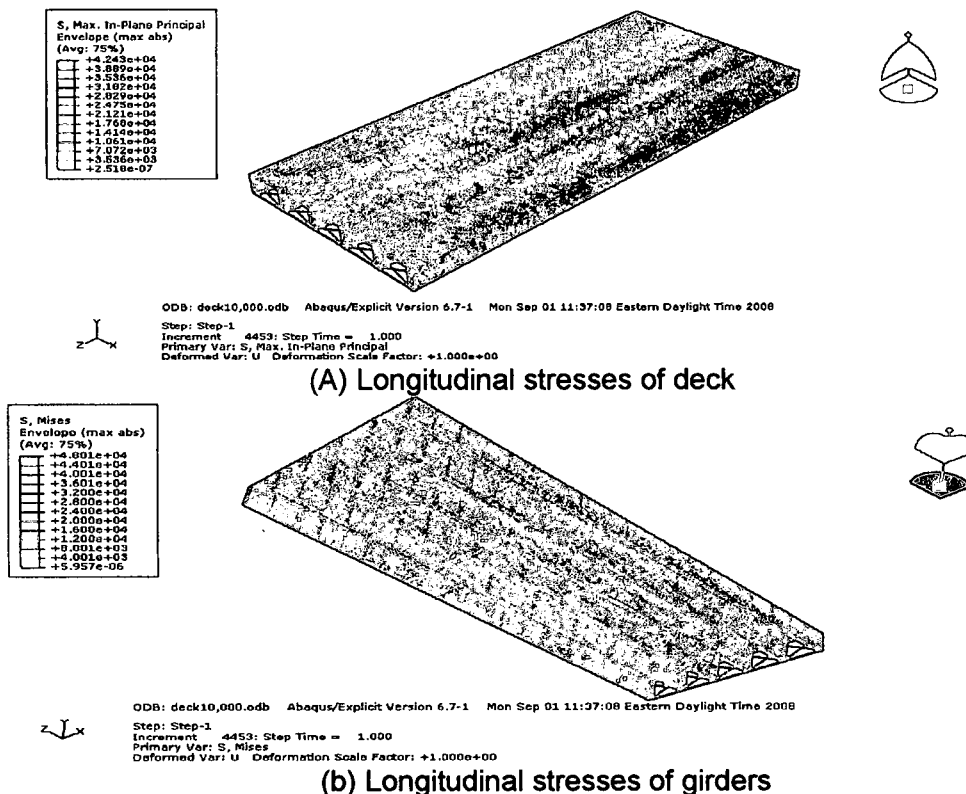


Figure (22) Deflection of deck due to 0.5N-lb blast load



(b) Longitudinal stresses of girders
Figure (23) Damage due to 0.5N-lb blast load

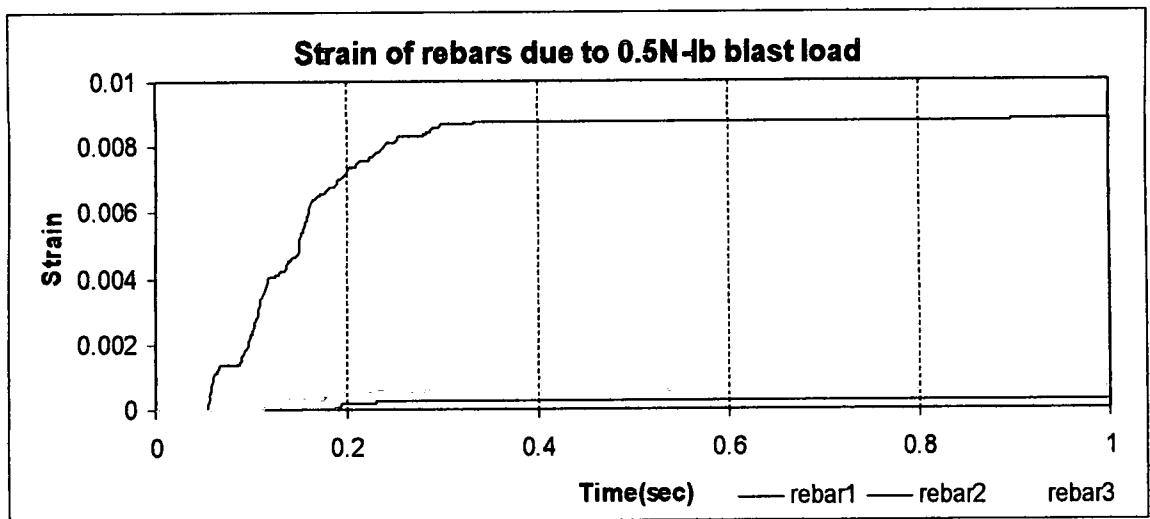
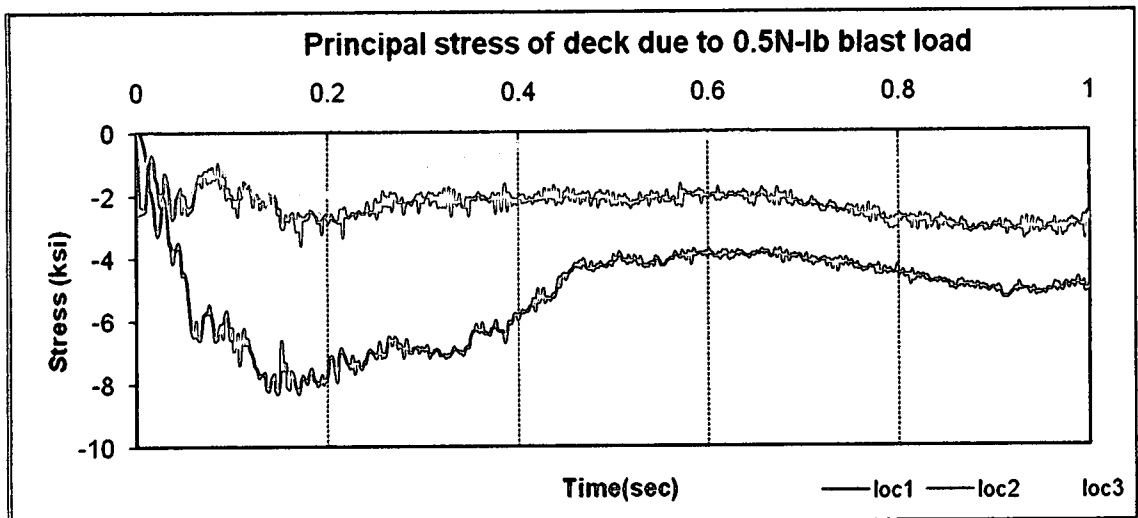
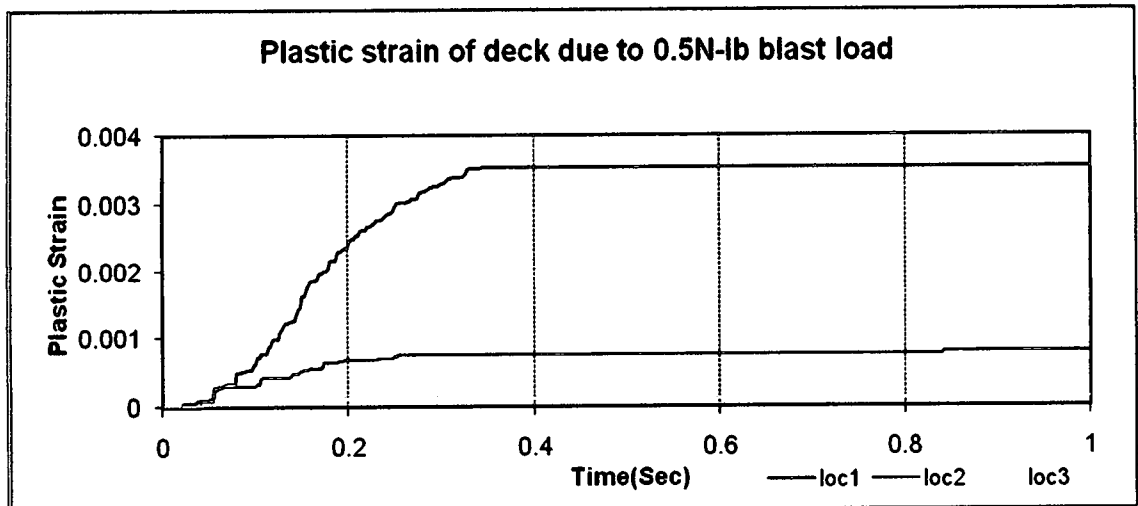


Figure (24) longitudinal stress and strain of deck and rebar due to 0.5N-lb blast load

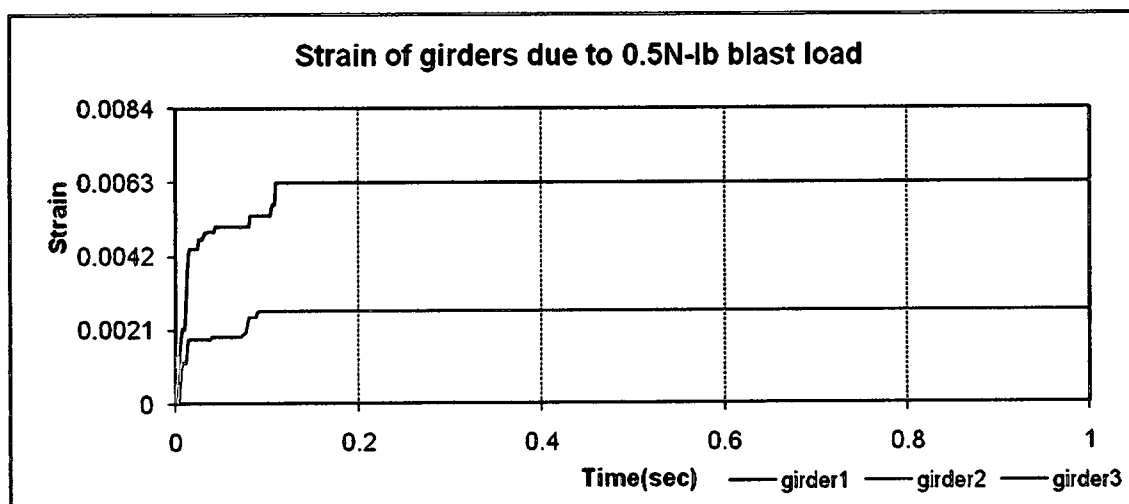
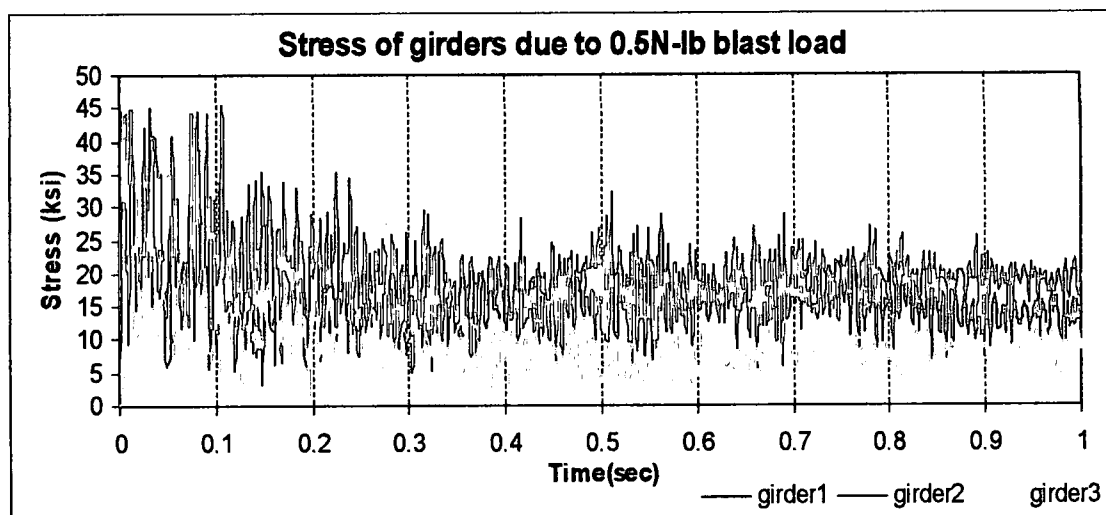
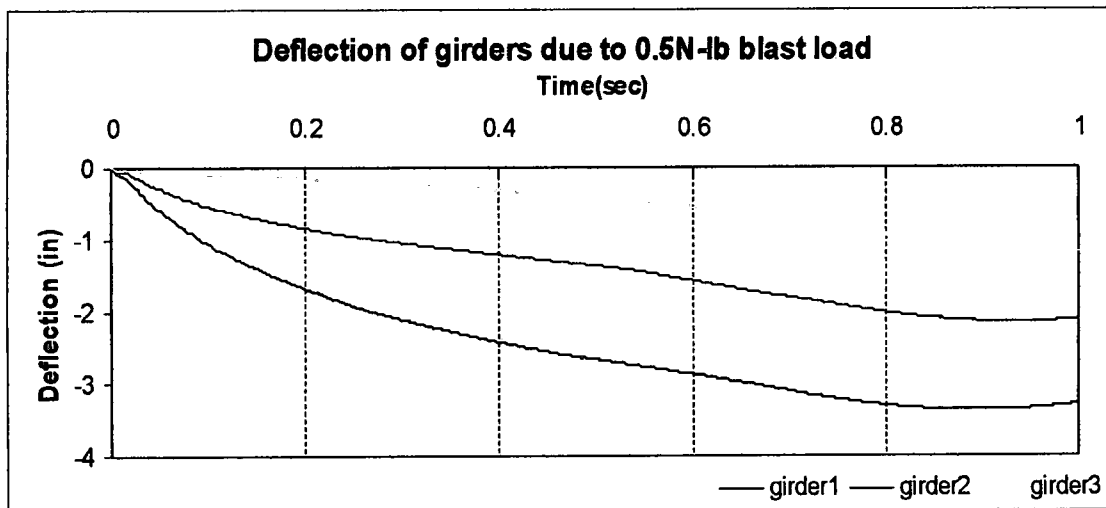


Figure (25) Deflections, longitudinal stresses and strains at girders due to 0.5N-lb blast load

5.4.4.2 Results

Deck: Table (6) and Figure (22-24) show that deflection of the concrete deck at loc1 is 4.17 in, and compressive strain of loc1 reaches yield strain, while rebar has not yielded. Based on this information, loc1 experiences minimal damage. There is no yielding of either steel or concrete in loc2 and loc3, which implies that the concrete deck at both locations experience no damage due to the 0.5N-lb charge size. Hence, with minimal repair to loc1, concrete deck can safely carry blast load of 0.5N-lb without affecting the structural stability and daily function.

Girder: As seen in Table (6) and Figure (25), a maximum deflection of 3.275 in occurs at girder1 which is equal to the allowable serviceability deflection of $L/360$. Longitudinal stress and strain have values less than plastic strain damage; as a result the girder is stable to carry design loads after 0.5N-lb blast load.

Charge Size 0.5N-lb	Parameter		Loc1		Loc2		Loc3	
			Deck	Rebar1	Deck	Rebar2	Deck	Rebar3
	Deflection	in	4.17	-	2.72	-	1.76	-
	Strain	-	0.0035	0.0088	0.0008	0.0003	0.00013	0.00065
	Stress	psi	8298	45904	3596	43566	2734	43673
	Failure		No	No	No	No	No	No
	Parameter		Girder1		Girder2		Girder3	
	Deflection	in	3.275		2.123		1.170	
	Strain	-	0.0063		0.00261		.1.10E-6	
	Stress	psi	45049		44210		4.263	
	Failure		No		No		No	

Table (6) Summary of structural response of girders

5.4.2. Scenario (2) 1N-lb Blast Load

The structural response of the bridge to 1N-lb blast at a distant of 5 ft above the deck is given in Figure (26) through Figure (29) which are deflection, longitudinal strains and stresses in concrete deck, rebar and girders. These responses are compared to damage criteria of Section (5.3.1).

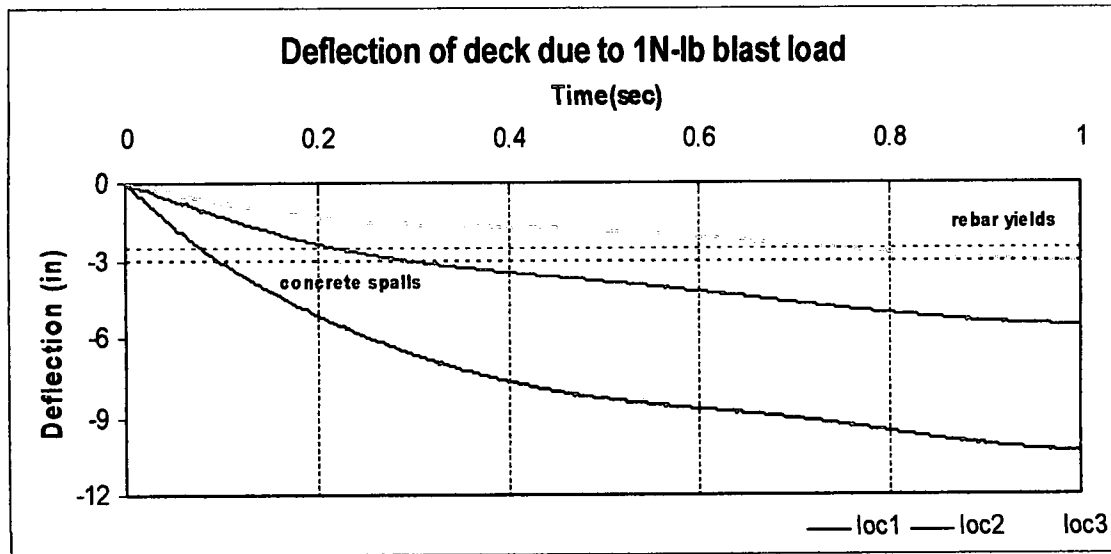
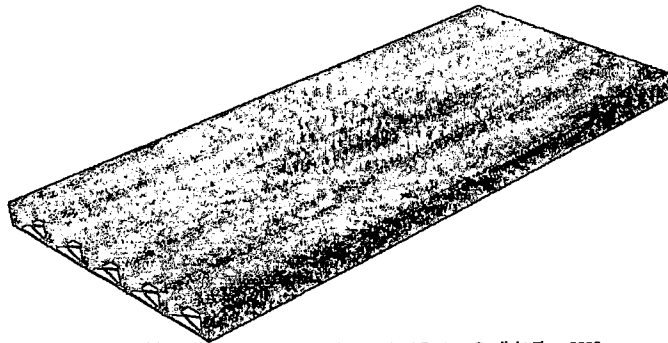
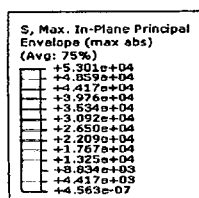


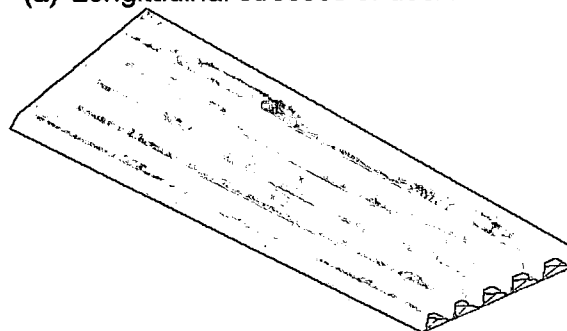
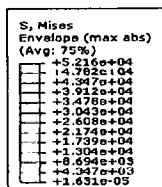
Figure (26) Displacement at concrete deck due to 1N-lb



ODB: 1000deck.odb Abaqus/Explicit Version 6.7-1 Sun Aug 31 11:16:14 Eastern Daylight Time 2008
 Step: Step-1
 Increment 4464: Step Time = 1.000
 Primary Var: S, Max. In-Plane Principal
 Deformed Var: U Deformation Scale Factor: +1.000e+00



(a) Longitudinal stresses of deck.



ODB: 1000deck.odb Abaqus/Explicit Version 6.7-1 Sun Aug 31 11:16:14 Eastern Daylight Time 2008
 Step: Step-1
 Increment 4464: Step Time = 1.000
 Primary Var: S, Mises
 Deformed Var: U Deformation Scale Factor: +1.000e+00



(b) Longitudinal stresses of girders

Figure (27) Damage due to 1N-lb blast load

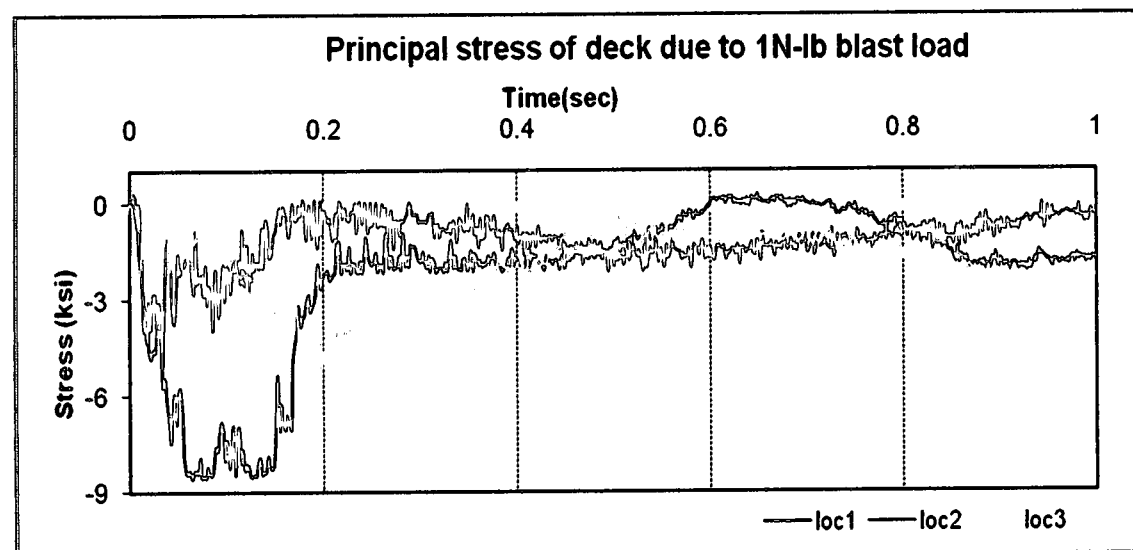
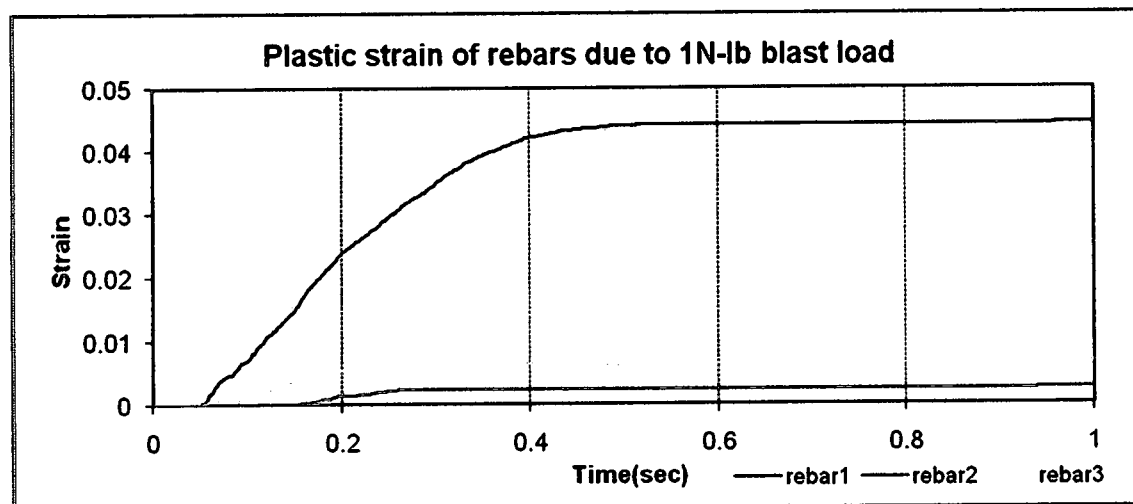
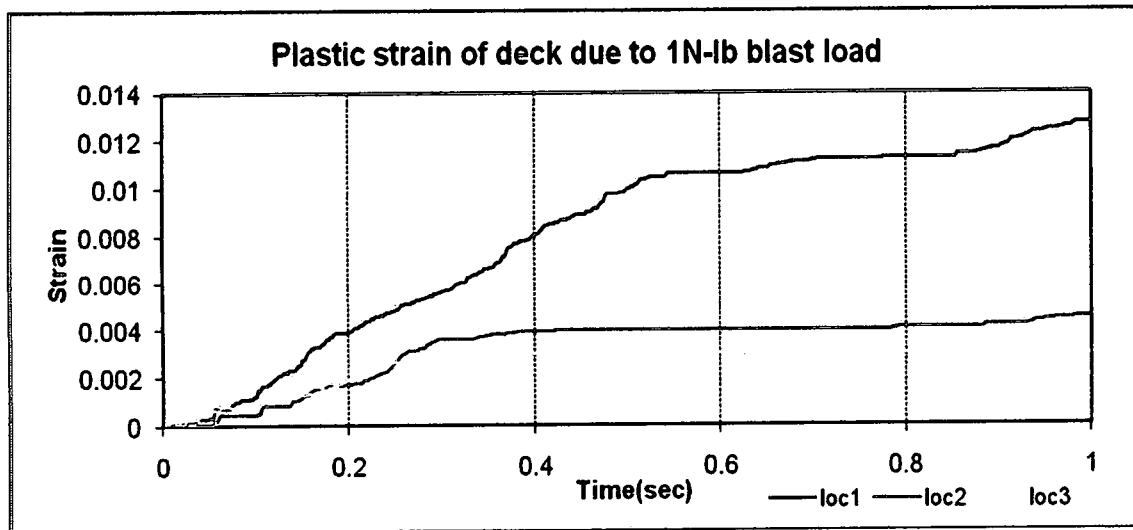


Figure (28) longitudinal stress and strain of deck and rebar due to 1N-lb blast load

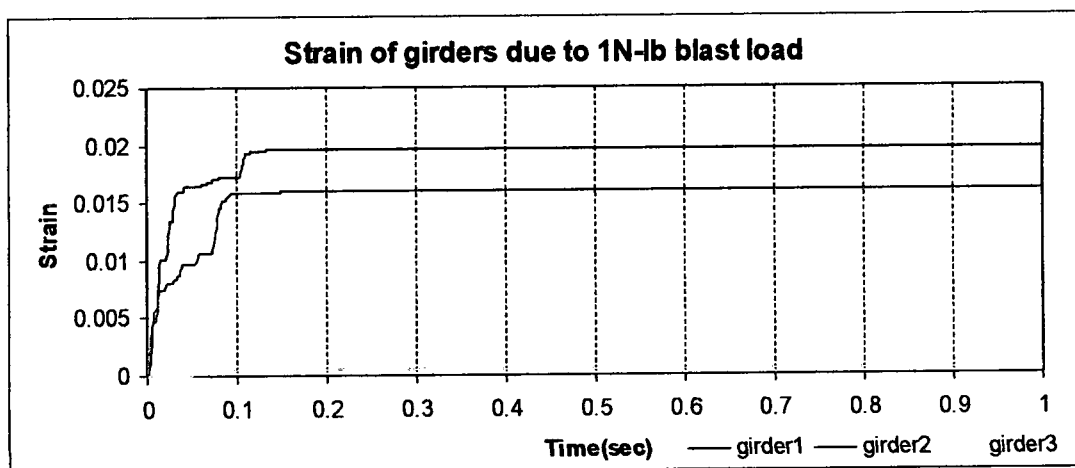
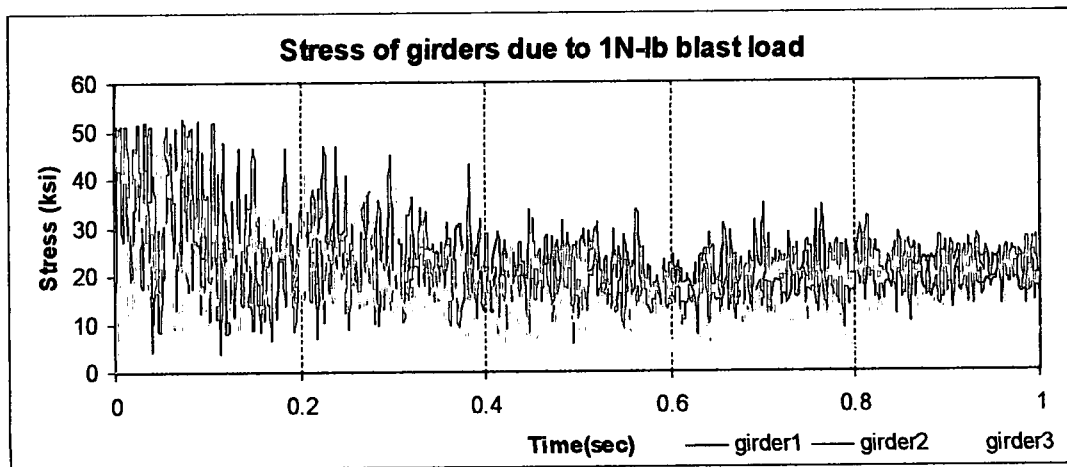
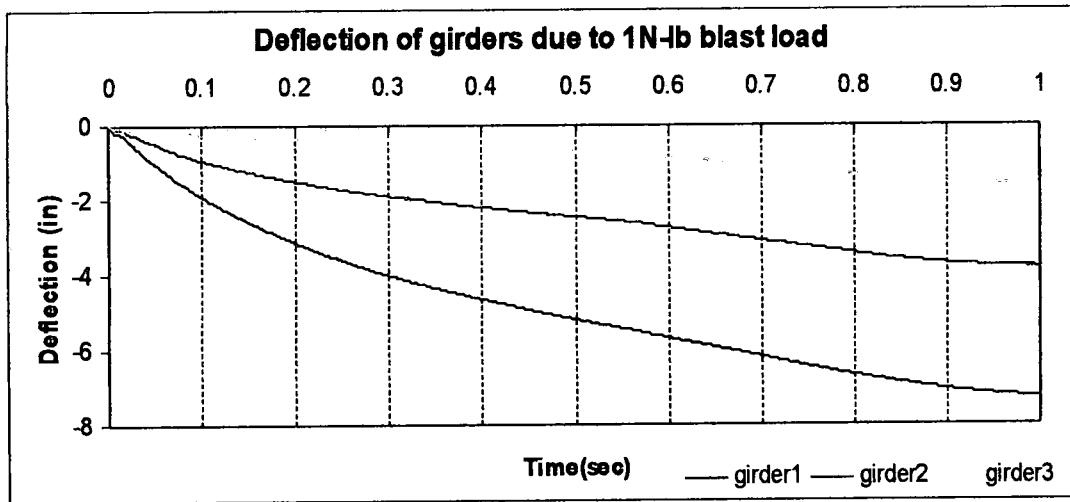


Figure (29) Deflections, longitudinal stresses and strains at girders due to 1N-lb blast load

5.4.2.3 Results of 1N-lb

Deck: Results indicate that the concrete deck at loc1 crushes accompanied by yielding of rebar1. Loc2 has strain value exceeding yield strain. Based on analysis results and damage criteria, loc1 sustains significant damage and would need to be replaced. Damage at loc2 and loc3 is considered minimal damage because rebar in both locations have not yielded.

Girders: Analysis shows that principal stress exceeds yield stress of 50 ksi with strain levels exceeding yield strain in girder1 and girder2 but less than plastic strain hardening. Deflection in girder1 is 7.265 in which exceeds serviceability static deflection of L/360, but less than assumed damage criterion of 13.105 in; as a result both girder2 and girder3 will continue to perform satisfactorily after 1N-lb blast load, while more investigation is required to assess girder1 structural damage.

Charge Size 1N-lb	Parameter		Loc1		Loc2		Loc3	
			Deck	Rebar1	Deck	Rebar2	Deck	Rebar3
	Deflection	in	10.33	-	5.57	-	3.03	-
	Strain	-	0.0127	0.0444	0.0045	0.0025	0.0029	0.0065
	Stress	psi	8582	50056	5114	50237	5198	5062
	Failure		Yes	Yes	No	No	No	No
	Parameter		Girder1		Girder2		Girder3	
	Deflection	in	7.265		3.82		1.61	
	Strain	-	0.0196		0.01596		0.000464	
	Stress	psi	51765		51501		49944	
	Failure		No		No		No	

Table (7) Structural response of steel girder to 1N-lb blast load

5.4.3 Scenario (3) 2N-lb Blast Load

The structural response of the bridge deck and girders to a 2N-lb blast load (deflections, stresses and strains) is presented in Figure (30) through Figure (33).

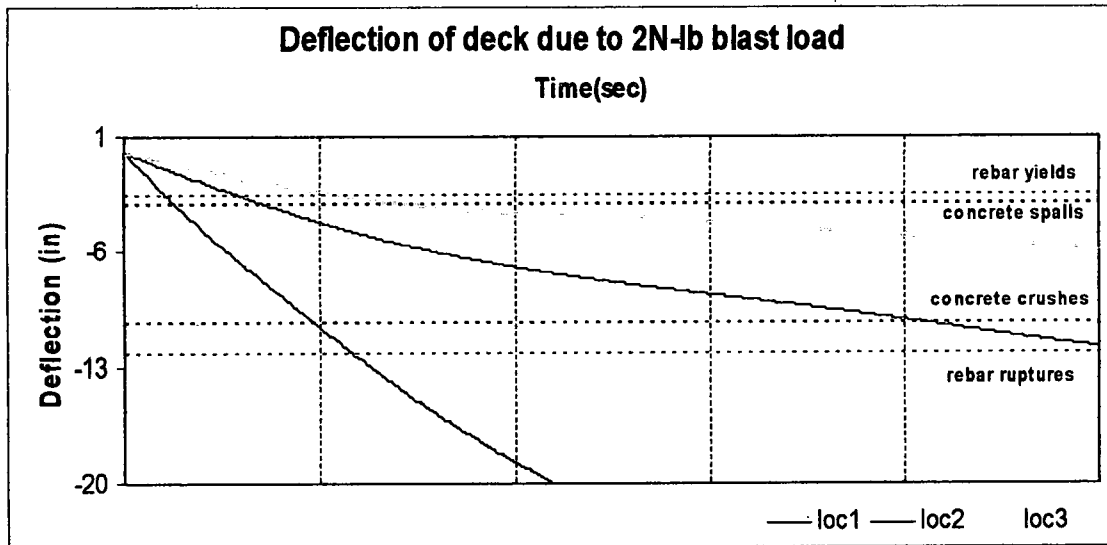
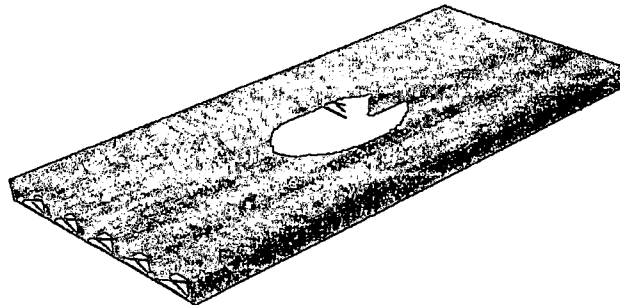
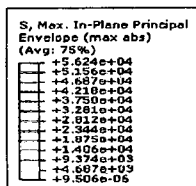
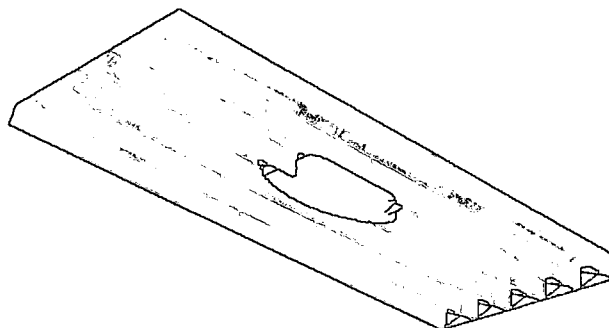
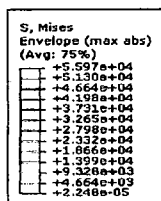


Figure (30) Displacement of deck due to 2N-lb blast load



ODB: 2000deck.odb Abaqus/Explicit Version 6.7-1 Sun Aug 31 13:39:10 Eastern Daylight Time 2008
 Step: Step-1
 Increment: 4489; Step Time = 1.000
 Primary Var: S, Max. In-Plane Principal
 Deformed Var: U Deformation Scale Factor: +1.000e+00

(A) Longitudinal stresses of deck



ODB: 2000deck.odb Abaqus/Explicit Version 6.7-1 Sun Aug 31 13:39:10 Eastern Daylight Time 2008
 Step: Step-1
 Increment: 4489; Step Time = 1.000
 Primary Var: S, Mises
 Deformed Var: U Deformation Scale Factor: +1.000e+00

(b) Longitudinal stresses of girders
 Figure (31) Damage due to 2N-lb blast load

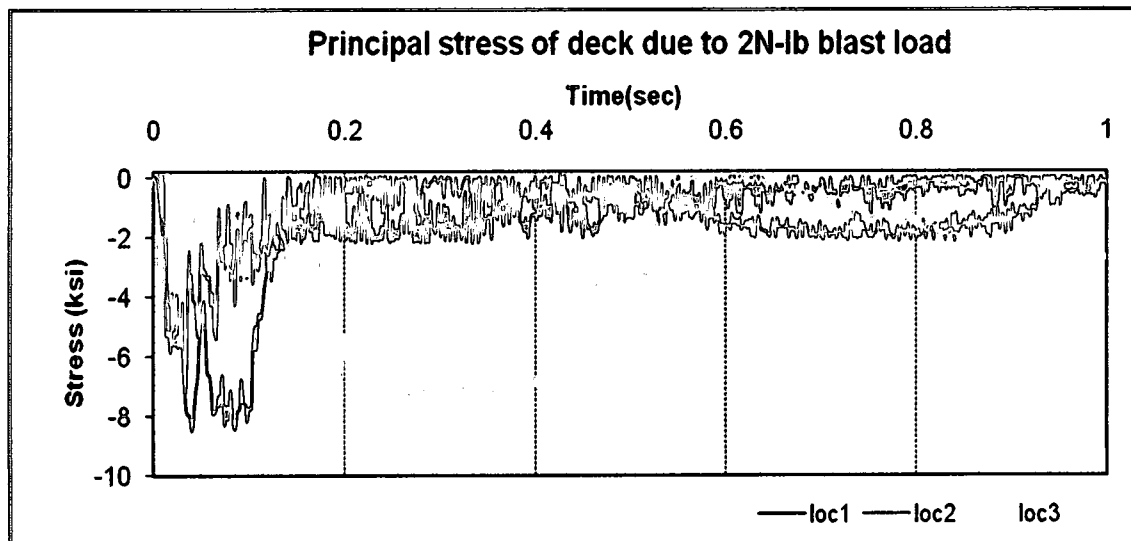
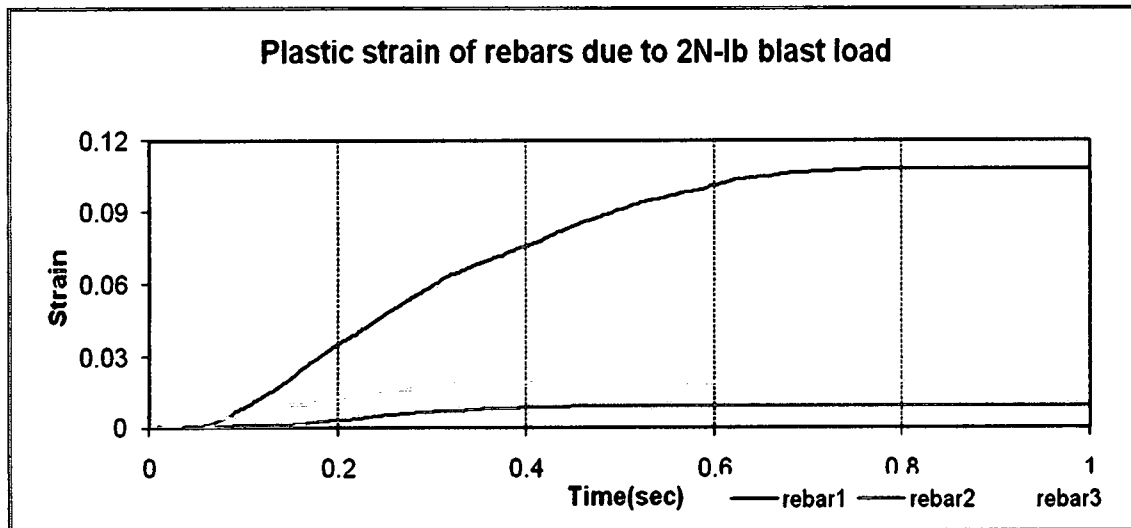
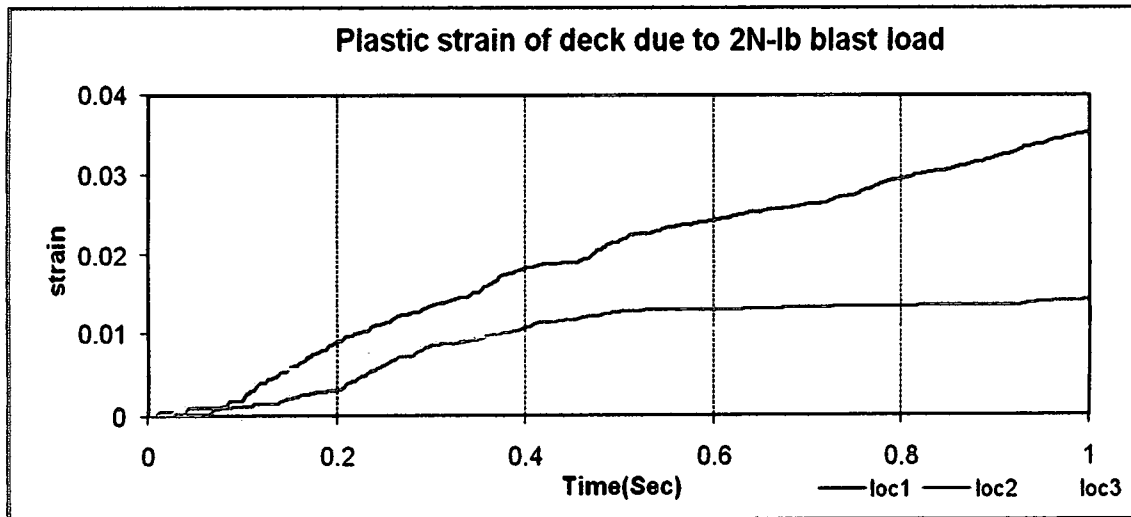


Figure (32) Longitudinal stress and strain of deck and rebar due to 2N-lb blast load

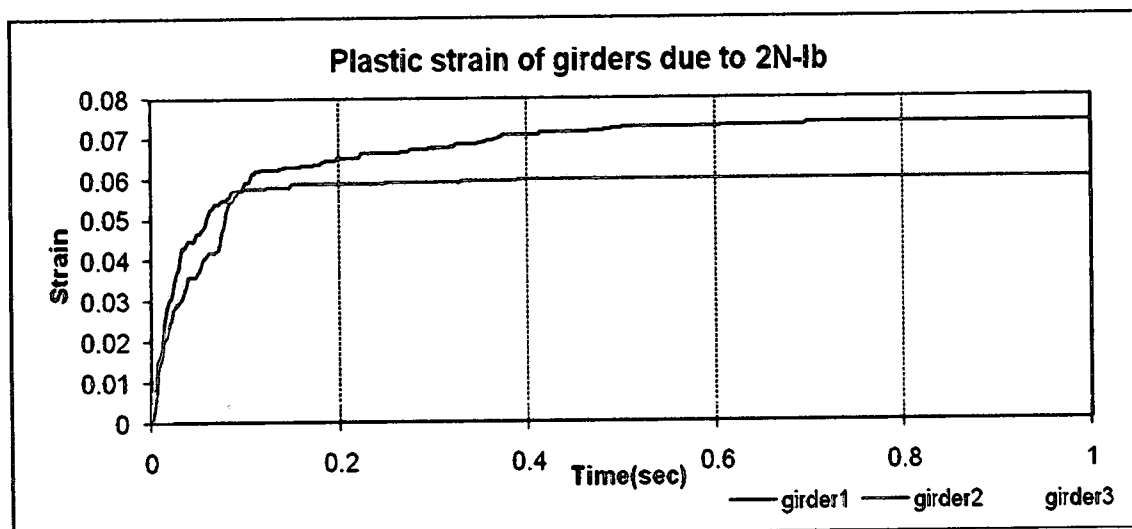
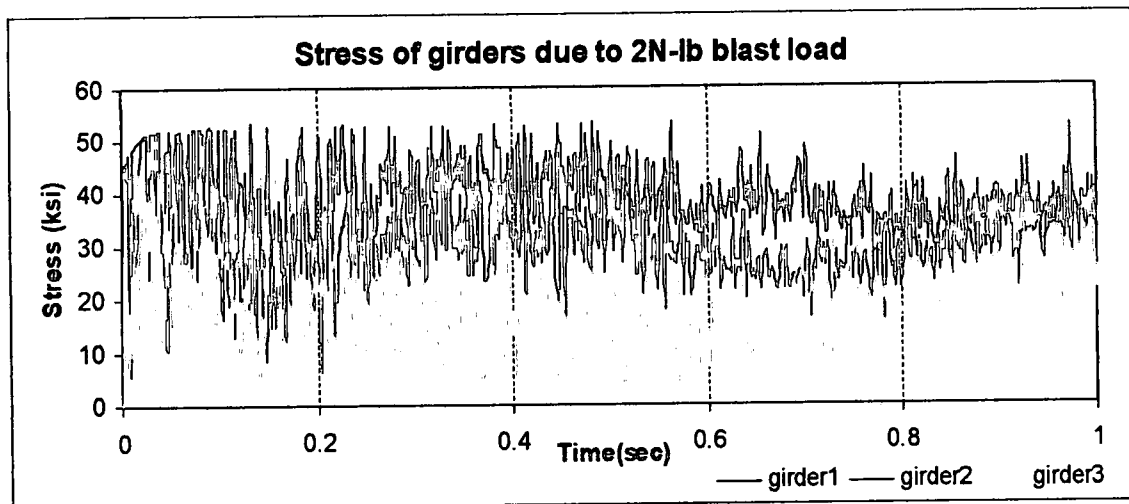
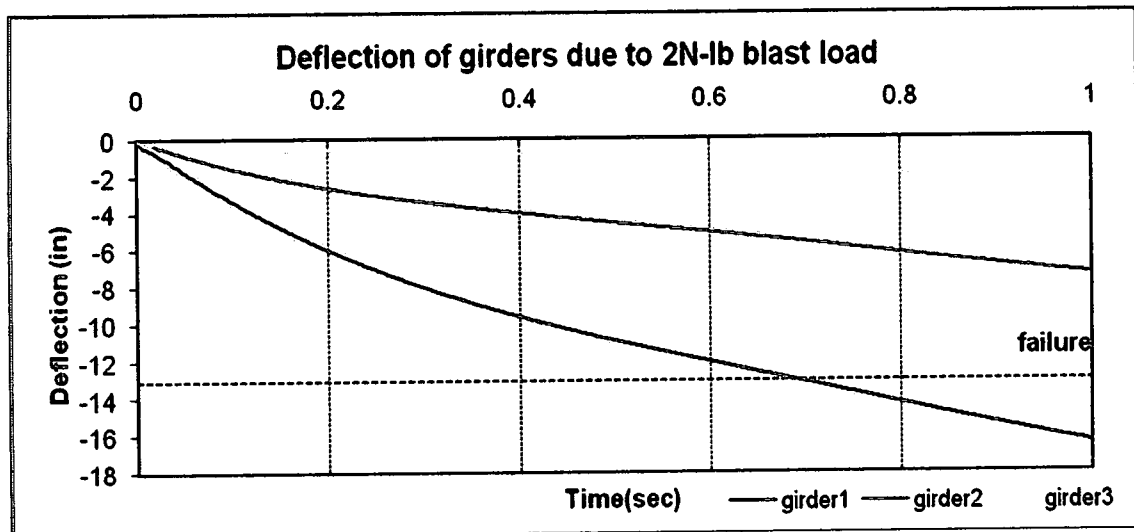


Figure (33) Deflections, longitudinal stresses and strains at girders due to 0.5N-lb blast load

5.4.3.3 Results

Deck: Results in Table (8) reveal that the strain of loc1, loc2 and loc3 is equal to or exceeding crushing strain. Rebar1 and rebar3 have longitudinal strain levels equals to or exceeding yield strain, while that at rebar2 is less than the yielding strain. Hence loc1 suffers a significant damage, loc2 and loc3 both suffer a repairable damage with crushing of concrete.

Girder: In Table (8) deflection of girder1 exceeds the allowable deflection of 13.105 in. Longitudinal strain and stress at girder1 and girder2 exceed yield strain and stress, but less than rupture strain. Hence, based on allowable deflection criterion, girder1 is considered not stable to carry design load after blast load, i.e., it has suffered a significant damage. Girder2 is subjected to further analysis to assess structural stability. Girder3 is safe to carry design load after 2N-lb blast load.

Charge Size 2N-lb	Parameter		Loc1		Loc2		Loc3	
			Deck	Rebar1	Deck	Rebar2	Deck	Rebar3
	Deflection	in	28.89		11.88		5.80	
	Strain	-	0.0353	0.108	0.0144	0.0094	0.01064	0.0190
	Stress	psi	8489	54602	7194	46023	7881	48673
	Failure		Yes	Yes	Yes	No	Yes	No
	Parameter		Girder1		Girder2		Girder3	
	Deflection	in	16.40		7.34		2.404	
	Strain	-	0.074		0.06		0.0046	
	Stress	psi	52948		52427		44359	
	Failure		Yes		No		No	

Table (8) Structural response of steel girder to 2N-lb blast load

5.4.4 Scenario (4) 3N-lb Blast Load

For 3N-lb blast load, Figure (34) through Figure (37) show deflection, longitudinal strain and stresses in concrete deck, rebar and steel girder due to 3N-lb blast load.

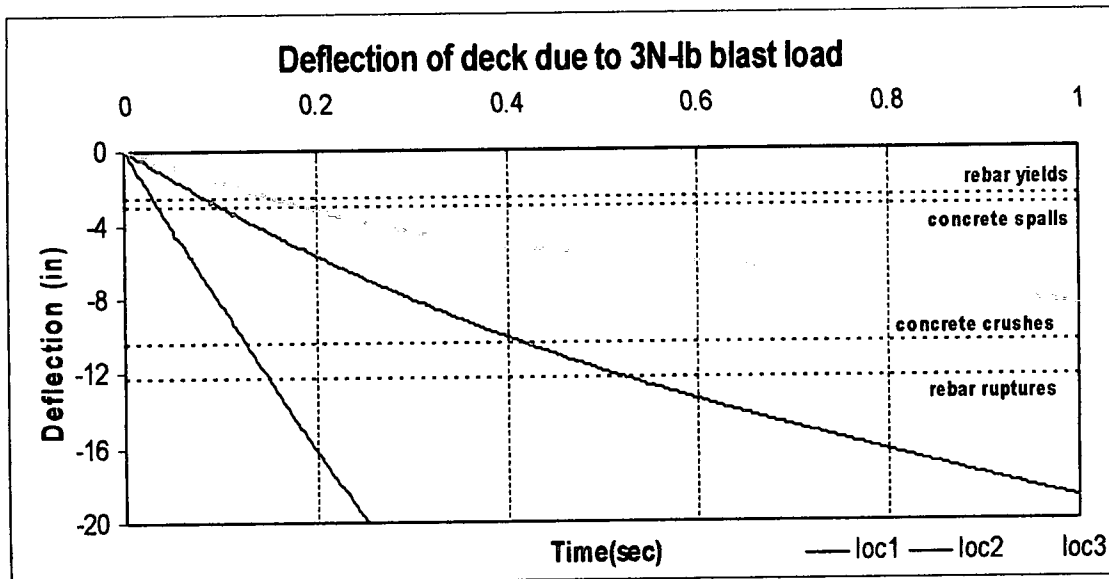
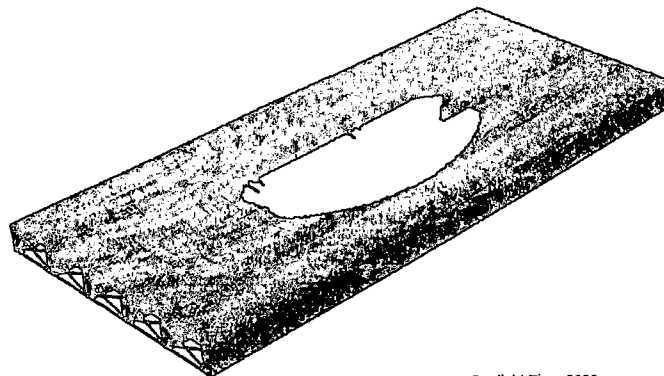
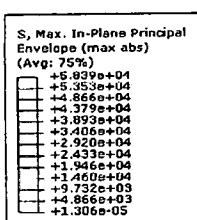


Figure (34) Deflection of deck due to 3N-lb blast load

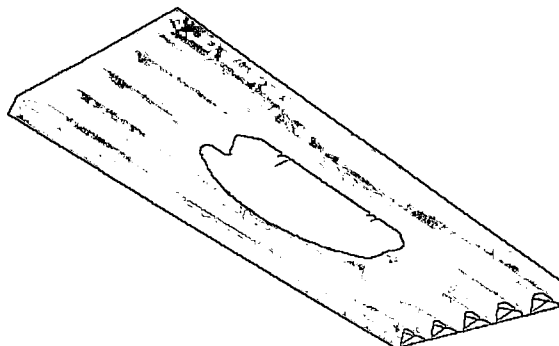
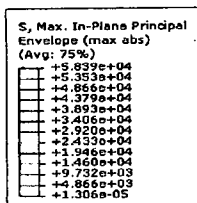


ODB: 3000girder.odb Abaqus/Explicit Version 6.7-1 Sun Aug 31 14:26:00 Eastern Daylight Time 2008



Step: Step-1
Increment 4583: Step Time = 1.000
Primary Var: S, Max. In-Plane Principal
Deformed Var: U Deformation Scale Factor: +1.000e+00

(A) Longitudinal stresses of deck



ODB: 3000girder.odb Abaqus/Explicit Version 6.7-1 Sun Aug 31 14:26:00 Eastern Daylight Time 2008



Step: Step-1
Increment 4583: Step Time = 1.000
Primary Var: S, Max. In-Plane Principal
Deformed Var: U Deformation Scale Factor: +1.000e+00

(b) Longitudinal stresses of girders

Figure (35) Damage due to 3N-lb blast load

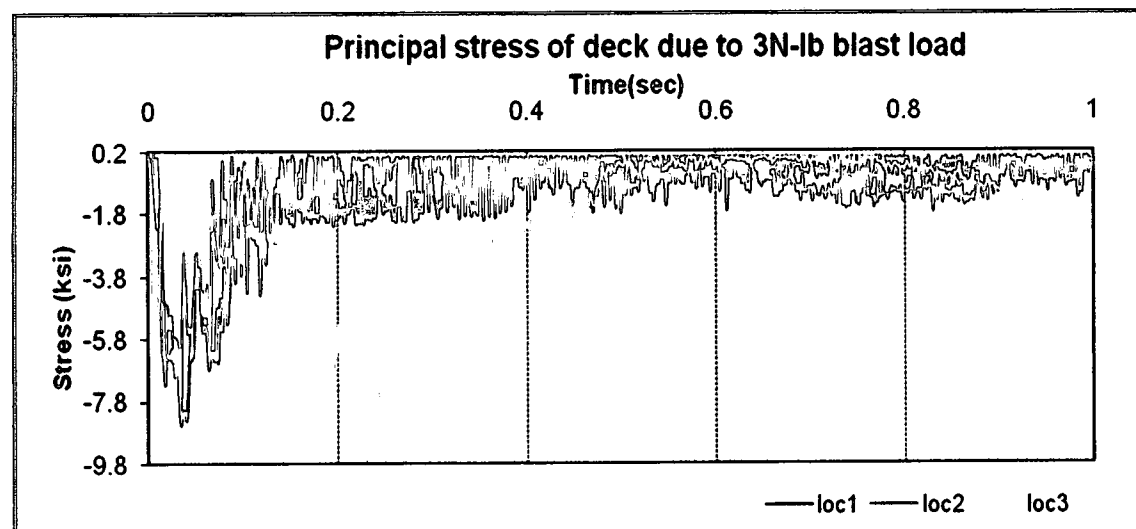
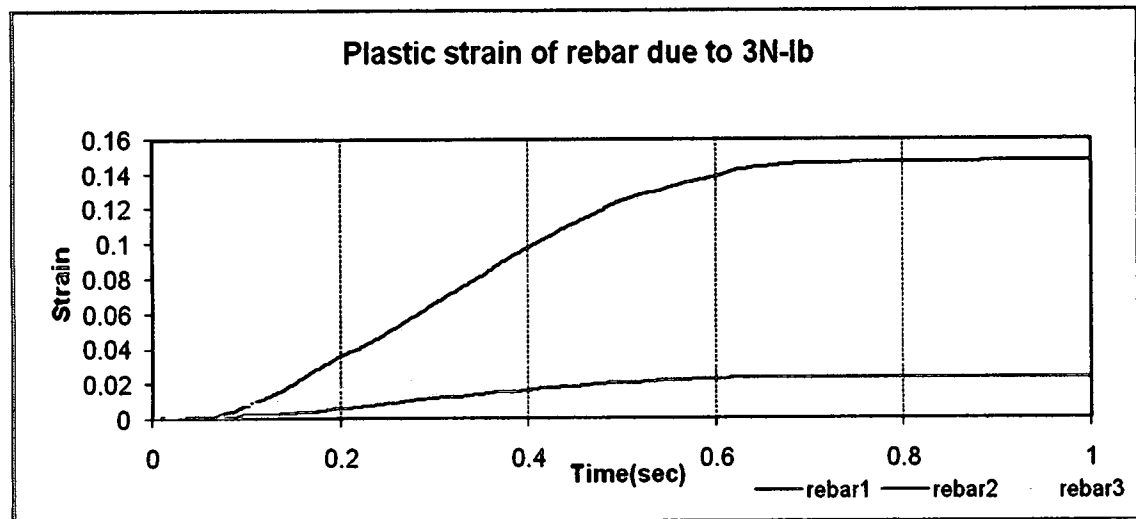
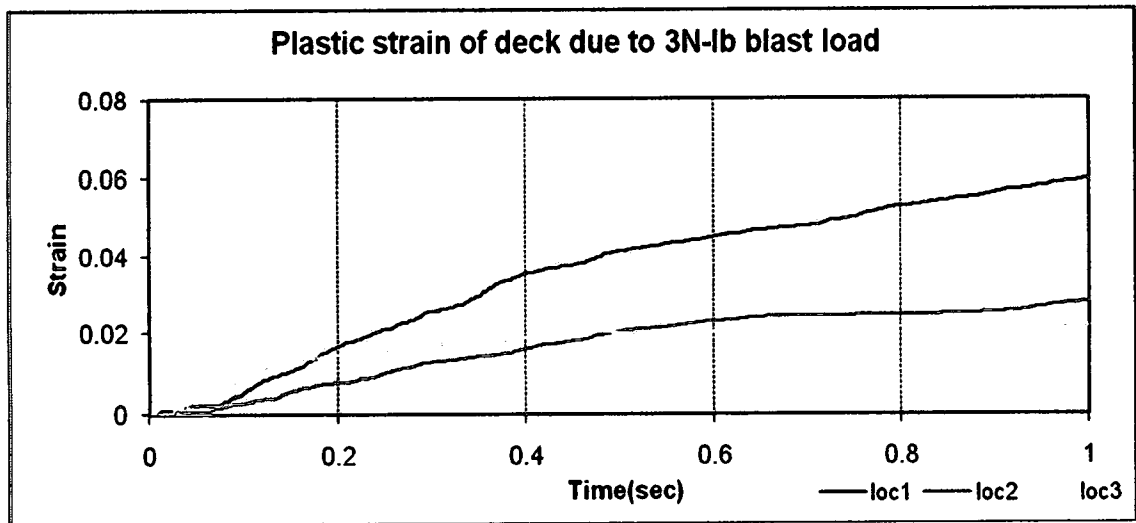


Figure (36) longitudinal stress and strain of deck and rebar due to 3N-lb blast load

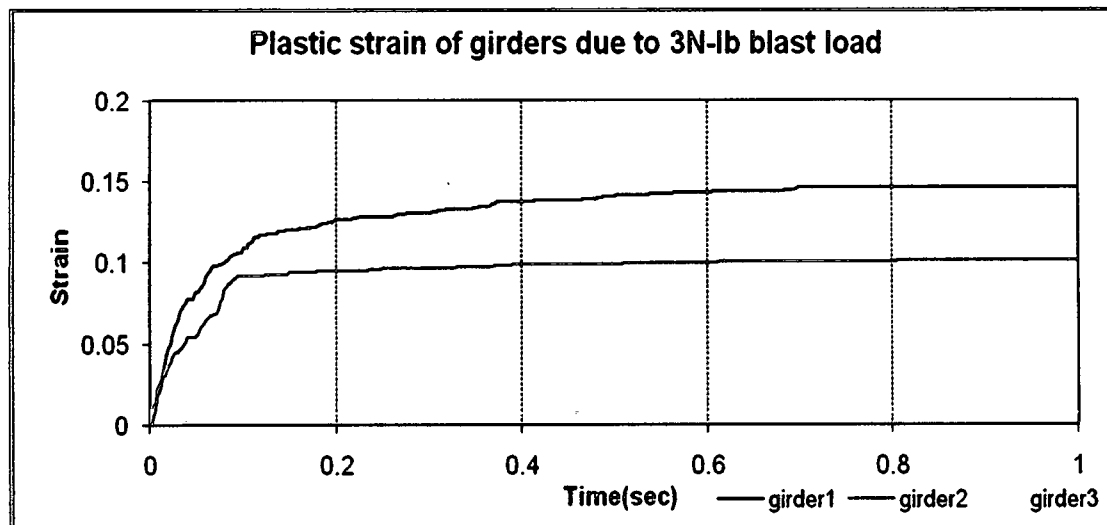
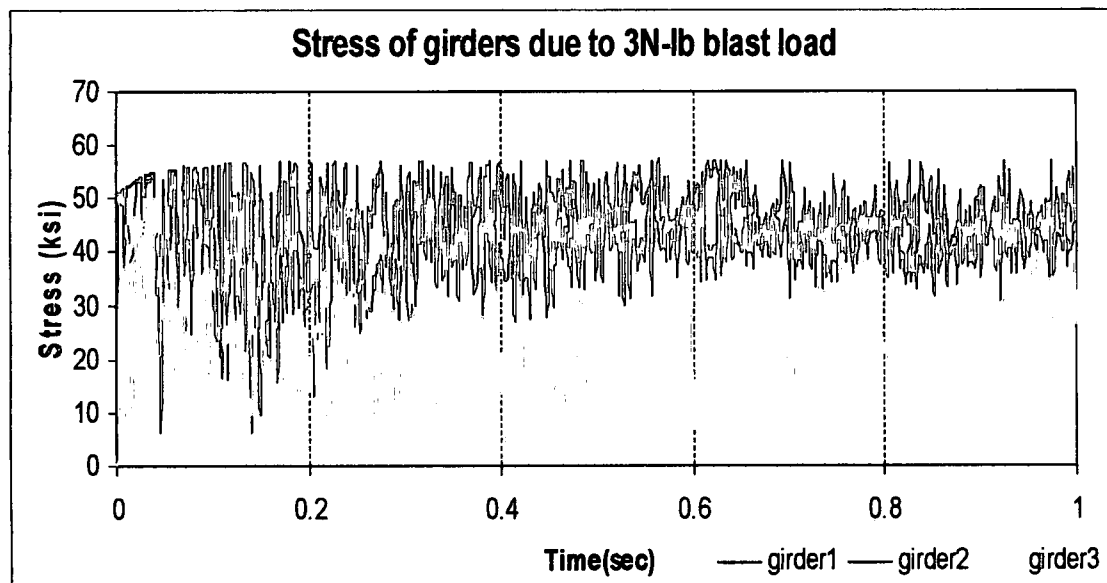
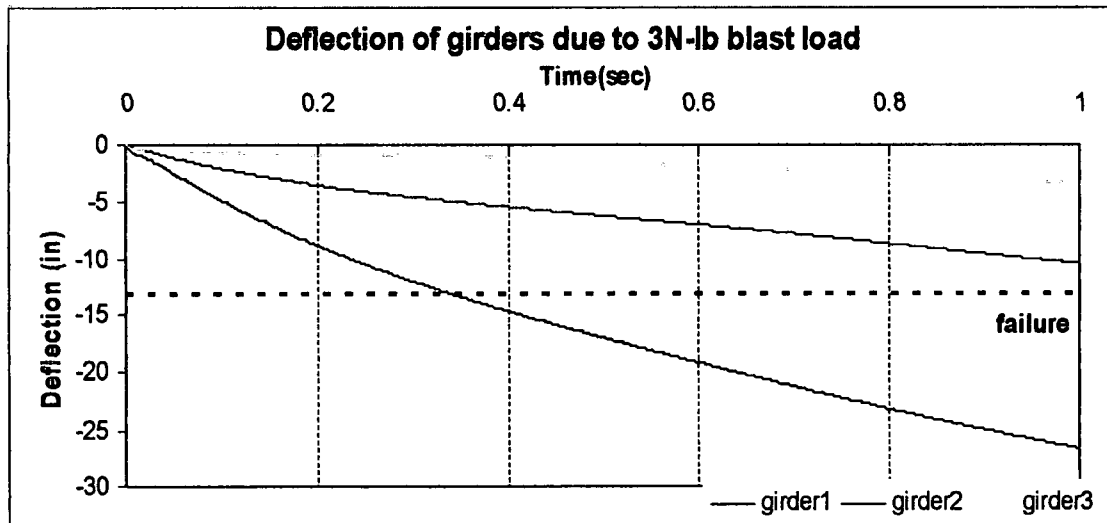


Figure (37) Deflections, longitudinal stresses and strains at girders due to 3N-lb blast load

5.4.3.3 Results

Deck: Results in Table (9) show that strain of loc1, loc2, loc3, rebar1, rebar2, rebar3 all exceeding crushing strains and yield strain, respectively. The deflection of loc1, loc2 and loc3 is 46.31in, 18.80 in and 8.50 in respectively, indicating that the concrete has already crushed. Hence, the plastic response of the concrete at all locations coupled with yielding of rebars and excessive deflection, classifies the damage as a significant damage. This implies that a charge size of 3N-lb will significantly damaged the concrete deck, making it unsafe for daily use.

Girder: Table (9) shows that the deflection of girder1 exceeds 13.105 in, deflection that causes significant damage. The longitudinal strain of girder1 is approximately equals to plastic strain hardening, while strain at girder2 is significantly greater than the yield strain. The value of stresses at all girders exceeds the yield stress. Due to excess deformation, girder1 is considered not stable to carry design load after blast load, i.e. has suffered a significant damage. Girder2 is subjected to further study in section (5.7.2) to assess its structural stability. Girder3 is considered safe to resist 3N-lb blast load.

Charge Size 3N-lb	Parameter		Loc1		Loc2		Loc3	
			Deck	Rebar1	Deck	Rebar2	Deck	Rebar3
	Deflection	in	46.31	-	18.80	-	8.498	-
	Strain	-	0.060	0.147	0.028	0.023	0.0214	0.032
	Stress	psi	8530	57591	8322	52232	7938	52824
	Failure		Yes	Yes	Yes	Yes	Yes	Yes
	Parameter		Girder1		Girder2		Girder3	
	Deflection	in	26.66		10.504		3.448	
	Strain	-	0.147		0.101		0.0077	
	Stress	psi	57209		56179		50693	
	Failure		Yes		No		No	

Table (9) Structural response of bridge to 3N-lb blast load

5.4.4 Scenario (5) 4N-lb Blast Load

The structural response of the deck and girders to 4N-lb blast load is presented in Figure (38) through Figure (41).

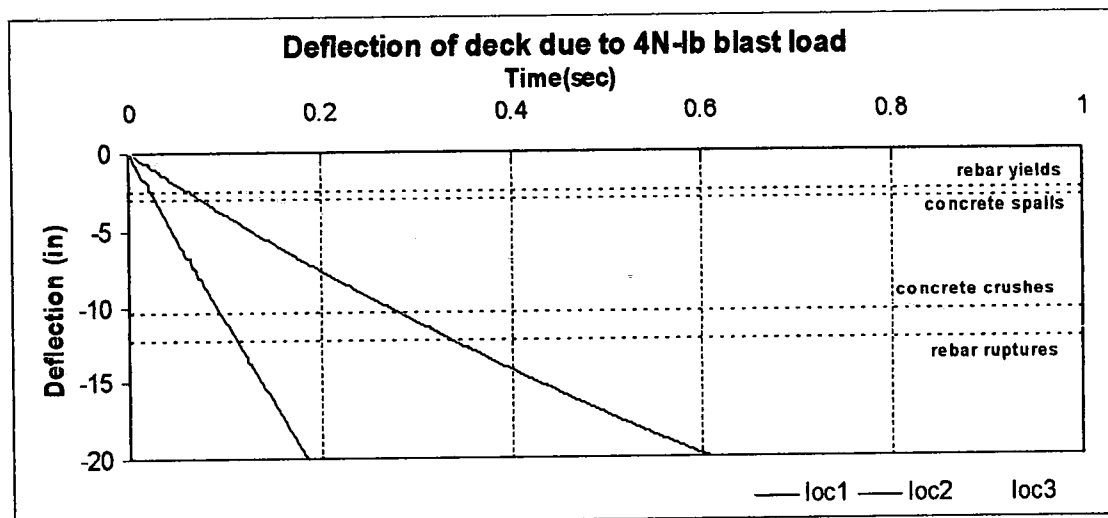
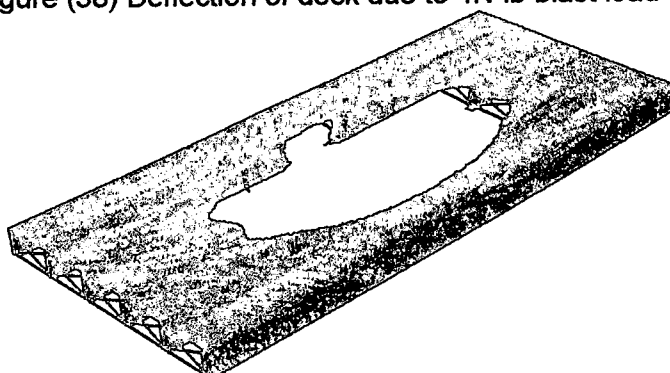
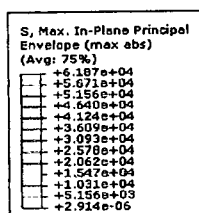


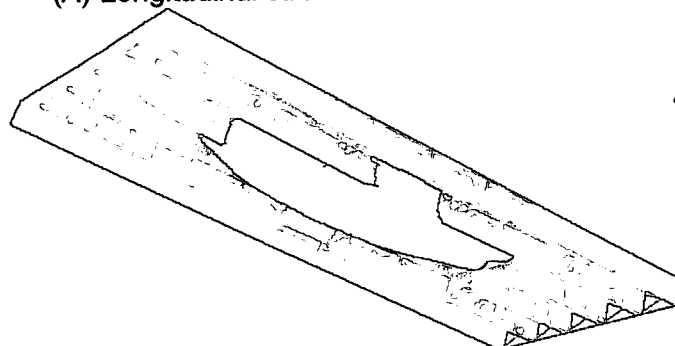
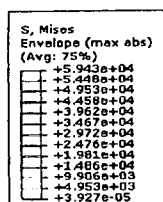
Figure (38) Deflection of deck due to 4N-lb blast load



ODB: 4000deck.odb Abaqus/Explicit Version 6.7-1 Mon Sep 01 19:00:19 Eastern Daylight Time 2008

Step: Step-1
Increment 5260: Step Time = 1.000
Primary Var: S, Max. In-Plane Principal
Deformed Var: U Deformation Scale Factor: +1.000e+00

(A) Longitudinal stresses of deck



ODB: 4000deck.odb Abaqus/Explicit Version 6.7-1 Mon Sep 01 19:00:19 Eastern Daylight Time 2008

Step: Step-1
Increment 5260: Step Time = 1.000
Primary Var: S, Mises
Deformed Var: U Deformation Scale Factor: +1.000e+00

(b) Longitudinal stresses of girders

Figure (39) Damage due to 4N-lb

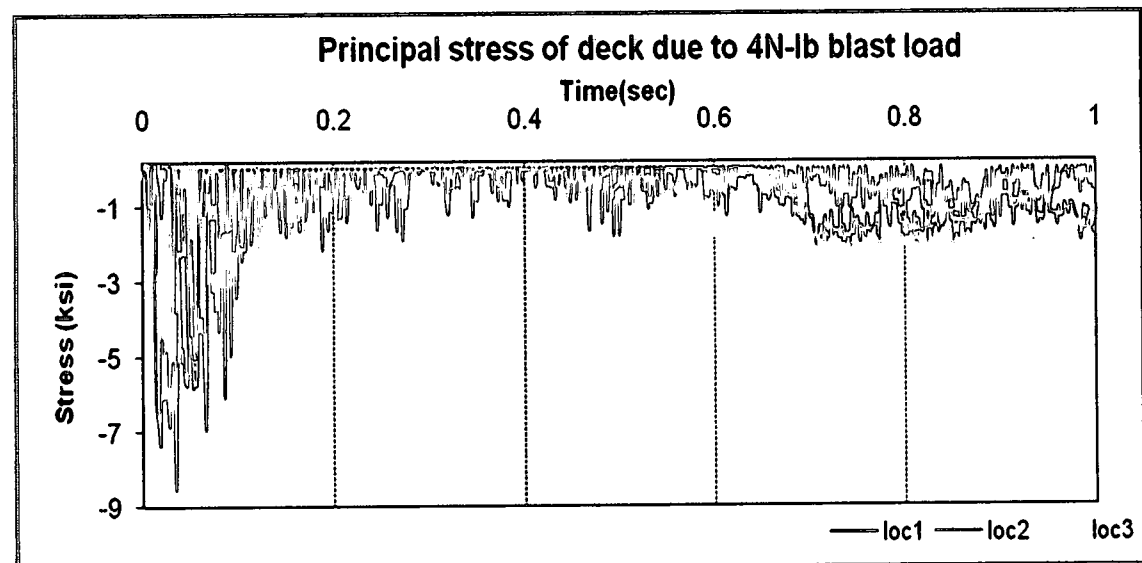
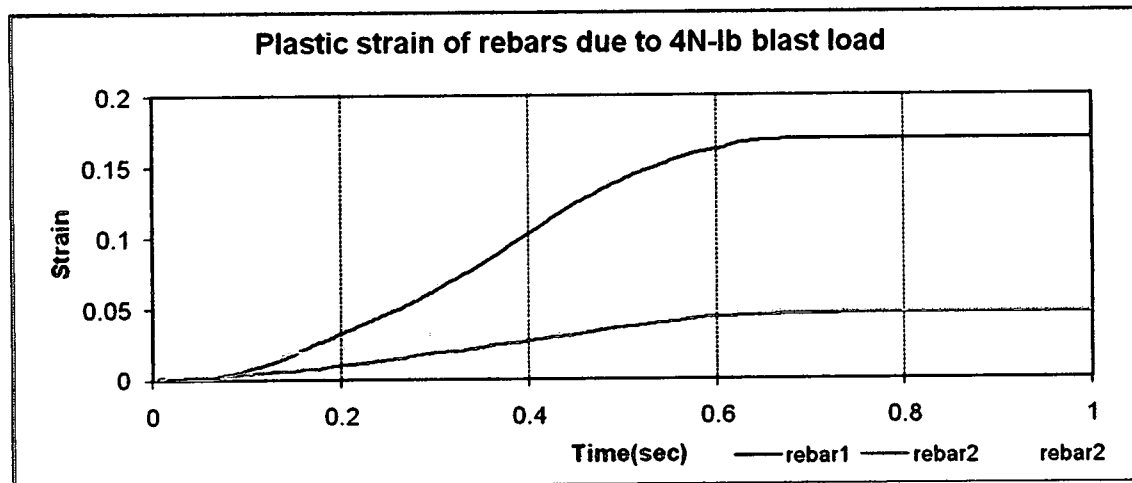
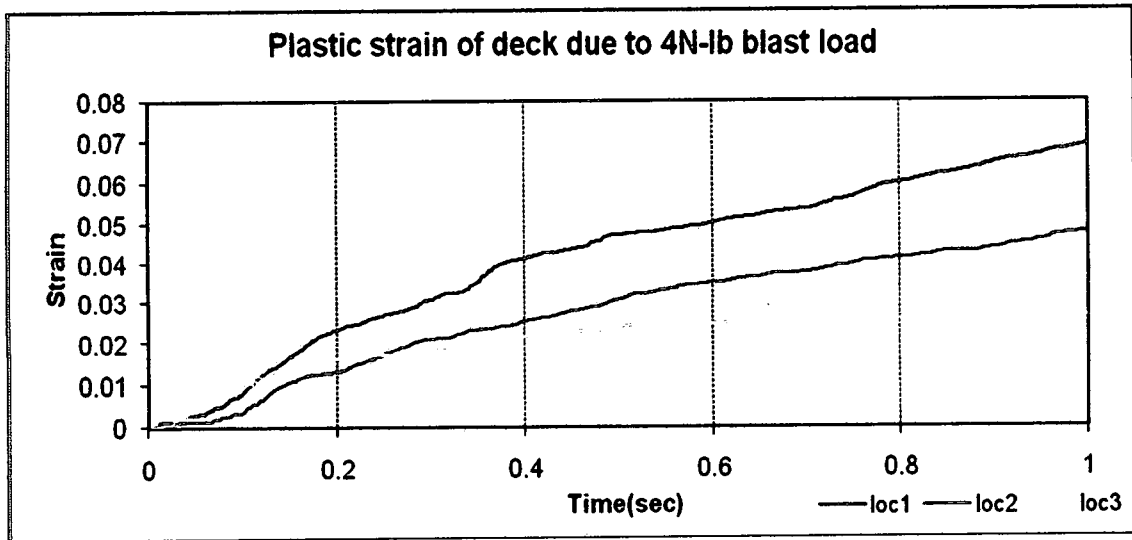


Figure (40) longitudinal stress and strain of deck and rebar due to 4N-lb blast load

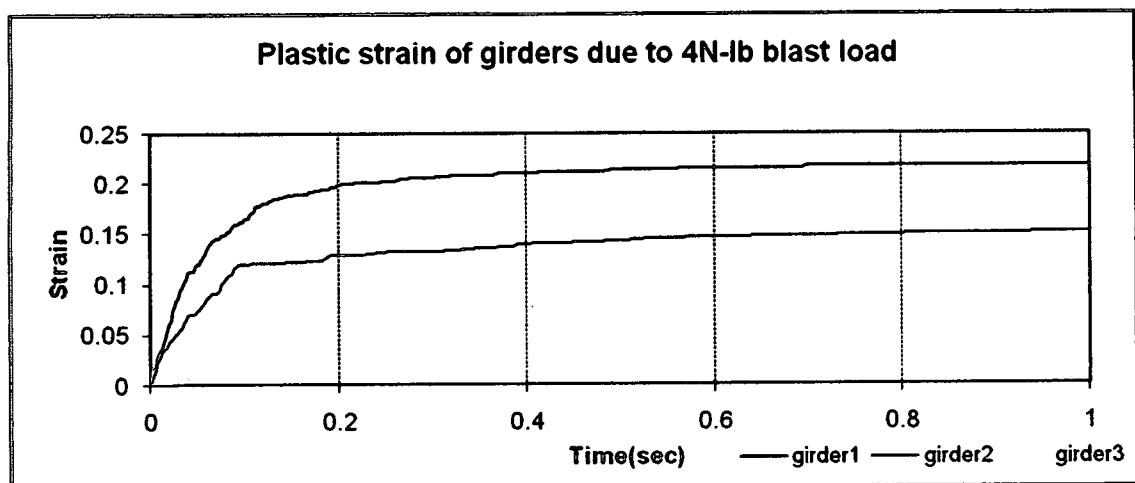
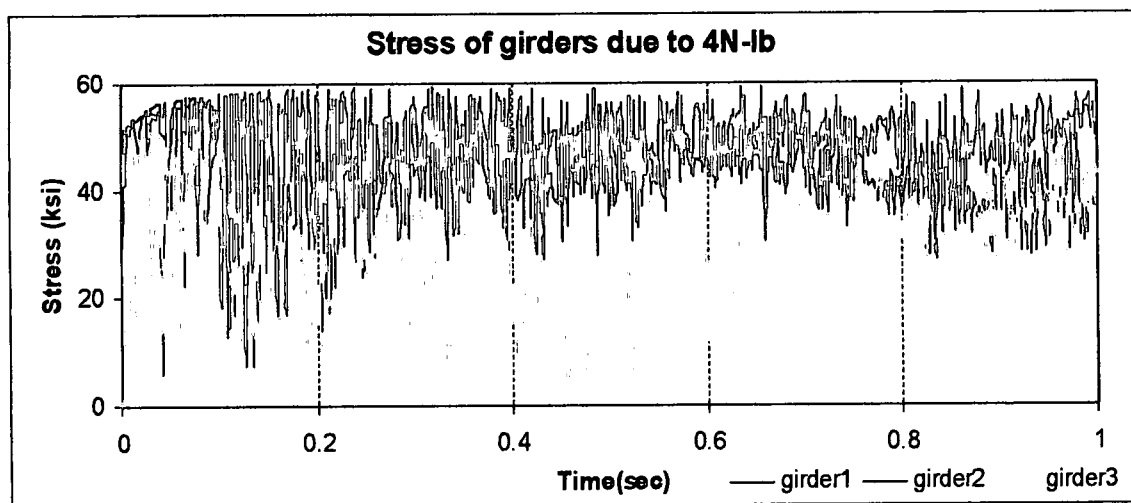
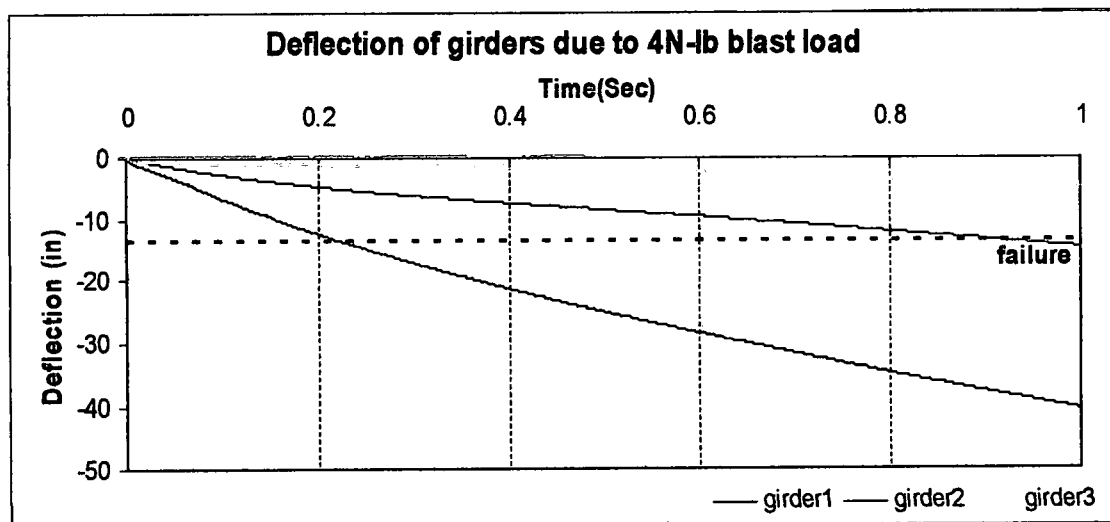


Figure (41) Deflections, longitudinal stresses and strains at girders due to 4N-lb blast load

5.4.3.3 Results

Deck: Results in Table (10) show that loc1 suffered a significant flexural deformation, crushing of concrete and yielding of rebar, hence the damage is considered a significant damage. Loc2 suffered a sizable deformation, crushing of concrete and yielding of rebar, thus considering it as a significant damage. A deflection of 11.82 in coupled with crushing of concrete and yielding of steel at loc3 is enough to consider the damage as a significant one. Hence all locations have failed in the concrete deck.

Girder: As seen in Table (10) deflection of girder1 and girder2 exceed maximum permissible deflection of 13.105 in, with a strain greater than plastic strain hardening in girder1 and equals to plastic strain hardening in girder2. Stress at all girders exceeds yield stress. Due to excessive deformation, both girder1 and girder2 suffered a significant damage, while girder3 is subjected to further study in section (5.7.2) to assess structural stability.

Charge Size 4N-lb	Parameter		Loc1		Loc2		Loc3	
			Deck	Rebar1	Deck	Rebar2	Deck	Rebar3
	Deflection	In	63.87	-	28.35	-	11.82	-
	Strain	-	0.069	0.169	0.0474	0.0459	0.0261	0.0465
	Stress	psi	5794	58218	8526	53545	4400	54568
	Failure		Yes	Yes	Yes	Yes	Yes	Yes
	Parameter		Girder1		Girder2		Girder3	
	Deflection	In	40.305		14.495		4.48	
	Strain	-	0.217		0.151		0.016	
	Stress	psi	58903		57652		51527	
	Failure		Yes		Yes		No	

Table (10) Structural response of bridge to 4N-lb blast load

5.5 Discussion of Results

Comparison of the response of the bridge's components to various blast loads is very instrumental to understanding the initiation and progress of structural damage while conducting post-blast analysis. Comparison is done with focus on the behavior and response of girders since global stability of the superstructure is dependent on girder response to blast and design loads.

5.5.1 Deck

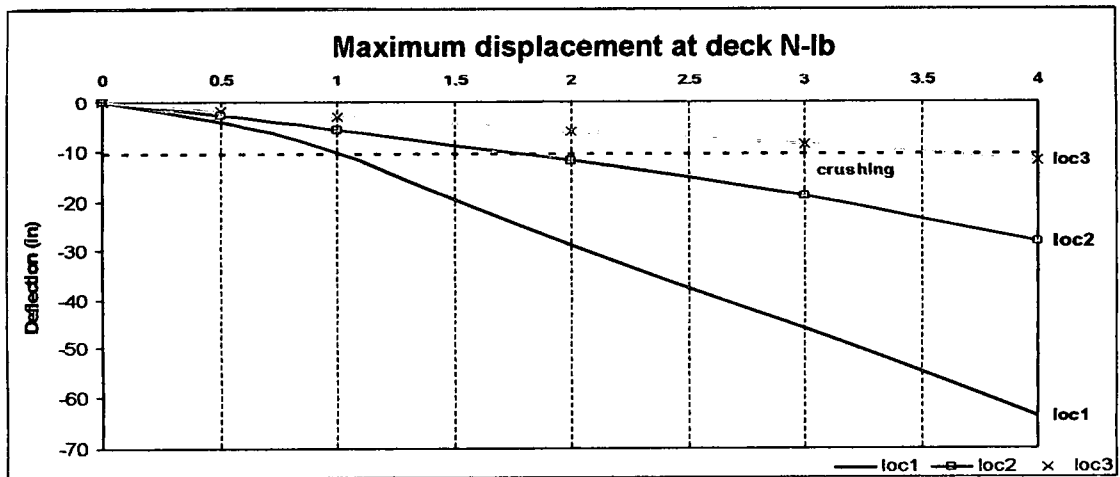
The largest deflection of the concrete deck occurred at loc1, as shown in Figure (42-a), is 63.87 in due to 4N-lb TNT blast load. Loc2 experiences a deflection of 28.35 in and loc3 has a deflection of 11.82 in for the same blast scenario. This trend of deflection shows the fact that deflection of the concrete deck is dictated by charge size and proximity to explosion center.

Figure (42-b) shows longitudinal strain of all three locations in the deck. It is clear that loc1 loses its structural integrity (crushes) after a blast load of 0.5N-lb TNT, loc2 crushes under a blast load of 1.75N-lb, and loc3 crushes for blast load of around 2.25N-lb blast load. This indicates that locations closest to blast load will be the first to crush, and damage progresses as a function of distance from blast center.

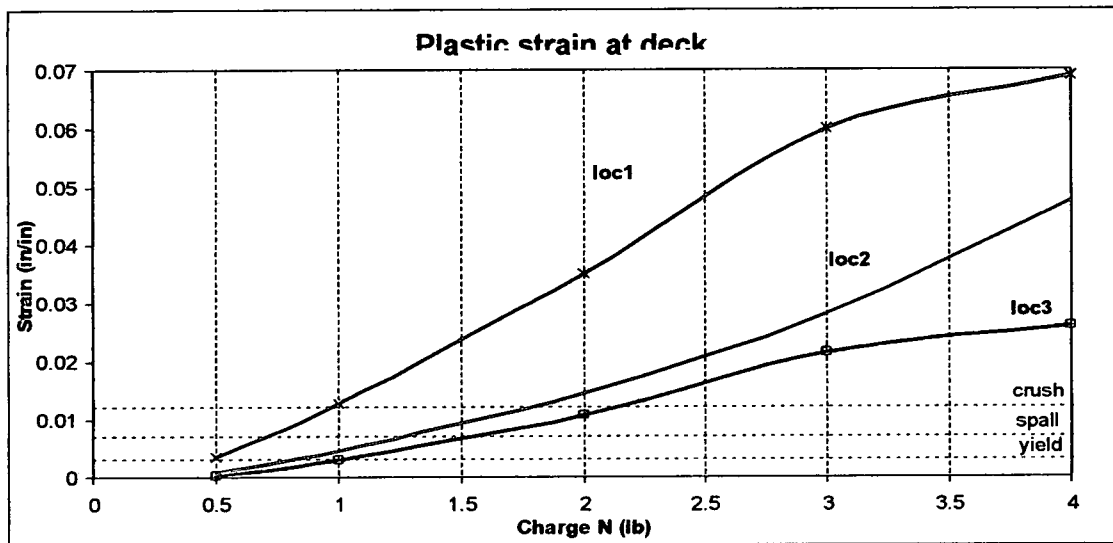
Figure (42-c) shows plastic strain in rebar. Rebar1 yields for charge size of 0.7N-lb, and rebar2 and rebar3 yield for charge size less than 3N-lb, while rebar3 yields for charge size around 3N-lb.

5.5.1.2 Conclusion

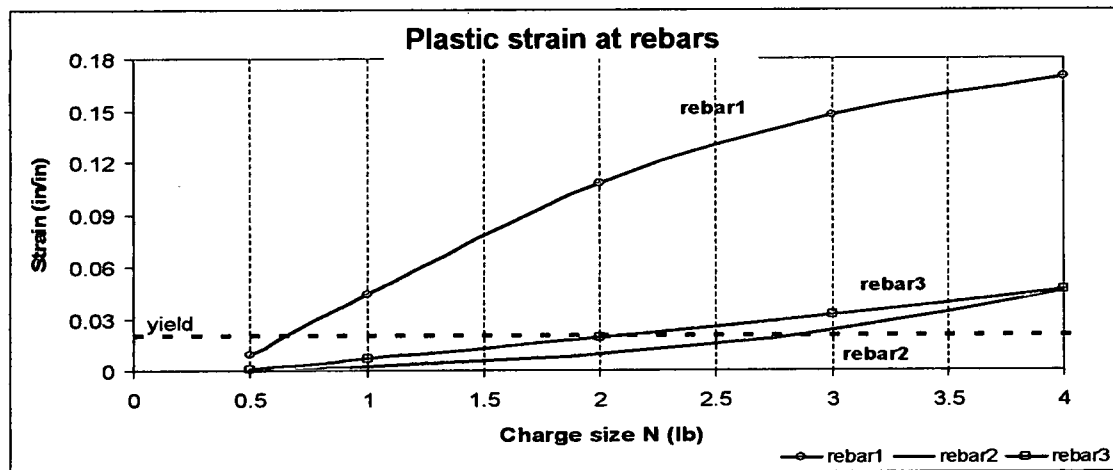
Since significant damage is characterized by major spalling, crushing of concrete and yielding of reinforcement steel, significant damage at loc1, loc2, loc3 is caused by charge sizes of 0.5N-lb, 1.75N-lb and 2.25N-lb TNT, respectively. If we assume that the loss of two-third of the area of the deck is total damage, then a charge size of 1.75N-lb is assumed to be the blast load that puts the deck out of surface.



(a) Deflections at deck



(b) Plastic strain of deck



(c) Plastic strain of rebar

Figure (42) Comparison of blast load results

5.5.2 Girders

As seen in Figure (43), the deflection of girder1 is 40.31in due to 4N-lb blast load. Girder3 has a deflection of 4.48 in indicating that girders closest to the explosion center suffer the largest damage.

As seen from the strain diagram in Figure (44), girder1 reaches yield strain for charge sizes greater than 1N-lb. Girder2 reaches yield strain for charge sizes greater than 1.15N-lb and girder3 experiences no yield strain for all charges.

Figure (45) shows stresses at girders due to various charge sizes. Approximately both girder1 and girder2 reach yield stress for charge sizes greater than 0.75N-lb. Girder3 reaches yield stress for charge size between 2.5N-lb and 2.75N-lb TNT.

Figure (46) and Figure (47) show the history of damage of girder1 and girder2 respectively. It is observed that yielding time decreases as charge size increases. Girder1 starts to yield 0.0061 sec due to 4N-lb blast, girder2 starts to yield 0.0081 sec for the same charge size. This indicates that damage history is a function of proximity of girders to blast center. The closest girder yields first.

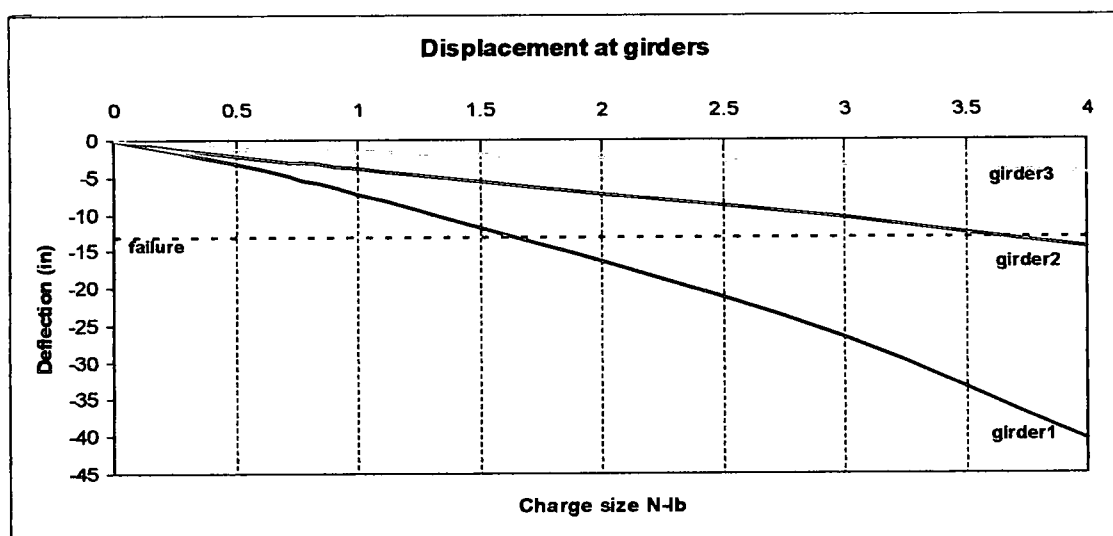


Figure (43) Comparison of displacement of girders at mid-span

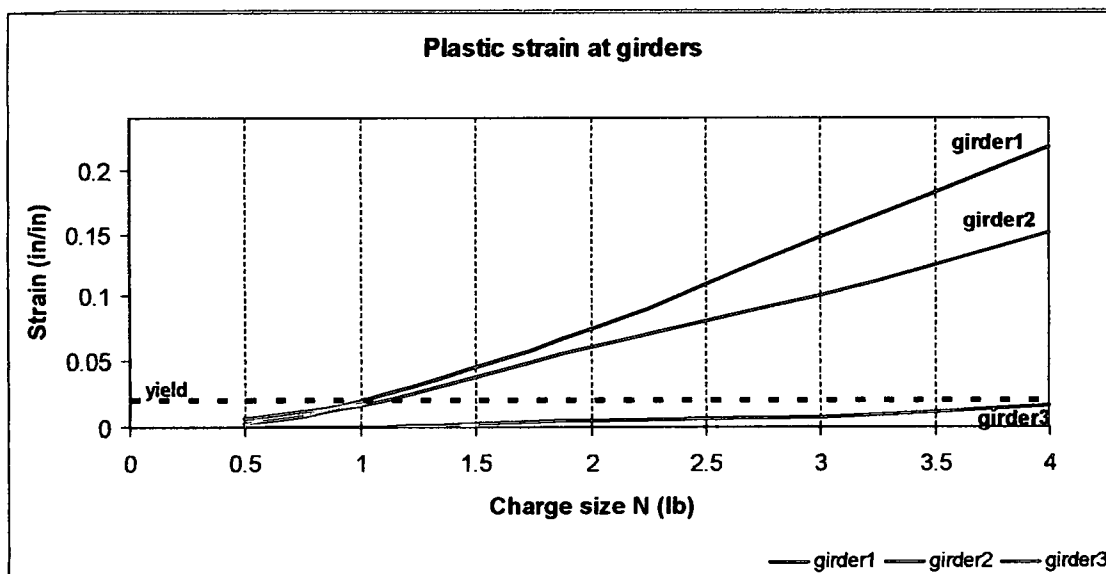


Figure (44) Comparison of plastic strain of girders at mid-span

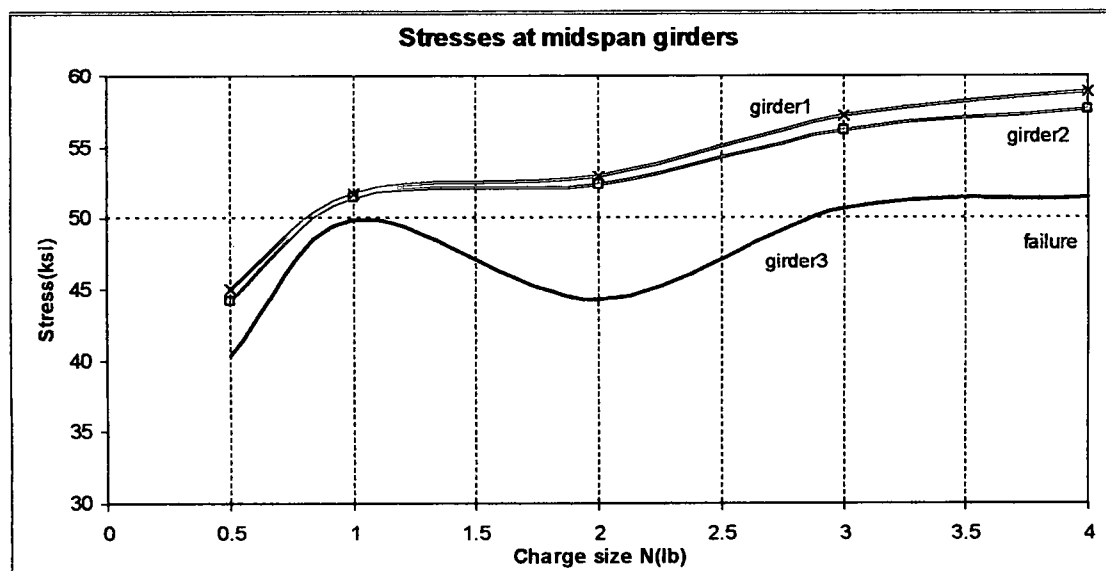


Figure (45) Comparison of stresses at girders

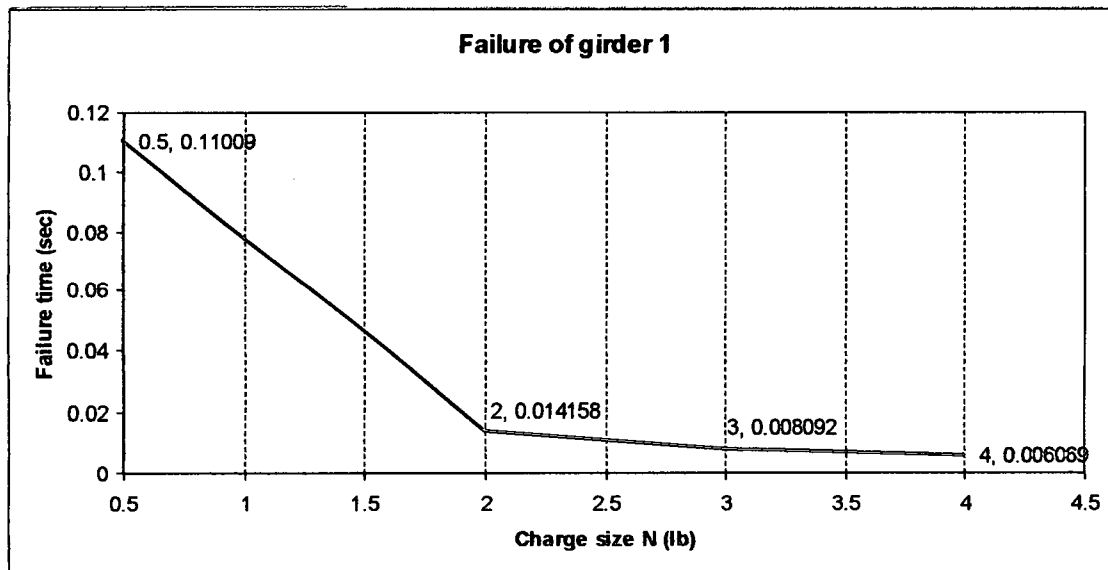


Figure (46) Damage to girder1

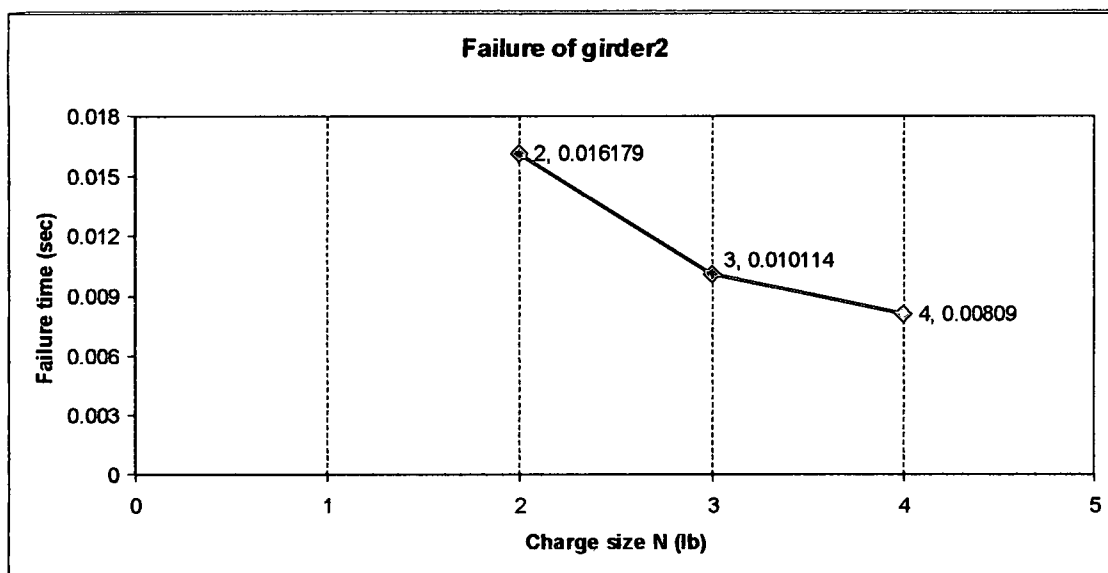


Figure (47) Damage to girder2

5.6 Post-Blast Analysis

5.6.1 Design Load

The post-blast analysis of the bridge will determine whether the bridge has passed or failed an explosion event, and hence its adequacy for daily use. The best index of failure is whether the structural member has reached its ultimate strength. Ultimate strength is chosen as a failure criterion because a blast is an extreme loading event that is not considered in analysis and design using serviceability limits criteria. It is also apparent the bridge will undergo large strains, plastic deformations and redistribution of load before collapse occurs, all of these are information that ultimate strength is reached. For the bridge, the most critical members are girders. Failure of girders means the failure of the superstructure; hence the post-blast analysis will focus on the response of girders.

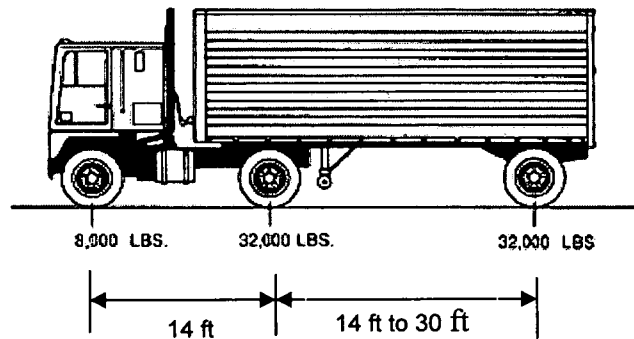
The analysis is conducted by applying HS20 design truck loading⁽²⁶⁾ and uniform lane loading, shown in Figure (48), to the bridge deck after the blast event has taken place. The HS20 design truck load is applied to the bridge on patches; the front two patches have a dimension 12×18 in and each carry a pressure of 37 psi. The two middle and rear patches each have the dimension of 20×18 in and each carry a pressure of 45 psi. To ensure that the patch does not carry any pressure it is assigned a very small modulus of elasticity of 0.1 psi and a thickness of 0.05 in. The design truck is placed in such a manner that its center of gravity lies exactly on the mid-span. The design load is given by

$$W_d = 1.25 \times DL + 0.5 \times LL$$

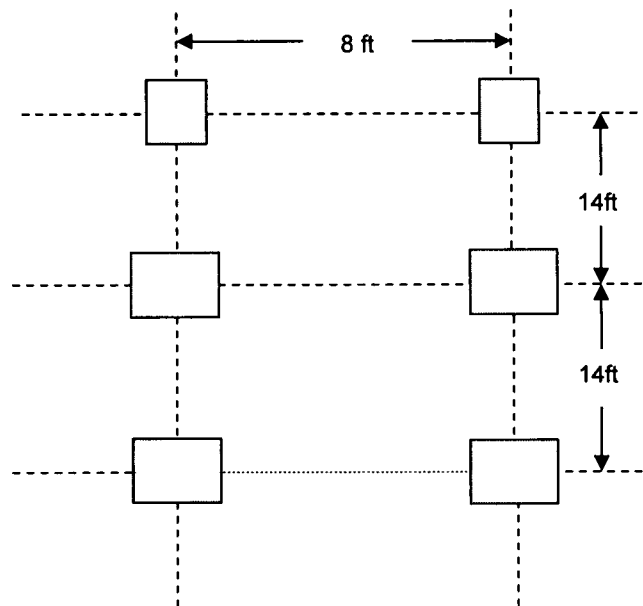
W_d is design load, DL is dead load, LL is live load.

If girders reach or exceed ultimate strength due to live load then the whole girder fails; otherwise it is still capable of carrying live load.

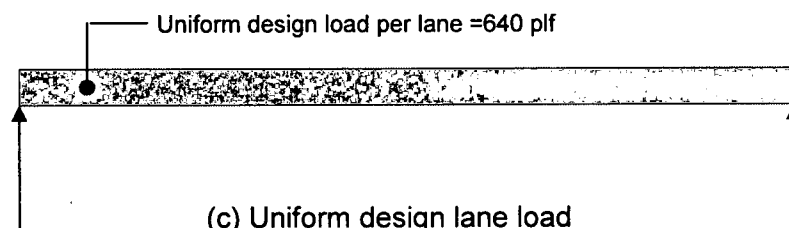
Recommendations are made on whether the bridge has partially failed or completely failed.



(a) AASHTO HS20 truck loading



(b) HS20 Truck Design load distribution



(c) Uniform design lane load

Figure (48) Design load

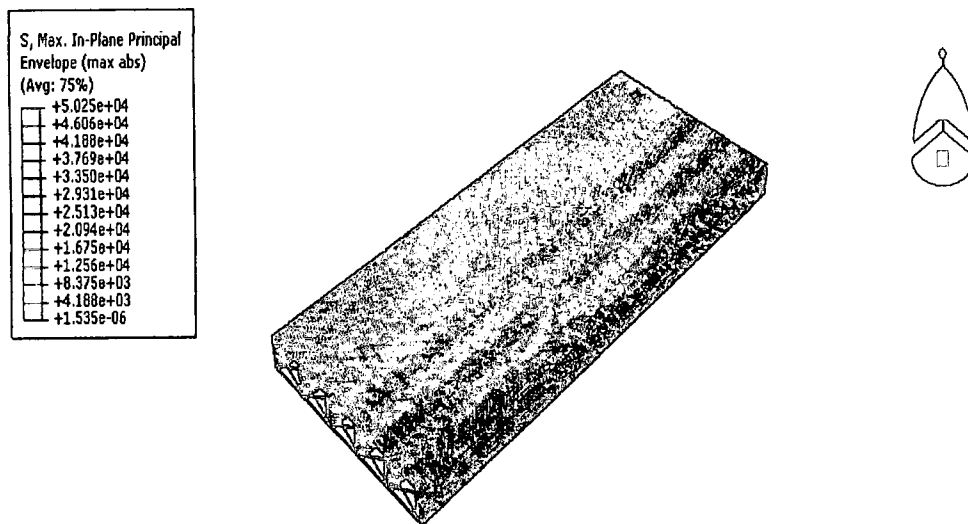
5.6.2 Results of Post-Blast Analysis

5.6.2.1 0.5N-lb Blast Load

For the case of a bridge subjected to 0.5N-lb blast load, the post-blast analysis, as indicated in table (11), reveals a decrease in deflection at girder1 and girder2, with girder1 having a deflection of 2.77 in down from 3.275 in due to blast load. Strain levels remain the same after application of the design load. This indicates that all girders are able to carry design loads as shown in Figure (49) without any major structural problems after exposure to blast load.

Charge Size 0.5N-lb	Parameter	Girder1	Girder2	Girder3
		Midspan	Midspan	Midspan
	Deflection (in)	3.275	2.123	1.170
		2.77	1.79	1.20
	Strain	0.0063	0.00261	1.1E-6
		0.0063	0.00261	1.1E-6
	Stress (psi)	45049	44210	40263
		16727	19140	9746

Table (11) Response of girders to 0.5N-lb blast load



ODB: deck10,000.odb Abaqus/Explicit Version 6.7-1 Mon Sep 01 11:37:08 Eastern Daylight Time 2008



Step: Step-2
Increment 891: Step Time = 0.2000
Primary Var: S, Max. In-Plane Principal
Deformed Var: U Deformation Scale Factor: +1.000e+00

Figure (49) Structural response of the bridge due to 0.5N-lb and live load

5.6.2.2 1N-lb Blast Load

After application of the design load to a bridge subjected to 1N-lb blast load, the deflection of girder1 decreases from 7.265 in to 7.146 in while strain values remain constant at 0.0196. Girder2 has a deflection 3.71 in and strain of 0.01596. Post-blast analysis indicates that girder1 and girder2 both have stress and strain values exceeding the elastic range. The deflection criterion of 13.1 in is not exceeded by any girder. The summary of response is presented in Table (12)

Charge Size 1N-lb	Parameter	Girder1	Girder2	Girder3
		Midspan	Midspan	Midspan
	Deflection (in)	7.265	3.82	1.614
		7.146	3.71	1.621
	Strain	0.0196	0.01596	0.000464
		0.0196	0.01596	0.000464
	Stress (psi)	51765	51501	449944
		29096	28064	13939

Table (12) Response of girders to 1N-lb blast load

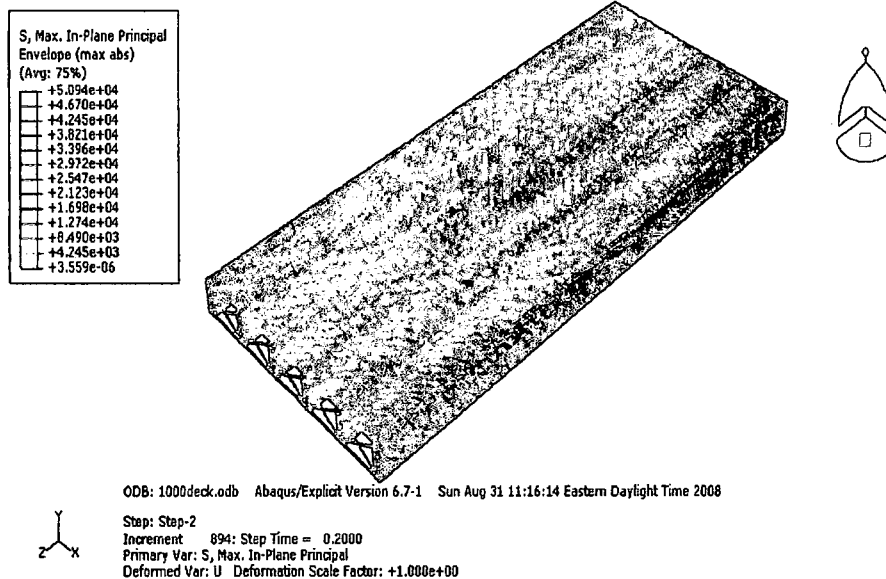


Figure (50) Structural response of the bridge due to 1N-lb and live load

5.6.2.3 2N-lb Blast Load

After application of a design load to a bridge exposed to a 2N-lb blast load, the deflection of girder1 increases from 16.40 in to 18.05 in while the strain remains constant at 0.074. Girder2 has a deflection of 8.54 in and strain of 0.06. Post-blast analysis indicates that girder1 will experience flexural deflection greater than the allowable deflection criterion. Although girder2 has strain and stress levels exceeding elastic limits, it has not suffered excessive deflection; hence two central girders suffer significant damage as shown in Figure (51). The summary of the post-blast study is detailed in Table (13).

Charge Size 2N-lb	Parameter	Girder1	Girder2	Girder3
	Deflection (in)	16.40	7.34	2.404
		18.05	8.54	2.32
	Strain	0.074	0.060	0.0046
		0.074	0.060	0.0050
	Stress (psi)	52948	52427	44359
		41574	25287	22174

Table (13) Response of girders to 2N-lb blast load

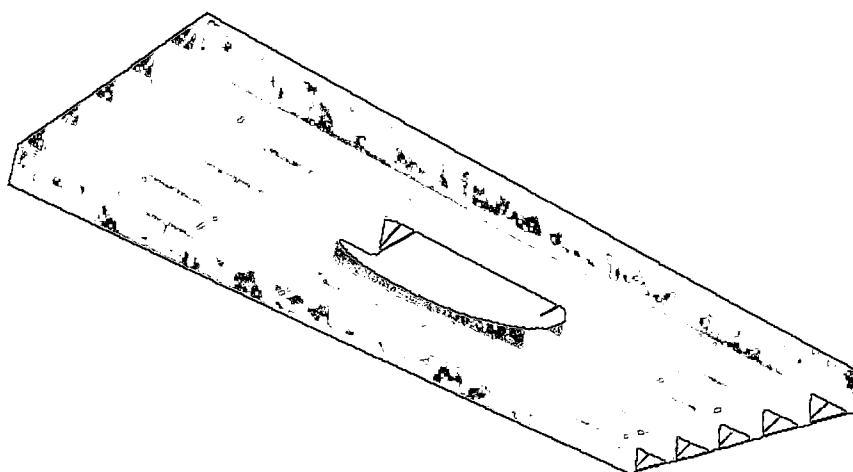
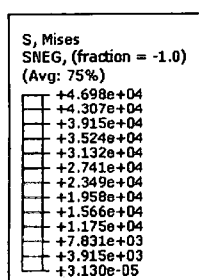


Figure (51) Structural response of the bridge due to 2N-lb and live load

5.7.2.4 3N-lb Blast Load

Application of design load to bridge exposed to a 3N-lb blast load results that girder1 and girder2 experience flexural deflection 37.00 in and 16.08 in, and plastic strains of 0.148 and 0.102, respectively. Girder3 has a deflection of 4.28 in. Hence, based on the failure criterion, four central girders will fail to carry design loads as shown in Figure (52). This implies that the whole bridge is not safe to carry design loads after explosion and all four girders would have to be replaced. The summary of structural response is detailed in Table (14)

Charge Size 3N-lb	Parameter	Girder1	Girder2	Girder3
	Deflection (in)	26.66	10.54	3.45
		37.00	16.08	4.28
	Strain	0.147	0.101	0.0077
		0.148	0.102	0.0079
	Stress (psi)	57209	56179	50693
		55991	55964	46775

Table (14) Response of girders to 3N-lb blast load

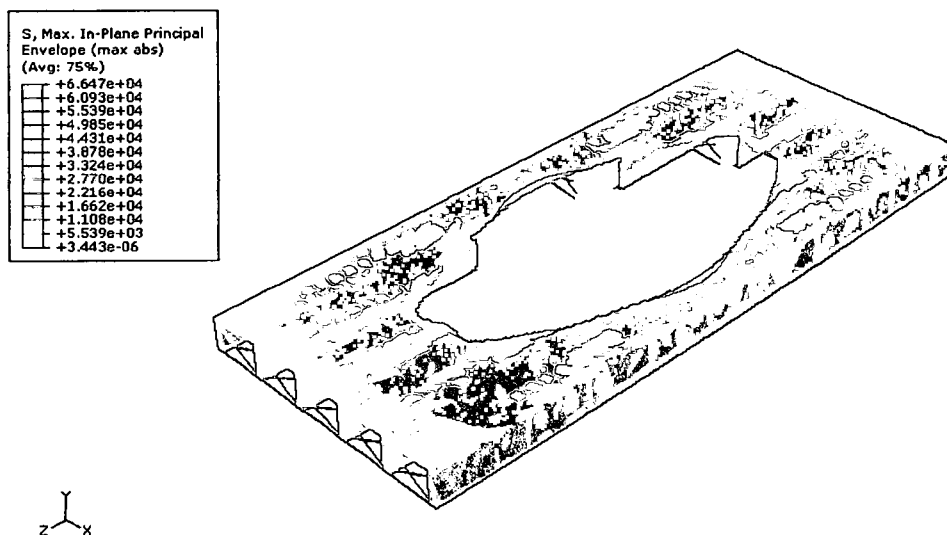


Figure (52) Structural response of the bridge due to 3N-lb and live load

5.7.2.4 4N-lb Blast Load

Application of design load to a bridge exposed to 4N-lb blast load results that deflection of girder1 and girder2 increased from 40.31 in to 45.48 in, and 14.50 in to 17.14 in, respectively. Strain levels of girder1 and girder2 both exceed the strains hardening limits. Gider3 has a deflection of 5.27 in. Based on the damage criterion, four of six girders fail, as shown in Figure (53), to carry design load. This implies that the whole bridge is not safe to carry design loads after 4N-lb blast, and the decision to replace the whole bridge becomes inevitable. The summary of structural response is detailed in Table (15)

Charge Size(lb) 4N	Parameter	Girder1	Girder2	Girder3
	Deflection	40.31	14.50	4.48
		59.75	26.71	6.58
	Strain	0.217	0.151	0.0159
		0.217	0.156	0.0172
	Stress (psi)	58903	57652	51527
		35767	53591	22174

Table (15) Response of girders to 4N-lb blast load

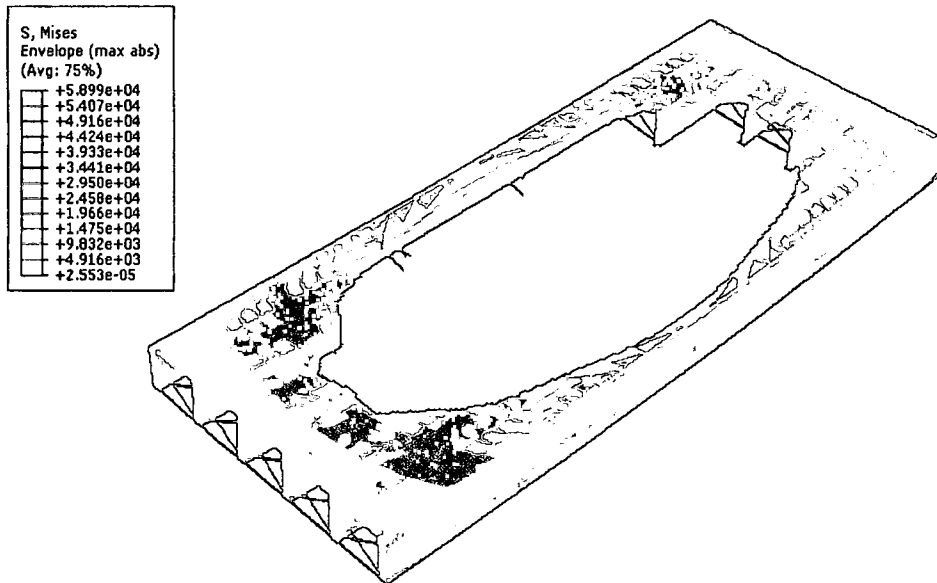


Figure (53) Structural response of bridge due to 4N-lb and live load

Chapter VI

Conclusion and Future Research

6.1 Conclusion

The finite element analysis of a typical highway steel bridge subjected to various blast load charges presents a better understanding of the structural response and vulnerabilities of these types of bridges. It also provides a better insight into the retrofitting process, structural hardening and, ultimately, design of blast-resistant bridges. The following conclusions are reached in the current study:

1. In the case of 0.5N-lb TNT blast over the deck, locations closest to explosion center on the deck will exceed ultimate strain and although severely damaged, will not spall or crush if the concrete model exhibits ductile behavior.
2. For a 0.5N-lb TNT blast load, and for the various levels of ductility investigated, a 4000 psi concrete responds better than a 6000 psi concrete and 10,000 psi. Hence a low strength concrete deck resists blast loads better than high strength concrete due to the intrinsic ductility of lower strength concrete.
3. There is no substantial difference in displacement between low strength concrete deck and high strength concrete deck (only 3 percent decrease), and hence using high strength concrete has no significant effect in reducing the effect of blast load.
4. The post-blast analysis conducted on the steel girder bridge revealed that the two central girders closest to the explosion center can resist an explosion of

1N-lb magnitude or less. The two central girders fail for blast magnitude of 2N-lb or more.

5. It has been observed in post-blast analysis that for a steel girder to resist blast load it should have a deflection to span ratio of 1.2 percent, and hence 1.2 percent can be adopted as the new deflection criterion for steel girders when analyzing for extreme loads for this type of bridges.
6. Post-event analysis reveals that a blast load of 0.75N-lb can cause significant damage to the concrete deck in the vicinity of the explosion center. A blast load of 1.75N-lb and greater can cause irreparable levels of damage.
7. All blast loads investigated resulted in severe deck damage exhibited by a crater of diameter proportional to charge sizes i.e. a crater of about 40 percent of width of the bridge is observed for 2N-lb load, and a crater of 60% is observed for 4N-lb explosion.
8. Based on the study conducted, the steel girder can safely resist 0.5N-lb TNT blast load, specified in Blue Ribbon Panel for Bridge and Tunnel security⁽²⁾ as a potential minimum blast load a vehicle can carry. The steel girder bridge will be completely out of service if a blast load of 2N-lb TNT or greater.

6.2 Future Research

1. The study conducted is basically for an over the deck explosion. A detailed finite element analysis study should be done on a similar bridge considering various locations of explosion.
2. A similar study is recommended to be done on the substructure of the bridge including bearing, and seats. Structural integrity of bridges is dependent on the behavior of all components combined.
3. Research should be conducted to understand blast load distribution on structures. The distribution of blast load considered in this study, though rigorous, is still approximate.
4. Since excessive deflection is the main reason for failure of girders, research should be done to decrease the flexural response of girders to blast load.
5. Further studies should be conducted on blast-resistant bridges, and on retrofitting existing bridges to safely resist blast loads. New materials such as fiber reinforced polymer, structural hardening, and alternative load path are the feasible measures to create a blast-resistant bridges. Design codes similar to seismic design codes should be formulated to design important highway bridges.

APPENDIX A

Verification Examples

To validate the accuracy of ABAQUS analytical capability to analyze bridges, various structural component of the bridge has been solved conventionally using hand calculation, and numerically by ABAQUS. Results are compared for validation purposes.

A-1 Concrete Beam

Two cases of a simply supported reinforced concrete beams were analyzed by ABAQUS, and structural response such as stresses, strains and deflection were compared to conventional analysis using hand calculations.

Geometry and modeling

The first case is an unconfined reinforced concrete beam subjected to a uniformly distributed load of 355 lb/in applied instantaneously on the beam. The beam is 10-in wide, 25-in deep and has a span of 20-ft. The beam is modeled by 60×3 S4R shell elements. Reinforcement bars are incorporated to the beam in properties module. No mesh refinement was done, since the problem is simple and involves insignificant nonlinear plastic response. The concrete has an ultimate strength f'_c of 6000 psi, modulus of elasticity E_c 4,420 ksi, and Poisson's ratio of 0.18. The total area of reinforcement is 2.37 in², yield stress of 60 ksi and modulus of elasticity of 29,000 ksi.

Results

Figure (54) show stresses, displacement, sectional moment and strain of the beam computed by ABAQUS. The comparison of mid-span deflection, Figure (55), and stress distribution across the top surface of the beam, Figure (56) was done between ABAQUS results and conventional methods of analysis results. As seen in both Figures, the deflection (0.27429-in) and stress (2453.88 psi) at mid span computed by ABAQUS is largely consistent with conventional "hand calculation" results of 0.26647-

in and 2453.73 psi respectively. More convergence of results can be improved through mesh refinement process.

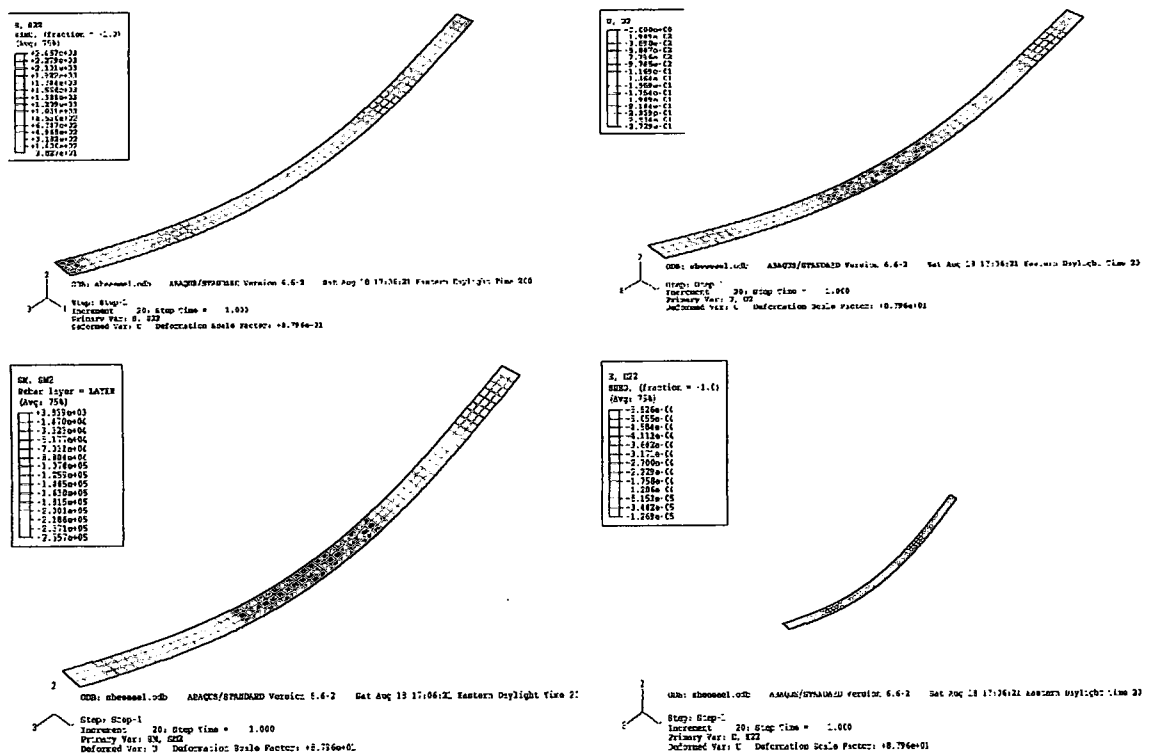


Figure (54) ABAQUS results

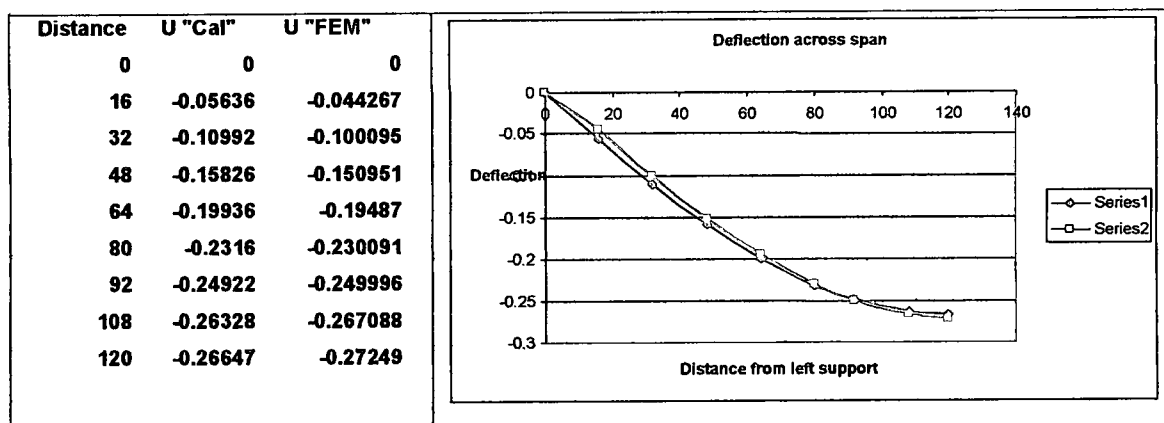


Figure (55) Deflection across half of the beam

Distance	Stress (Cal)	Stress (FEM)
0	0	0
16	-610.706	-467.717
32	-1134.16	-1014.34
48	-1570.381	-1472.37
64	-1919.361	-1843.16
80	-2181.092	-2126.71
92	-2320.137	-2282.12
108	-2429.191	-2412.98
120	-2453.729	-2453.88

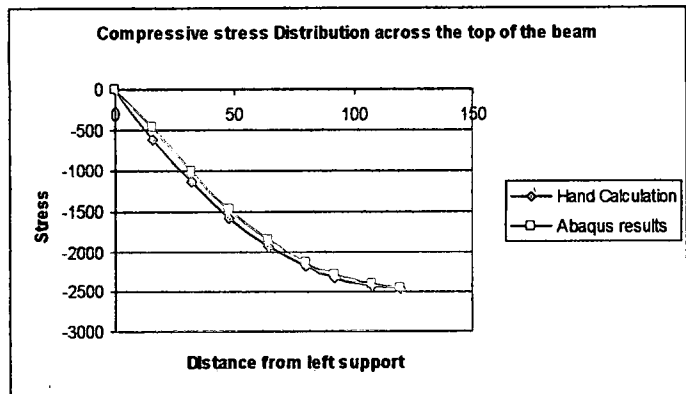


Figure (56) Compressive stress at the top of beam.

A-2 Rectangular Concrete Beam with Reinforcement.

The aim of this verification problem is examine the plastic behavior of a reinforced concrete beam subjected to two concentrated loads of 70,000 lb. Concrete damaged plasticity model in ABAQUS/Explicit is capable of representing the permanent damage that may occur due to the formation of tensile cracks and change of stiffness. ABAQUS/Explicit also has tension stiffening capability which is efficient in modeling the interaction between steel and concrete.

Geometry and Modeling:

The beam is 16 in × 33 in modeled using S4R shell elements. The beam is reinforced by 11 bars of # 4 with $A_s = 1.4 \text{ in}^2$. The beam was modeled by extremely fine mesh of 900 elements. The beam has modulus of elasticity of $3.2\text{E}+6$ psi, Poisson's ratio of 0.2. Cracking failure stress of 489 psi and ultimate strength of 5500 psi. The load is applied at 5% increments to monitor the detailed behavior of bending and curvatures.

Results:

The moment-curvature relationship shown in Figure (57) clearly matched an established plastic moment-curvature curve. The ultimate moment was calculated to be 11.6×10^6 , which is also captured using ABAQUS software. Moment-deflection

curve shown in Figure (58) matches the hand calculations. The curve behavior is linear for the first part of the curve. At 86% of ultimate moment value, the reinforcing steel started to yield; hence the concrete lost some of its stiffness which is shown by the change in slope of the curve. The maximum deflection was found to be 2.44 in.

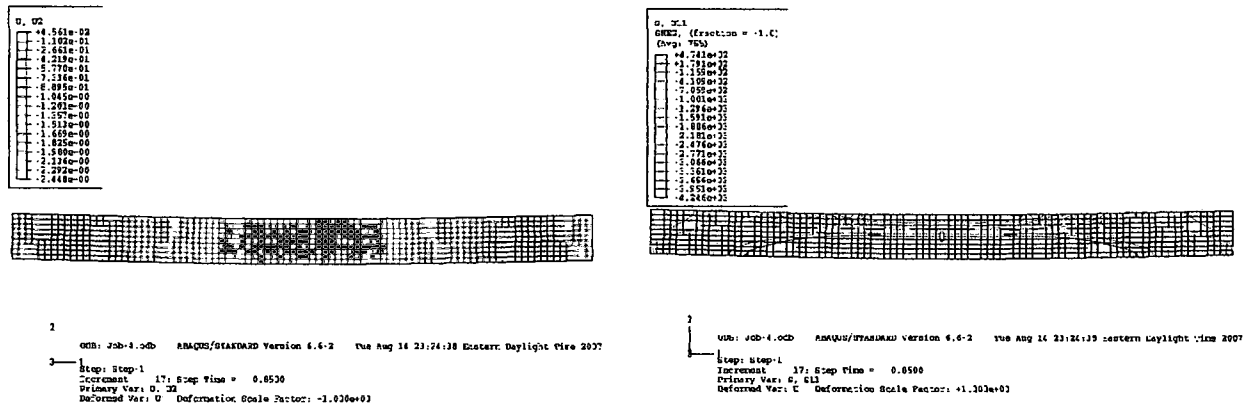


Figure (57) Response of reinforced concrete beam

Curvature	Moment
0	0
1.743E-04	1494900
1.867E-03	9276300
7.277E-03	10701900

$$M_{cr} = 1.74 \times 10^6$$

$$M_y = 4.68 \times 10^6$$

$$M_p = 11.6 \times 10^6$$

$$EI_g \text{ "Cal"} = 1.53 \times 10^6$$

$$FE EI = 1.647 \times 10^6$$

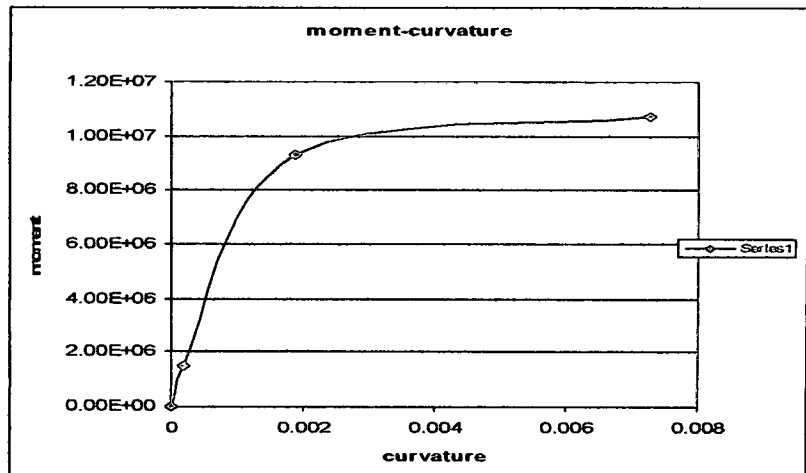


Figure (58) Moment-curvature for reinforced concrete beam

A-3 Nonlinear Analysis of Reinforced Concrete Slab

Nonlinear dynamic analysis of a simply supported reinforced concrete slab is performed to examine structural response to a concentrated load. ABAQUS/Explicit brittle crack model is used to model concrete, and tension stiffening was added to model the interaction between reinforcing steel and concrete. Brittle crack feature of ABAQUS allows for the detection of initial tensile cracks, and tension stiffening transforms loads across cracks to the reinforcement, hence loading the slab to collapse.

Geometry and Modeling:

The slab is 6 ft by 7 ft and has a thickness of 7.5 in. It is modeled by S4 shell elements with 9 integration points across the thickness. S4 element is capable of modeling bending behavior accurately. The slab is modeled by 224 elements (2in by 2in), so that each reinforcing steel bar be positioned alone inside a mesh. The slab is reinforced at the top and bottom using # 5 @ 6 in spacing. Two tensions stiffening value of 0.0015 and 0.003 were used to depict the loss of tensile strength after first crack failure. The slab is subjected to an incremental load 110 kips.

The Concrete's Modulus of Elasticity is $4.2\text{E}+6$ psi, Poisson's ratio is 0.18, ultimate strength is 6000psi, yield stress is 4000 psi, failure stress is 5500 psi. Cracking failure stress is 375 psi. For the Steel, yield stress is 60 ksi, modulus of Elasticity is $29\text{E}+6$ psi. Tension stiffening varies linearly from zero strain to either 0.0015 or 0.003.

Results:

As shown in Figure (59) Tension stiffening 0.0015 was not able to represent the full interaction between the concrete and rebar, hence the slab fails due to load 82500 lb. By using tensile softening strain of 0.003, Figure (60), the slab was able to carry all the applied load of 110 kips, and mid span deflection was 0.05 in.

Deflection	Load
0	0
0.001043	5500
0.0020863	11000
0.00535	27500
0.01283	55000
0.02082	71500
0.02527	77000
0.03108	82500

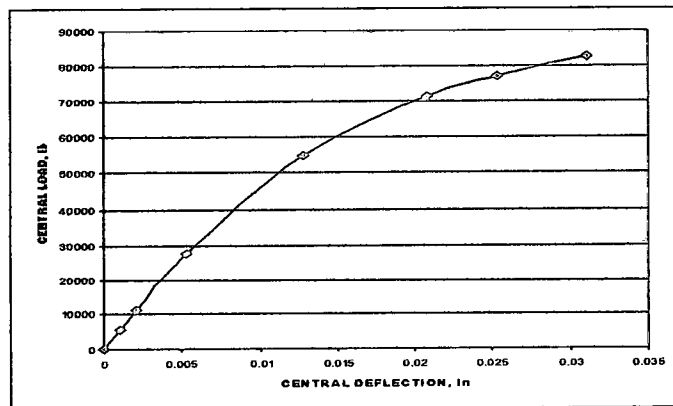


Figure (59) Load – Deflection diagram, Tension Stiffening = .0015

Deflection	Load
0	0
0.001043	5500
0.002086	11000
0.005344	27500
0.01247	55000
0.02446	82500
0.04372	104500
0.05161	110000

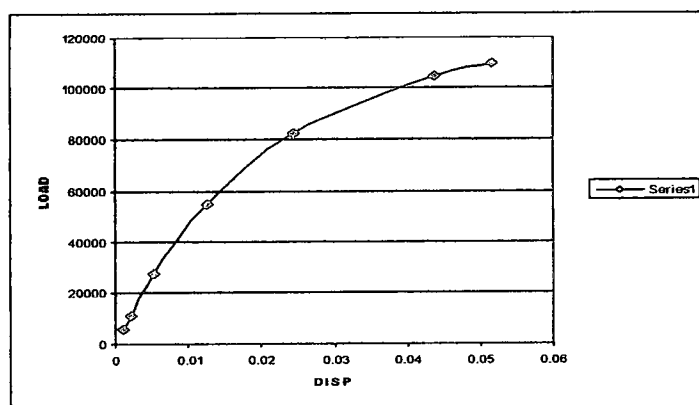


Figure (60) Load – Deflection diagram, Tension Stiffening = .003

Maximum value of deflection at mid span was calculated to be 0.0516 in, and the maximum compressive stress found was 5871.82 psi.

A-4 Slab used in the Thesis

The dimension of the slab is as identified in section (3.2) with the exception that the width of the slab is 12 in. The slab is loaded till failure and three distinct values are recorded i.e. the displacement that causes the concrete to spall and crush, and also the displacement at which reinforcement steel will yield and rupture. Figure (61) shows these responses as obtained by ABAQUS. From the Figure it can be deduces that the concrete deck start to spall when the deflection is 3.079 in and crushes when the deflection is 10.47 in.

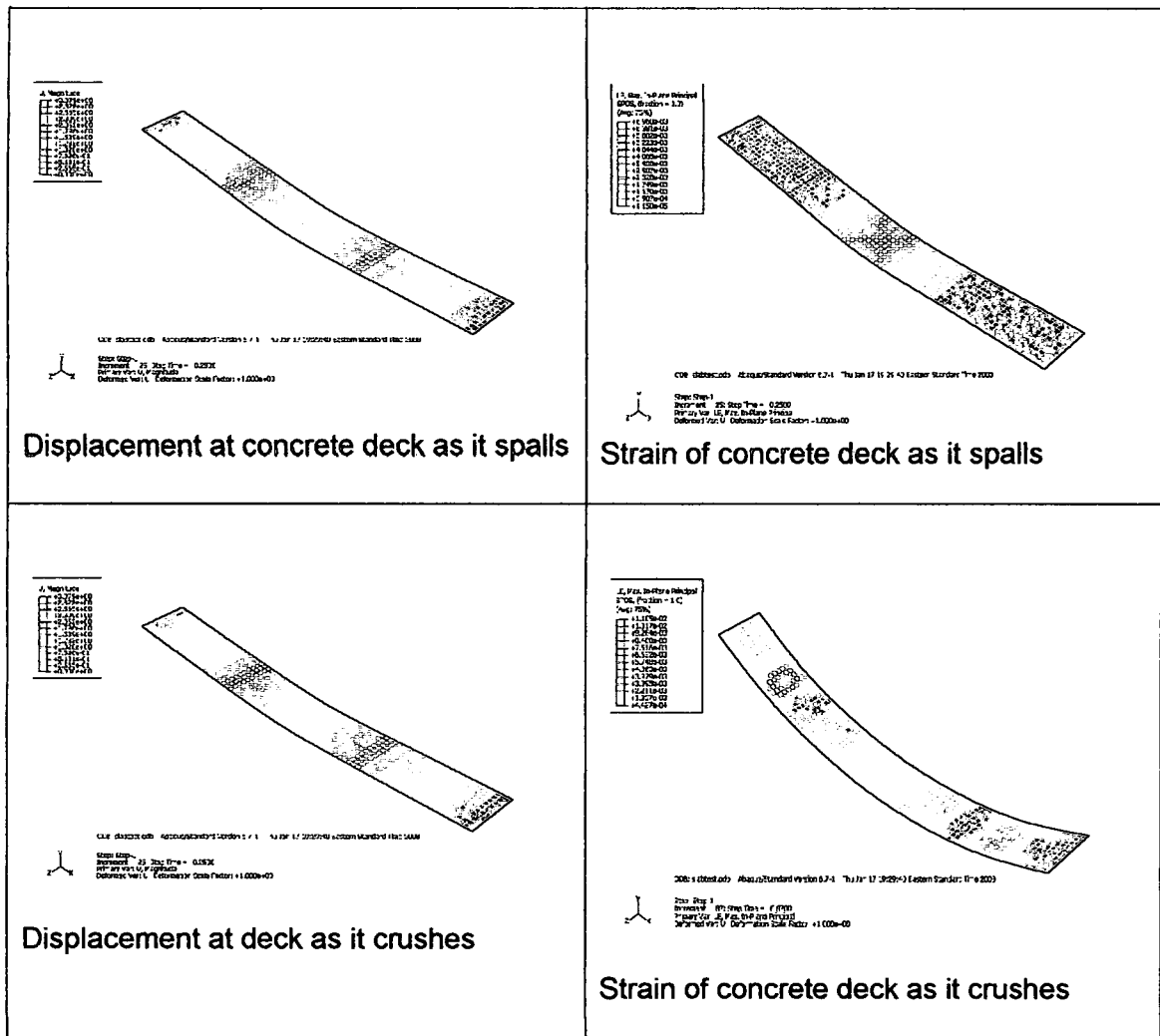


Figure (61) Concrete Slab response to failure load

Also Figure (62) shows that rebars starts to yield at deflection of 2.569 in of the concrete deck and starts to rupture at deflection of 12.28 in. These two values are used in determining the failure of the superstructure.

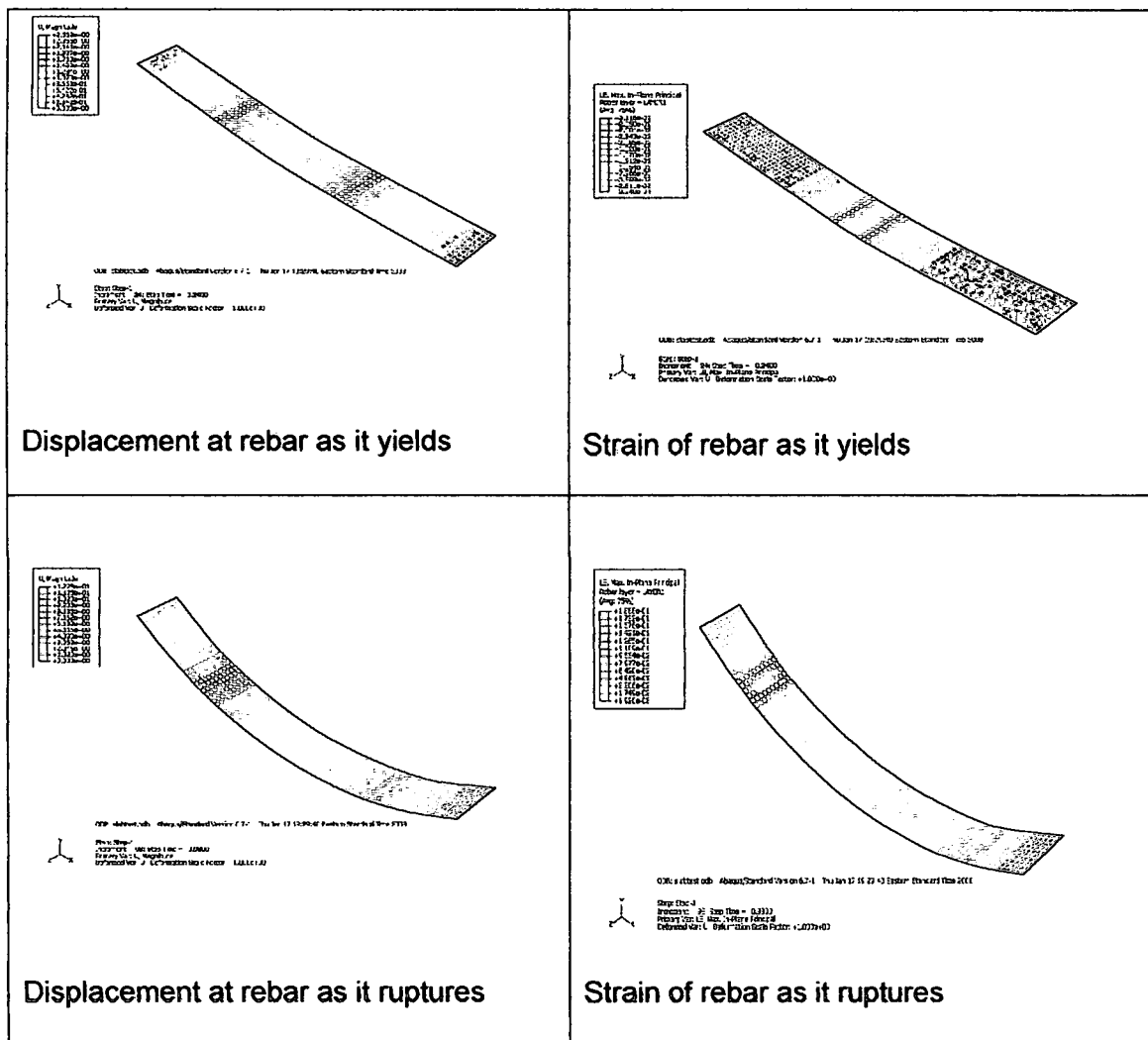


Figure (62) Structural Response of the steel reinforcement

A-4 Linear Elastic/Nonlinear Plastic Analysis of a Composite Beam

This practice is performed to verify the accuracy of ABAQUS in analyzing composite beams. The structural responses were compared to established examples for validity. ABAQUS results should comply with the fact that the composite beam has to behave as an integral unit that has uniform stress-strain curve from the top fiber of the concrete deck to the flange of the steel girder.

For this purpose a composite beam with dimensions shown in Figure (63) is studied. The beam has a length of 40 ft. and spacing between girders is 90.55in. The beam is subjected to UDL of 1.74 psi. The following material property was considered:

Concrete:

- | | |
|-------|--|
| 8673. | Compressive stress is 5500 psi. at inelastic strain of 0.002 |
| 8674. | Tensile stress is 460 psi |
| 8675. | Young's Modulus is 3200 ksi. |
| 8676. | Poisson' ratio is 0.18 |
| 8677. | Density is .087 lb/in ³ |

Steel:

- | | |
|-------|---------------------------------------|
| 8678. | Yield stress of steel $f_y = 36$ ksi. |
| 8679. | Young's Modulus is 29000 ksi |
| 8680. | Poisson' ration = .3 |
| 8681. | Density is .284 lb/in ³ . |

Reinforcement:

The concrete deck is reinforced at top and bottom by using 20 - # 5 bars. $F_y = 60$ ksi.

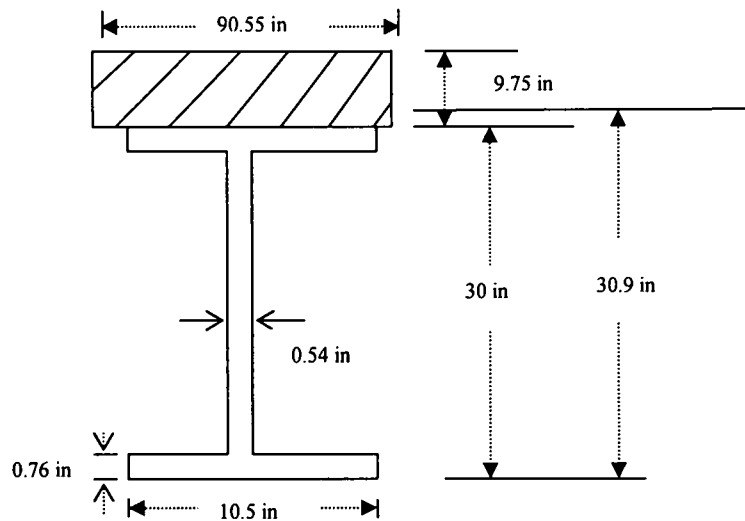


Figure (63) Cross-section of the composite beam

FE model

Element Type, Geometry and Meshing:

Shell element S4R was used to model the steel girder and the concrete deck. The element is capable of accurately representing flexural behavior as well as transverse shear. The composite action is achieved by using a command TIE, which basically make the bottom surface of the concrete deck and the top surface of the steel girder to act as a unit. A fine mesh was adopted such that the girder has 440 elements at the web level, 80 elements at each web, and deck has 320 elements. No mesh refinement study was conducted. The vertical displacement of both ends of the beam is restricted, while the other degrees of freedom are allowed.

Linear Static Analysis:

The composite beam was subjected to a load of magnitude of 1.74 psi. A linear static analysis was conducted to compute values of stresses, strains and deflection at mid-span of the beam, and these values were compared to established values. Figure (64) shows stresses, strains, displacement and moment at the composite beam.

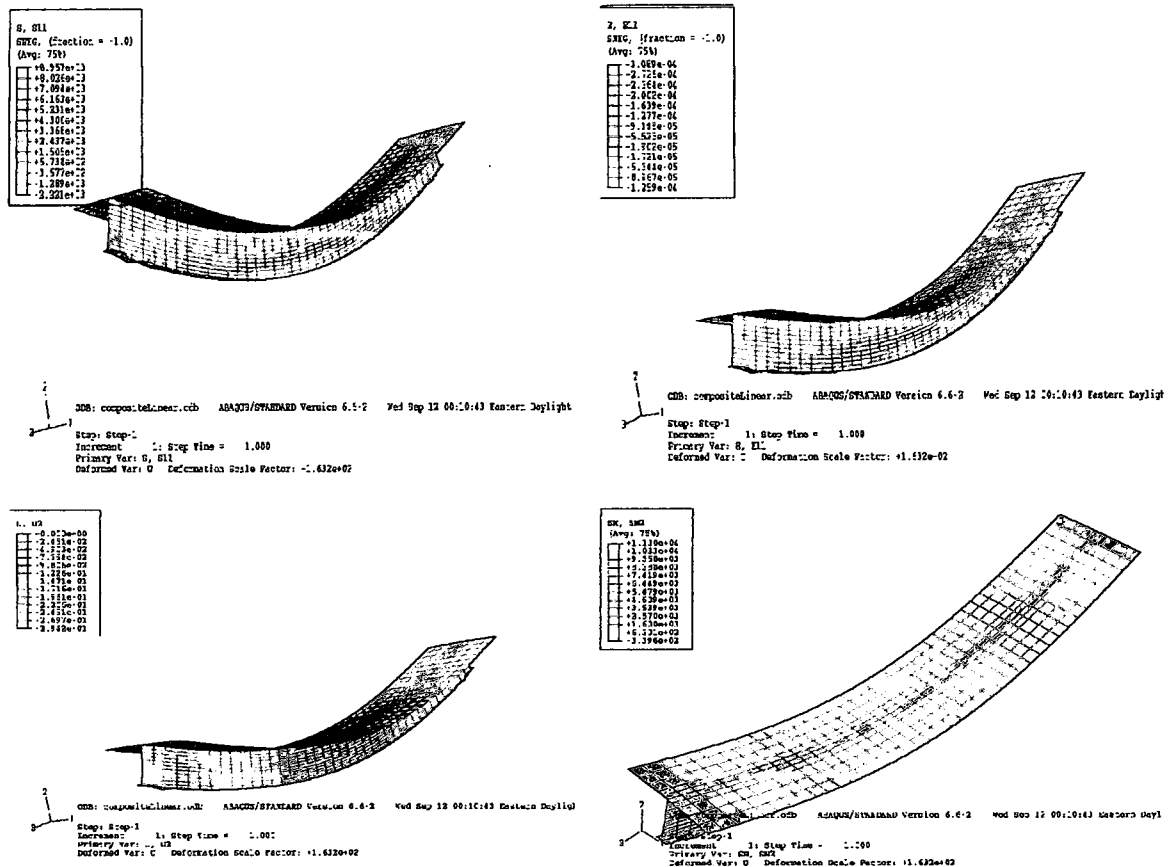


Figure (64) Response of composite beam

Concrete Slab:

The maximum compressive stress computed at top surface of the deck was -352.2 psi while the hand-calculated stress was found to be -384.9 psi. The variation in the results is about 9.28%. The maximum strain was found to be 107.55×10^{-6} while the hand-calculated value is 87.66×10^{-6} . The variation in results is attributed to the fact that FE analysis conducted was a 3-d analysis while the equations considered for hand calculation considers usually a one dimension cases.

Steel Girder:

The maximum stress and strains at the top, middle and bottom slab compared to hand calculated values are all shown in Table (16). It can be seen that all values showed remarkable convergence to the established values except for the stress at the top

flange of the girder which is connected to the concrete deck. This value is linked to the 3-D load distribution at top slab, and hence its value is greatly affected, since it is calculated using 1-D equations.

The composite beam was found to deflect 0.29 in. in mid-span, which 21% more than the established value of 0.24 in, but matches the ratio of FE strain to calculated strain.

The moment calculated for the composite beam section was found to be 895 ft-lb which is 21% more than the hand calculated moment of 737.4 ft-lb.

		FEM	Conventional	% divergence from accurate results
Stress	Top Flange	302.374	300.3	0.7%
	Web	4597.99	4658.6	1.32 %
	Bottom Flange	8957.05	9016.85	0.7%
Strain	Top Flange	12.69×10^{-6}	10.35×10^{-6}	22%
	Web	159.6×10^{-6}	160.5×10^{-6}	0.56%
	Bottom Flange	308.86×10^{-6}	310.7×10^{-6}	0.6%

Table (16) Stress and strain of the girder.

A-5 Plastic Analysis of the composite beam

This analysis is conducted to evaluate the nominal strength of the composite beam.

The plastic stress distribution method was used in hand calculation to obtain the nominal strength. The plastic neutral axis 'PNA' was found to be 8.85 in below the top surface of concrete deck. Hence the PNA is within the concrete slab. In this case the maximum strain at the concrete top fiber should be 0.003, and stress at the same location is $0.85 f'_c$, while the steel girder will attain the full yielding stress F_y , as seen in Figure (65).

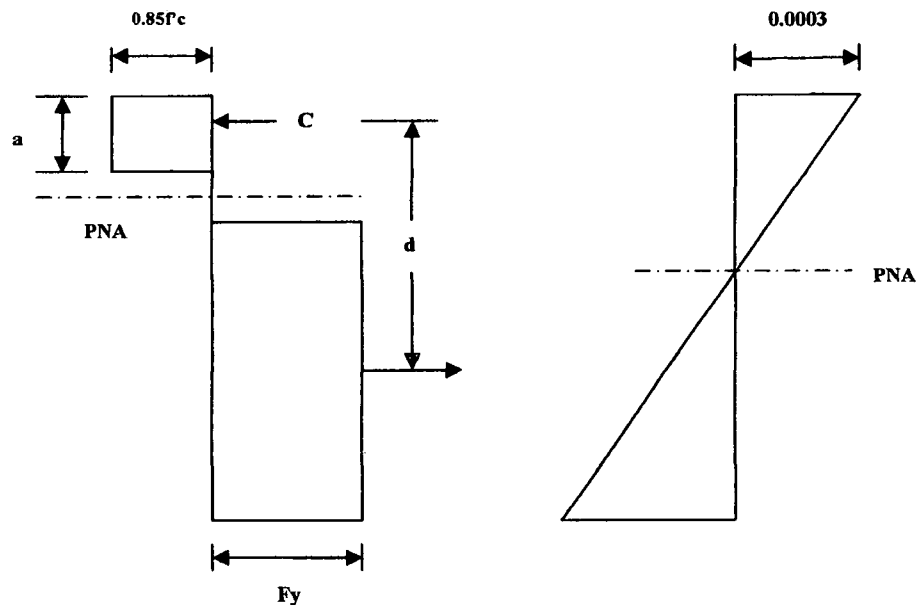
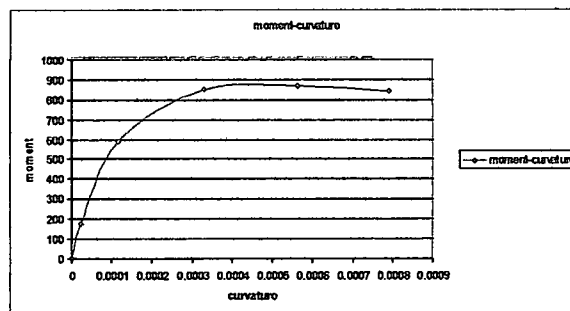


Figure (65) Plastic stress and strain distribution at ultimate moment

Figure (66) shows the moment-curvature diagram, and moment-strain diagram

Curvature	Moment kip-ft
0	0
0.0000221	174.2333
0.000116	590.2788
0.00033	851.834
0.000563	867.3181
0.00079	842.0924



Strain	Moment kip-ft
0	0
0.000222	174.233292
0.000897	590.278849
0.0018	851.834033
0.00254	867.318083
0.003016	842.092363

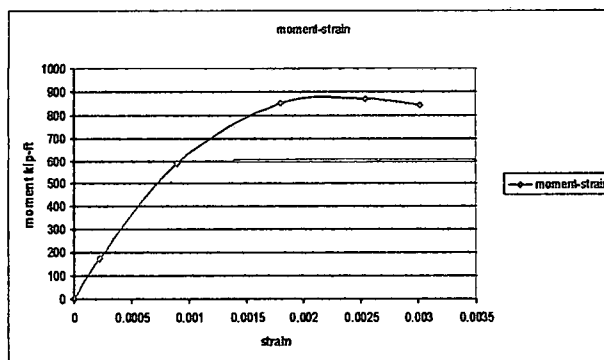


Figure (66) Moment curvature and moment-strain diagram

At the beginning of loading the response was linear, which indicated that no cracks have been detected. The steel girder started to yield when the moment was 68% of the nominal moment M_n i.e. at moment of 590 kip-ft, hence there will be a reduction in stiffness. The ultimate/nominal strength is reached when the moment is 867 kip-ft i.e. when steel reaches its full yield capacity the calculated ultimate moment is 873 kip-ft, as shown in Figure (67). The percentage of difference is 3% which deemed acceptable if mesh refinement is conducted.

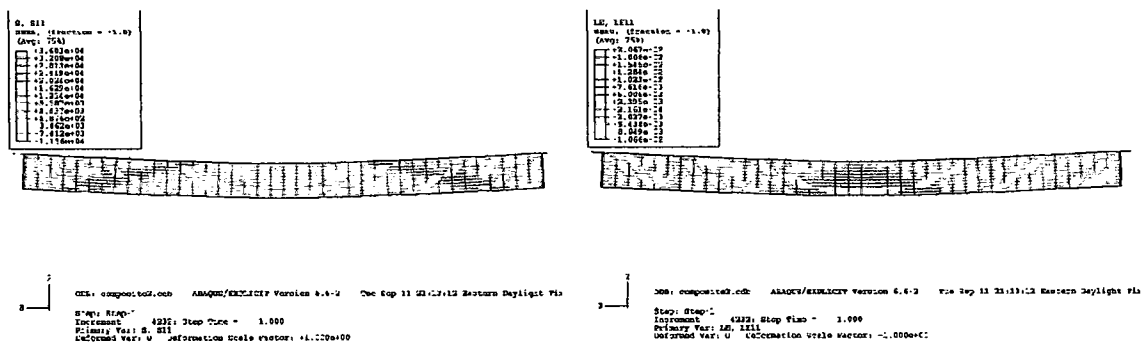


Figure (67) Plastic analysis of concrete beam

The compressive strain at top surface of the concrete when the nominal strength is reached is -0.003016, which confirms the maximum compressive strain of -0.003. While the strain in the girder is .0207. The maximum compressive stress at the deck is -5419.82 which is greater than $0.8f'_c$, but the maximum tensile stress at the girder matches exactly the yield stress is, as shown in Table (17).

	Concrete Deck	Steel Girder
Stress	-5419.82	36000
Strain	-.003016	.0207

Table (17) Analytical values of stress and strain of the composite beam.

Hence after comparing results of both linear elastic and plastic analysis, it can be concluded that the shell element used (S4R) and the model scheme applied are capable of representing the structural behavior of a composite beam, hence ABAQUS can be employed with increasing confidence to analyze bridges that consists of series of similar composite beams.

APPENDIX B

Alternative Mesh Refinement Study

To study mesh refinement, a simple geometry of one span simply supported bridge is constructed as shown in Figure (68). The bridge has steel girder and concrete deck. The overall width of the bridge is 24 ft. and the span between supports is 98 ft. It is assumed that an explosion equivalent to 5N Lb of TNT occurred 10ft on the middle of the top surface of the concrete deck. ATBlast software was utilized to convert blast load into uniformly distributed pressure on the bridge surface as shown in Figure (69). The blast load is applied in concentric fashion as explained in section 4.1.3. Several studies suggested that overpressure resulted from blast wave incident at 90° is to be considered as a design blast load. But since the effect of reflected pressure can be multiple times greater than the effect of overpressure, the mesh refinement study was done also for reflected pressure.

ABAQUS/Explicit considers both material and geometrical nonlinearity in analysis and is best-suited to solve high-speed dynamic events of explosions. Since mesh refinement practice can be a time consuming process, the time duration of the explosion event is assumed to be 0.05 second. Time increment between steps is generated automatically by ABAQUS/Explicit. Structural response such as compressive stress and strain, tensile stress and strain, and deflection in mid-span are examined for results convergence.

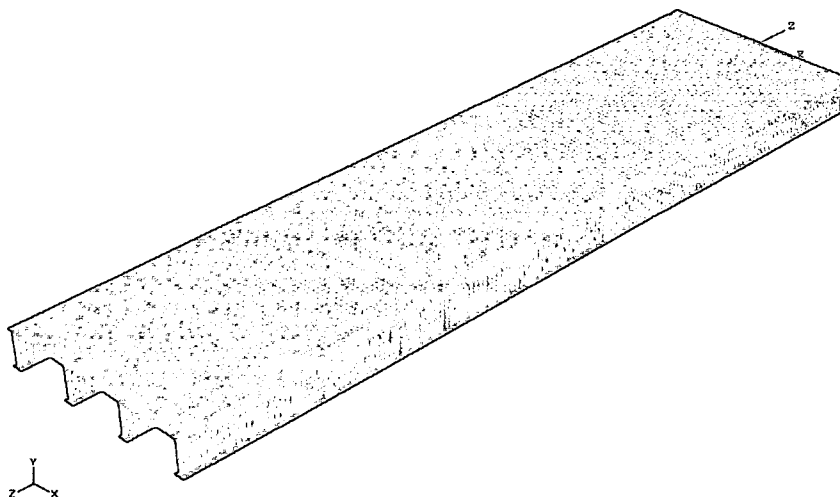


Figure (68) Mesh of bridge 'simplified model'.

Six mesh schemes are considered for mesh refinement study of the deck. The numbers of elements in these schemes are 147, 588, 2352, 4182, 5992, and 6912 respectively. Additional refinement beyond the last scheme will exceed the limited capacity of 'ABAQUS teaching version' nodes.

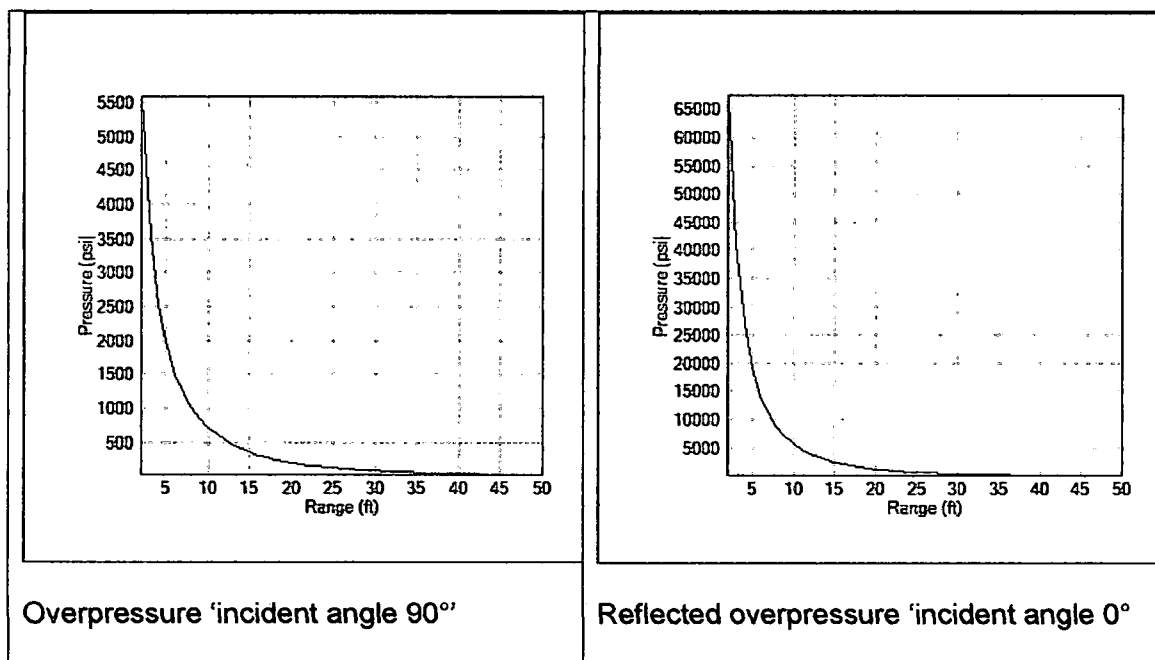
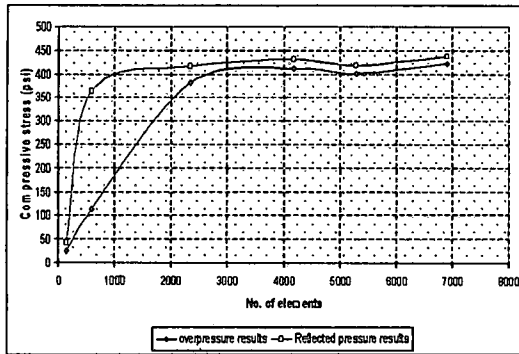


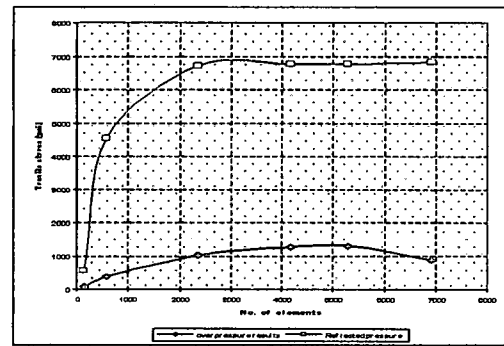
Figure (69) Distribution of pressure due to overpressure and reflected pressure

Results:

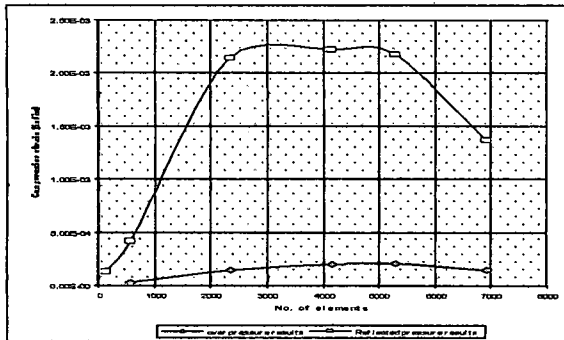
The response of the bridge due to mesh refining for blast loads is shown in Figure (70) Figure (71) and table (18). It is clear that mesh refining yields convergence of various structural responses, but virtually more refining beyond 5992 elements does not lead to any more convergence in cases of compressive strain and tensile strain. Hence that number of elements is excluded from consideration. From table (18), it can be observed that as the number of elements increases the convergence occurs faster for both the overpressure and reflected pressure response. The rate of percentage of convergence of deflection response at mid span is 16% at the start of refining process and 1.2%, which shows that even using 4182 elements '3% convergence' is sufficiently enough to yield accurate results. But tensile stresses do not converge smoothly at 4182 elements; instead they converge to within 4% accuracy for 5992 elements for both load cases. This shows that deflection due to blast load for the bridge deck converges faster than stresses and strains. Hence 5992 elements 'which means 8 in square element' are used to discretized the bridge deck to study blast load response. This is slightly higher than the mesh proposed by the wave propagation study, but will yield acceptable results.



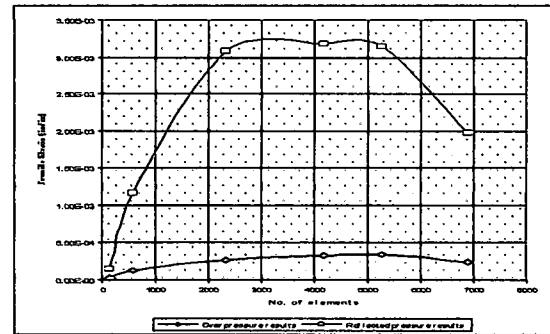
(a) mesh refinement and comparison of overpressure and reflected pressure response of compressive stress



(b) mesh refinement and comparison of overpressure and reflected pressure response of tensile stress



(c) mesh refinement and comparison of overpressure and reflected pressure response of compressive strain



(d) mesh refinement and comparison of overpressure and reflected pressure response for tensile strain

Figure (70) Stress and strain response for mesh refinement.

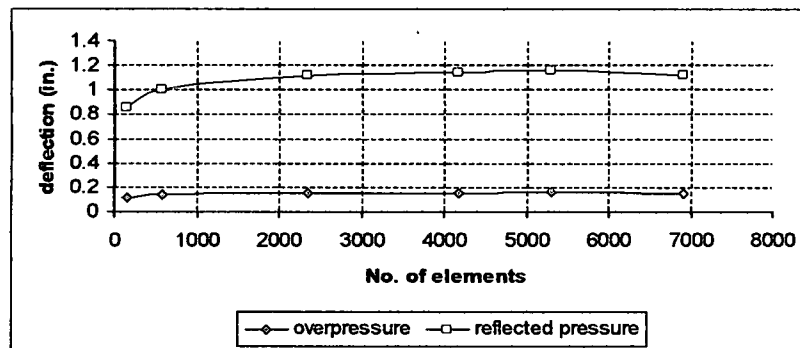


Figure (71) Deflection at mid-span due to mesh refinement

Mid-span Comparative mesh refinement study

PARAMETER	MESH DENSITY	% CONVERGENCE	
		90° reflected	0° incident
Deflection	147	0	0
	588	16	17.5
	2352	10.6	11.6
	4182	3	1.6
	5992	1.2	.81
	6912	2.5	2.96
Compressive stress	147	0	0
	588	354.3	787
	2352	238	14.4
	4182	7.3	3.47
	5992	2.3	2.98
	6912	5	4.4
Tensile Stress	147	0	0
	588	394	692
	2352	157.3	48
	4182	22.5	.86
	5992	3.4	1
	6912	30.5	.17
Compressive strain	147	0	0
	588	248.6	240
	2352	40.2	416
	4182	41	4
	5992	4.139	2
	6912	31.6	3
Tensile strain	147	0	0
	588	555	774
	2352	103.6	165
	4182	24.3	3.5
	5992	2.8	1.4
	6912	30	37

Table (18) Response due to mesh refinement

APPENDIX C

Distribution of blast load on bridge deck

The pressure profile of every charge, obtained from ATBlast software, is shown in Figure (72). The methodology used to distribute blast load on the concrete deck is explained below.

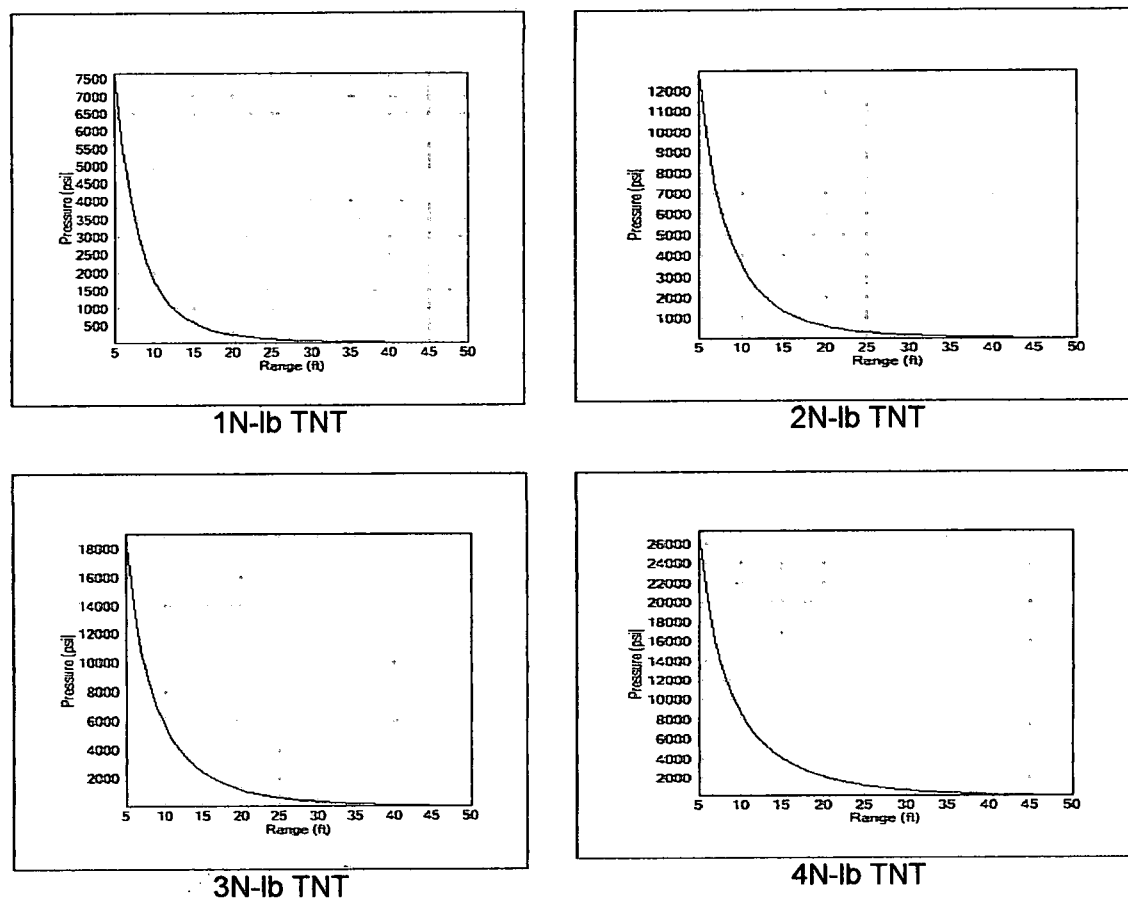


Figure (72) Blast load profile

The blast load is distributed on the bridge deck in form of rings. The first ring has a radius of 2 ft, and subsequent rings have radius that increases by 2 ft. AT Blast software is used to obtain the reflected pressure P_r and time of arrival and duration of blast load t_d .

Example:

Assume that a blast load 0.5N lb is applied 5 ft above the bridge deck.

First Ring:

The radius of the ring is chosen to be 2 ft, $R = 5$ ft, scaled distant Z is given by

$$Z = \frac{R}{W^{1/3}}$$

From which $Z = 0.62996$

In ATBlast software substitute the value to Z for a zero incident angle, the following results will be generated

Time of arrival = 0.31 sec

Reflected pressure = 18979.07 psi

Time of peak reflected pressure = 0.67 sec

The total duration of blast load is given by expression:

$$t_d = \frac{980 \times W^{1/3} [1 + (Z/0.54)^{10}]}{[1 + (Z/0.02)^3] \times [1 + (Z/0.74)^6] \times \sqrt{1 + (Z/6.9)^2}}$$

Substituting, $t_d = 1.3277$

Decay Factor is given by:

$$\alpha = 0.3306Z^4 - 3.188Z^3 + 11.755Z^2 - 20.308Z + 15.12$$

Substituting, $\alpha = 6.247$

Hence the pressure at one-third the total time is given by expression

$$P(t) = P_o \{ 1 - t/t_d \} \exp^{-(\alpha t/t_d)}$$

Hence $P(1/5 t_d) = 0.229 P_o$

$$P(2/5 t_d) = 0.0493 P_o$$

$$P(3/5 t_d) = 0.00943 P_o$$

$$P(4/5 t_d) = 0.00135 P_o$$

$$P(\text{average}) = 0.258 P_o$$

Hence two pressure distributions are considered in design, the first pressure is maximum reflected pressure which arrives, and the second is the average pressure.

Second Ring:

Time of arrival = 0.38 sec

Reflected pressure = 14738.04 psi

Time of peak reflected pressure = 0.66 sec

Total duration of blast load t_d = 1.7286 sec

Decay Factor α = 5.82187

Average pressure $P(\text{average}) = 0.264441$

By using an excel sheet, the distribution of pressure is given in Table (19)

Similar calculation has been used to obtain distribution of 1N-lb, 2N-lb, 3N lb and 4N lb TNT charge.

R (ft)	W (lb)	Z (ft)	alpha	T arrival (sec)	T dur. (sec)	Pr1 (psi)
5	5N	0.629961	6.246803	0.31	1.327715	18979
5.39	5N	0.679097	5.821871	0.38	1.728589	16795
6.4	5N	0.806349	4.856084	0.44	2.913986	12633
7.81	5N	0.983998	3.791319	0.59	4.597818	8986
9.43	5N	1.188106	2.897333	0.8	6.163592	6401
11.18	5N	1.408592	2.229355	1.05	7.601456	4611
13	5N	1.637897	1.76404	1.34	8.998373	3368
14.87	5N	1.873503	1.441812	1.69	10.41948	2491
16.76	5N	2.111628	1.208193	2.08	11.84785	1868
18.68	5N	2.353533	1.019841	2.52	13.30518	1418
20.62	5N	2.597957	0.859549	3.01	14.78707	1089
22.56	5N	2.842382	0.737011	3.55	16.28317	848
24.52	5N	3.089326	0.688153	4.14	17.80259	595
26.48	5N	3.336271	0.780796	4.78	19.33508	533
28.44	5N	3.583215	1.110771	5.64	21.05053	431
30.41	5N	3.83142	1.808131	6.19	22.42317	353
32.39	5N	4.080884	3.037037	6.96	24.80279	291
34.37	5N	4.330349	4.985364	7.78	26.41572	243
36.35	5N	4.579813	7.874201	8.64	28.03273	205
38.33	5N	4.829277	11.95537	9.54	29.58477	174
40.31	5N	5.078742	17.51141	10.41	31.29293	130
42.3	5N	5.329466	24.8978	11.47	32.9314	113

Pr(1/5)	Pr(2/5)	Pr(3/5)	Pr(4/5)	Paverage	Tr1
0.229350449	0.049314	0.009425	0.001351041	0.257888	0.98
0.249694343	0.058451	0.012162	0.001898038	0.264441	1.01
0.302897652	0.086013	0.021711	0.004110112	0.282946	1.11
0.374783309	0.131684	0.041127	0.009633653	0.311446	1.27
0.448157697	0.188292	0.070321	0.019696701	0.345293	1.52
0.512213136	0.245965	0.104989	0.033610339	0.379355	1.82
0.562169644	0.296283	0.138801	0.048768524	0.409204	2.19
0.599591923	0.337041	0.168406	0.063109268	0.43363	2.64
0.628271979	0.370055	0.193746	0.076078302	0.45363	3.15
0.652390653	0.399013	0.216927	0.088450638	0.471356	2.73
0.673644042	0.425434	0.238826	0.100552284	0.487691	4.39
0.690357436	0.446806	0.257047	0.110908818	0.501024	5.12
0.697136415	0.455624	0.264694	0.11532969	0.506557	6.2
0.684338345	0.439049	0.250382	0.107091142	0.496172	6.81
0.640633444	0.384761	0.205409	0.082244805	0.462609	7.93
0.557234122	0.291103	0.135177	0.047078309	0.406119	8.76
0.435809115	0.178059	0.064666	0.01761389	0.33923	9.83
0.295166313	0.081678	0.02009	0.003706271	0.280128	10.98
0.165632513	0.025719	0.00355	0.000367496	0.239054	12.17
0.073225116	0.005027	0.000307	1.40382E-05	0.215715	13.8
0.024102855	0.000545	1.09E-05	1.64795E-07	0.204932	14.67
0.00550167	2.84E-05	1.3E-07	4.47351E-10	0.201106	16.11

Table (19) Distribution of 5N blast load

Appendix (D)
Constitutive Model of Concrete

Compressive strength (psi)	Unit Weight lb/in ²	Modulus of Elasticity (10 ⁶ psi)	Tensile Strength (psi)
3000	.084	3.15E+06	478
3500	.084	3.40 E+06	530
4000	.084	3.64E+06	570
4500	.084	3.86 E+06	630
5000	.084	4.07 E+06	673
6000	.086	4.6 E+06	759.4
8000	.087	5.48 E+06	920
10000	.09	7.04 E+06	1068

Table (20) Concrete properties

Strain (in/in)	Stress (psi)				
	3000	3500	4000	4500	5000
0	0	0	0	0	0
0.00025	774.2464	843.7749	906.9979	963.9466	1017.507
0.0005	1474.151	1638.352	1783.179	1909.674	2024.751
0.0015	2918.076	3427.397	3932.665	4429.509	4916.277
0.002	2995.942	3480.079	3960.333	4443.908	4933.979
0.0025	2889.18	3263.669	3607.6	3932.93	4243.111
0.003	2709.325	2953.503	3138.624	3279.182	3378.563
0.0035	2511.496	2636.467	2685.32	2677.387	2620.122
0.004	2319.839	2346.558	2292.362	2182.783	2030.943
0.0045	2143.546	2093.063	1965.638	1792.448	1591.127
0.005	1985.05	1875.298	1697.746	1487.556	1264.846
0.006	1718.575	1530.014	1297.746	1059.915	836.0581
0.008	1339.906	1083.394	828.0126	605.1905	424.4884

Table (21) Properties of Low Strength Concrete

Strain(in/in)	Stress (psi)		
	6000	8000	10000
0	0	0	0
0.00025	1150.051	1370.331	1760.253
0.0005	2296.802	2740.474	3520.49
0.0015	5915.902	7714.701	9992.236
0.001884	6013.35	8116.07	9475.803
0.002	5860.978	7856.463	8449.989
0.0025	4637.341	5291.662	3205.813
0.003	3263.989	2761.454	945.3636
0.0035	2223.294	1374.628	305.2582
0.004	1527.03	712.0593	112.3425
0.0045	1073.262	390.9349	46.28899
0.005	774.4424	226.9165	20.91299

Table (22) Properties of High Strength concrete

Time (sec)	Strain (in/in) of low strength concrete				
	3000-psi	3500-psi	4000-psi	4500-psi	5000-psi
0	0	0	0	0	0
0.005844	-0.0004	-0.00042	-0.00043	-0.00044	-0.00045
0.011771	-0.00209	-0.00208	-0.00206	-0.00204	-0.002
0.017691	-0.00241	-0.00231	-0.00222	-0.00217	-0.00213
0.023612	-0.00326	-0.00342	-0.00355	-0.00364	-0.00369
0.029533	-0.00474	-0.00449	-0.00428	-0.00429	-0.00432
0.035453	-0.00565	-0.00551	-0.00529	-0.00514	-0.00493
0.041374	-0.00662	-0.00667	-0.00653	-0.00623	-0.00573
0.047287	-0.00763	-0.00723	-0.00673	-0.00651	-0.00608
0.05	-0.00789	-0.00773	-0.00715	-0.00673	-0.00624

Table (23) Strain at for non-ductile concrete

Time (sec)	Strain (in/in) of low strength concrete (ductility of 0.008)				
	3000-psi	3500-psi	4000-psi	4500-psi	5000-psi
0	0	0	0	0	0
0.005844	-0.0004	-0.00042	-0.00043	-0.00044	-0.00045
0.011771	-0.00209	-0.00208	-0.00206	-0.00204	-0.002
0.017691	-0.00241	-0.00231	-0.00222	-0.00217	-0.00213
0.023612	-0.00326	-0.00342	-0.00354	-0.00364	-0.00369
0.029533	-0.00474	-0.00448	-0.00425	-0.00427	-0.00429
0.035453	-0.00564	-0.00543	-0.00516	-0.00496	-0.00479
0.041374	-0.00651	-0.00632	-0.00576	-0.0052	-0.00468
0.047287	-0.00712	-0.00608	-0.00534	-0.0048	-0.00427
0.05	-0.00733	-0.00641	-0.00539	-0.0046	-0.00392

Table (24) Strain for ductile concrete

Time (sec)	Lateral Strain (in/in) of High strength concrete		
	Due to 6000-psi	Due to 8000-psi	Due to 10000-psi
0	0	0	0
0.005844	-3.56E-04	-0.00038	-0.00051
0.011771	-1.46E-03	-0.00138	-0.0015
0.017691	-0.0018	-0.0018	-0.00207
0.023612	-0.00318	-0.00303	-0.00295
0.029533	-0.0037	-0.00333	-0.00361
0.035453	-0.00461	-0.00379	-0.00392
0.041374	-0.00542	-0.00369	-0.00493
0.047283	-0.00610	-0.00400	-0.00456
0.05	-0.00582	-0.00484	-0.00403

Table (25) longitudinal Strain for high strength concrete

BIBLIOGRAPHY

1. <http://www.fas.org/irp/offdocs/nspd/hspd-7.html>. "Critical infrastructure identification, prioritization and protection" Homeland Security Presidential Directive / HSPD 7.
2. Recommendation for Bridge and Tunnel Security, September 2003, AASHTO Blue Ribbon Panel for Bridge and Tunnel Security.
3. Polzin, Stephen "Security considerations in Transportation planning", (2002).
4. Karthik, Srinivasan "Transportation Network Vulnerability Assessment: a Quantitative framework", 2002.
5. Science Applications International Cooperation (SAIC), "A Guide to Highway Vulnerability Assessment for Critical Asset Identification and Protection" 2002
6. Blue Ribbon Panel for Bridge and Tunnel Security, "Multiyear Plan for Bridge and Tunnel Security Research, Development and Deployment, 2003.
7. Michael E. Stovall and Daniel S. Turner, "Methodlogy for Developing a Prioritized list for Critical and Vulnerable Local Government Highway Infrastructure", Dec. 2004.
8. Eric B. William and Davis G. Winget, "Risk Assessment and design of critical bridges for terrorist attacks", 2005.
9. Son, Jin. Astaneh Abolahassan. Rutner Marcus, "Performance of Bridge Deck Subjected to Blast Load, September, 2005
11. Son Jin, Astaneh Abolahassan, "Blast Analysis of Typical steel Bridges using MD Nastran, Dytran and Pytran", 2007.
10. A.K.M. Anwarul Islam, PhD dissertation 2005, 'Performance of AASHTO girder bridge under blast load'
12. Jiang, X. M., Chen, H., and Liew, J. Y. R. ~2002!. "Spread-of-plasticity analysis of three dimensional steel frames." J. Constr. Steel Res.58~2!, 193~212.
13. Liew, J. Y. R., and Chen, H. ~2002. "Inelastic transient analysis of steel frames subjected to explosion and fire." Research Rep. No. CE10/02, Dept. of Civil Engineering, National Univ. of Singapore, Singapore.
14. (7). ABAQUS Version 6.7 User Manual, 2005.
15. Smith PhD and Hetherington JG Blast and Ballistic Loading of Structures, Butterowrth- Heinemann, Oxford 1994.
16. FEMA 426, chapter 4, Explosive Blast.
17. Brode HL "Numerical solution of spherical blast waves", Journal of Applied Physics, June 1955, No.6.

R002594182

18. GSA "security Reference Manual Part 3 – Blast Design and Assessment Manual 2001".
19. ATBlast Production of Applied Research Associates, Inc, June 2004.
20. Coggin, John M. "Response of Isotropic and Laminated Plates to Close Proximity Blast Loads", Virginia 2000.
- 21 Popovics, S. (1973). "A numerical approach to the complete stress strain curve for concrete." *Cement and concrete research*, 3(5), 583-599
22. Optimized sections for High-strength Concrete Bridge Girder – Effects of Deck Concrete Strength, FHWA-HRT-05-058, October 2006.
23. FHWA, "Multiyear plan for bridge and tunnel security research, development and deployment", March 2006.
24. Rojan, Mayes and Nutt, Recommendation for improved AASHTO bridge design specification. April 2006.
25. AASHTO (2002); Standard Specification for Highways Bridges, 17th ed. American Association of State Highways and Transportation Officials, Washington D.C.